New Jersey Institute of Technology

Digital Commons @ NJIT

Summer 8-31-2015

Determining how stable network oscillations arise from neuronal and synaptic mechanisms

Diana Martinez
New Jersey Institute of Technology

Follow this and additional works at: https://digitalcommons.njit.edu/dissertations

Part of the Biology Commons

Recommended Citation

DETERMINING HOW STABLE NETWORK OSCILLATIONS ARISE FROM NEURONAL AND SYNAPTIC MECHANISMS

By

Diana Martinez

Many animal behaviors involve the generation of rhythmic patterns and movements. These rhythmic patterns are commonly mediated by neural networks that produce an oscillatory activity pattern, where different neurons maintain a relative phase relationship. This thesis examines the relationships between the cellular and synaptic properties that give rise to stable activity in the form of phase maintenance, across different frequencies in a well-suited model system, the pyloric network of the crab *Cancer borealis*. The pyloric network has endogenously oscillating 'pacemaker' neurons that inhibit 'follower' neurons, which in turn feed back onto the pacemaker neurons. The focus of this thesis was to determine the methods by which phase maintenance is achieved in an oscillatory network. This thesis examines the idea that phase maintenance occurs through the actions of intrinsic properties of isolated neurons or through the dynamics of their synaptic connections or both. A combination of pharmacological and electrophysiological techniques a used to show how identified membrane properties and short-term synaptic plasticity are involved with phase maintenance over a range of biologically relevant oscillation frequencies.

To examine whether network stability is due to the characteristic stable activity of the identified pyloric neuron types, the hypothesis that phase

maintenance is an inherent property of synaptically-isolated individual neurons in the pyloric network was first tested. A set of parameters were determined (frequency-dependent activity profile) to define the response of each isolated pyloric neuron to sinusoidal input at different frequencies. The parameters that define the activity profile are: burst onset phase, burst end phase, resonance frequency and intra-burst spike frequency. Each pyloric neuron type was found to possess a unique activity profile, indicating that the individual neuron types are tuned to produce a particular activity pattern at different frequencies depending on their role in the network. To elucidate the biophysical properties underlying the frequency-dependent activity profiles of the neurons, the hyperpolarization activated current (I_h) was measured and found to possess frequency-dependent properties. This implies that I_h has a different influence on the activity phase of pyloric neurons at different frequencies. Additionally, it was found that the I_h contribution to the burst onset phase depends on the neuron type: in the pacemaker group neurons (PD) it had no influence on the burst onset phase at any frequency whereas in follower neurons it acted to advance the onset phase in one neuron type (LP) and, paradoxically, to delay it in a different neuron type (PY). The results from this part of the study provided evidence that stability is due in part to the intrinsic neuronal properties but that these intrinsic properties do not fully explain network stability.

To address the contribution of pyloric synapses to network stability, the mechanisms by which synapses promote phase maintenance were investigated. An artificial synapse that mimicked the feedforward PD to LP

synapse, was used so that the synaptic parameters could be varied in a controlled manner in order to examine the influence of the properties of this synapse on the postsynaptic LP neuron. It was found that a static synapse with fixed parameters (such as strength and peak phase) across frequencies cannot result in a constant activity phase in the LP neuron. However, if the synaptic strength decreases and the peak phase is delayed as a function of frequency, the LP neuron can maintain a constant activity phase across a large range of frequencies. These dynamic changes in the strength and peak phase of the PD to LP synapse are consistent with the short-term plasticity properties previously reported for this synapse.

In the pyloric network, the follower neuron LP provides the sole transmitter-mediated feedback to the pacemaker neurons. To understand the role of this synapse in network stability, this synapse was blocked and replaced by an artificial synapse using the dynamic clamp technique. Different parameters of the artificial synapse, including strength, peak phase, duration and onset phase were found to affect the pyloric cycle period. The most effective parameters that influence cycle period were the synaptic duration and its onset phase.

Overall this study demonstrated that both the intrinsic properties of individual neurons and the dynamic properties of the synapses are essential in producing stable activity phases in this oscillatory network. The insight obtained from this thesis can provide a general understanding of the contribution of

intrinsic properties to neuronal activity phase and how short-term synaptic dynamics can act to promote phase maintenance in oscillatory networks.

DETERMINING HOW STABLE NETWORK OSCILLATIONS ARISE FROM NEURONAL AND SYNAPTIC MECHANISMS

by
Diana Martinez

A Dissertation
Submitted to the Faculty of
New Jersey Institute of Technology
and Rutgers, The State University of New Jersey – Newark
in Partial Fulfillment of the Requirements for the Degree of
Doctor of Philosophy in Biological Sciences

Federated Biological Sciences Department

August 2015

APPROVAL PAGE

DETERMINING HOW STABLE NETWORK OSCILLATIONS ARISE FROM NEURONAL AND SYNAPTIC MECHANISMS

Diana Martinez

Dr. Farzan Nadim, Dissertation Advisor	Date
Professor of Biological Sciences, New Jersey Institute of Technology	

Dr. Dirk Bucher, Committee Member	Date
Associate Professor of Biological Sciences, New Jersey Institute of Technology	

Dr. Eric Fortune, Committee Member	Date
Associate Professor of Biological Sciences, New Jersey Institute of Technology	

Dr. Jorge Golowasch, Committee Member	Date
Professor of Biological Sciences, New Jersey Institute of Technology	

Dr. Michael P. Nusbaum, Committee Member	Date
Professor of Neuroscience, University of Pennsylvania, School of Medicine	

BIOGRAPHICAL SKETCH

Author: Diana Martinez

Degree: Doctor of Philosophy

Date: August 2015

Undergraduate and Graduate Education:

- Doctor of Philosophy in Biological Sciences,
  New Jersey Institute of Technology, Newark, NJ, 2015

- Neural Systems and Behavior Course
  Marine Biological Laboratory, Woods Hole, MA, 2013

- Master of Science in Biological Sciences,
  Rutgers the State University, Newark, NJ 2011

- Bachelor of Arts in Biological Sciences
  New Jersey Institute of Technology, Newark, NJ, 2007

  Major: Biology

- Associate of Science in Biological Sciences
  Associate of Science in Chemistry
  County College of Morris, Randolph, NJ, 2004

- Certificate in Applied Transgenics
  County College of Morris, Randolph, NJ
  Rockefeller University, New York, NY, 2003

Presentations and Publications:

Tseng H, Martinez D, Nadim F (2014) "The Frequency Preference of Neurons
     and Synapses in a Recurrent Oscillatory Network," Journal of
     Neuroscience 38:12933-45

Martinez D, Matveev V, Nadim F (2013) "Short Term Synaptic Plasticity in
     Central Pattern Generators," In: Jaeger D., Jung R. (Ed.) Encyclopedia of

Computational Neuroscience: SpringerReference Springer-Verlag Berlin Heidelberg,

Martinez D (2014) "Activity Signature of Oscillatory Network Neurons," *Biological Sciences Colloquium,* Rutgers University, Newark, NJ

Roeser A, Martinez D, Fortune E, (2014) "Decoding Brain Mechanisms for Sexual Signaling," *Dana-Knox Student Research Showcase,* New Jersey Institute of Technology, Newark, NJ

Martinez D, (2013) "Activity Signature of Neurons in an Oscillatory Network," *Neurobiology & Behavior Seminars*, McGill University, Montreal, CA

Martinez D, Nadim F (2013) "Distinct Activity Signatures of Neurons in an Oscillatory Network," Society for Neuroscience Annual Meeting 2013, San Diego, CA

Martinez D, Nadim F (2013) "Activity Signature of Pyloric Neurons," 18th Annual Neuroscience and Post Doctoral Research MiniSymposium, Rutgers University, Newark, NJ, May 2013

Martinez D (2012) "Activity Signature of Pyloric Neurons and Synapses," Society for Neuroscience, Satellite Small Circuits Meeting, New Orleans, LA, October 2012

Martinez D (2012) "Activity Signature of Pyloric Neurons," Small Circuits and Behavior Meeting, University of Pennsylvania Perelman School of Medicine, August 2012

Dedicated to my loving brother,

who walked with me during each step of this journey.

In memoriam of my loving, beautiful, supportive parents:

I am because you were.

"*The best scientist is open to experience and begins with romance - the idea that anything is possible.*"
-Ray Bradbury

ACKNOWLEDGEMENT

I am forever changed.

First, I would like to thank my parents, Xiomara and Luis, I will never be able to express enough gratitude for everything. You have given me so many gifts: the penchant for hard work (I still haven't taken that vacation), my curious and caring nature, and the courage to smile in the hardest of times, I hope to carry on all that you have taught me.

To my brother, during those moments when I felt that the weight of it all became too much, it was you who encouraged me and carried me through. I could have not made it through without you, in science and in life. I am lucky that your wife has become the sister I never had.

Farzan, I could never thank you enough for being an incredible mentor, advisor and friend. You have led my journey through the development of becoming a young scientist. You opened my eyes and encouraged me to look at scientific questions differently, and to always look beyond the problem at hand. I'll never forget our conversations about science, life and everything in between. You have witnessed the highs and lows of my graduate career. I'll miss you greatly as I continue on my path.

To my committee, Dr. Dirk Bucher, Dr. Eric Fortune, Dr. Jorge Golowasch, and Dr. Michael Nusbaum, thank you for being part of this journey.

Eric thanks for the long talks and for the thousands of cups of coffee and tea. We have had some unforgettable scientific discussions that provided a

different perspective. You have become my co-advisor, both in science and in life, that I could always count on and I can never thank you enough. I truly appreciate all of the writing advice and help that you provided. Thank you for supporting me during those times when I needed it the most. Even in the midst of chaos, interestingly enough you were always the one to make sure I remained focused.

Dirk, you've managed to provide me with very helpful thesis advice. You opened my mind to many new possibilities, you always offered straight to the point criticism. On a personal note, you made my days brighter, you made me laugh and I guess you'll always have to hand it to me.

Jorge, you've been there since the beginning of my journey as an undergraduate to PhD. You encouraged me to stay in the lab and pursue my scientific career. You offered some exceptional advice throughout my time here, and a smile on those days when I truly needed one.

Even though not a part of my committee, I'd like to also thank Dr. Horacio Rotstein, Dr. Amit Bose, and Dr. Gal Haspel. Horacio, has become my matlab yoda and without him some of the figures in this thesis would have not been created. Amit, thank you for accepting me into the UBM program and believing in me through these year. Your advice over the years has been quite valuable to me. Gal, thank you so much for your invaluable input, during my time here. I will not forget our chats about science and the advice you have given me.

To my fellow labmates, the most dysfunctional family I have had the privilege to be a part of, I cannot thank you enough for all of your support. We've had some great times that have definitely kept me smiling and will be the moments I miss the most. Thank you to Liz, Jordan, Nelly and Michael, for taking the time to read chapters in this document. Remember, it all started in Boyden.

Lastly to all of my friends who have been part of this crazy journey, I cannot thank you all enough. To Kim, I love you more than words can say, just do not call me at 3:00 am. To Matt, Moe, Pamela and Karen thank you for being supportive, and helping me achieve my dream. To Best Friends 2013, NS&B would have not been the same experience without you all.

To all of those who have been a part of this journey, I thank you.

TABLE OF CONTENTS

LIST OF TABLES

LIST OF FIGURES

CHAPTER 1

GENERAL INTRODUCTION

1.1 Background

Oscillations are a dominant feature of many neural networks. Oscillatory behavior is known to underlie or correlate with a variety of behaviors including sensory, motor, learning and memory formation (Sirota and Buzsaki, 2005, Nokia and Wikgren, 2010). Oscillatory systems have been studied with the potential of elucidating the mechanisms and principles involved in the generation, control and maintenance of rhythmic activity.

Rhythmic activity is often generated in neural networks called Central Pattern Generators (CPGs). CPG activity arises from the interplay of neuronal intrinsic properties and the synaptic interaction between neurons in a network (Marder and Calabrese, 1996). An important characteristic of oscillatory activity in a CPG is its ability to maintain rhythmic activity despite a lack of patterned sensory input (Marder and Calabrese, 1996, Marder et al., 2005). Some of the behaviors generated through CPGs include: heartbeat generation in leech, swimming in lamprey, feeding in crustaceans, breathing in vertebrates and locomotion in insects.

One particular area of study is to understand how neurons can maintain phase in different conditions (Bucher et al., 2005, Goaillard et al., 2009). In order for CPGs to maintain functional and stable motor outputs across different frequencies, the relative timing (phase) of the components of the network must

be maintained. Phase is defined as the fraction an event (bursting) takes during one cycle. Networks can produce stable activity that maintains a specific phase relationship across different frequencies (Bucher et al., 2005, Goaillard et al., 2009). This flexibility of network output requires neurons to adjust temporal characteristics such as burst duration, firing rate and interburst interval in order to maintain phase during changes in frequency (Mouser et al., 2008, Hooper et al., 2009, Soofi et al., 2012). The need for a system to maintain phase is important for a system or behavior to be stable as it changes frequencies. The mechanism by which phase maintenance occurs in motor networks is not fully understood.

Oscillatory motor activity frequently requires that network output to muscles arrive in a precise sequence. For CPGs, this requires distinct activity phases of the different neurons within the network; this is clearly demonstrated in lamprey and crayfish locomotion. For example, during lamprey swimming, the neural circuits that are located in the segments of the spinal cord, fire with a one percent phase lag with respect to each other (Hill et al., 2003). This phase lag occurs independently of the frequency of lamprey swimming. If this 1% phase lag is not maintained, the customary sinusoidal swimming action of the lamprey cannot be achieved. The swimmeret system in crayfish is responsible for propelling a crayfish forward through the water (Mulloney and Smarandache-Wellmann, 2012). When active, the right and left swimmeret of each segment moves in phase through cycles of power and return strokes. The periodic movements are started by the posterior pair of swimmerets, and

swimmerets on the adjacent segments differ in phase by 25%. The action of this system is driven by the activity of two types of motor neurons: the power-stroke and the return-stroke neurons. The actions of these neurons are coordinated in order to maintain the proper phase relationship between segments. Therefore, the order that these muscles are activated is an important property of the network. The actions of these neurons are coordinated in order to maintain the proper phase relationship between segments.

In addition to locomotion, proper phase maintenance is also important in the leech heart beat generation. The leech possesses two tubular hearts, which move blood through a closed circulatory system. The beating pattern, with a period of 4-10s, is asymmetric. One heart generates high systolic pressure through a wave directed along its length, which moves blood forward; the second generates low systolic pressure through near-synchronous constriction and pushes blood into the peripheral circulation (Norris et al., 2007b). The network responsible for heartbeat generation in leech is characterized as two coupled segmental oscillators. Both of these segmental oscillators drive muscles whose temporal sequence is important in producing stable motor output (Norris et al., 2007b). Therefore, identifying how CPGs generate oscillatory activity and maintain phase, can help reach an understanding of how neural networks adjust their activity to promote stable and useful behavior.

Phase maintenance is primarily a property of motor networks. However, it is not a necessary function of all oscillatory networks.   Such distinct patterns of activity, in other systems, are also important for non-motor rhythmic activity. For instance in mammals phase synchronization, particularly in the gamma frequency range, establishes transient associations between brain regions that represent the particular details of a stimulus (Fell and Axmacher, 2011). Phase synchronization, in mammals, is also responsible for linking different brain regions that process different aspects of one stimulus (Eckhorn et al., 1988, Fries, 2005). For instance, if the stimulus is the picture of a black BMW Z4, the different properties of the car are processed in different brain areas. Information about the car such as: the color - black, the type of stimulus i.e. the car, and the motion (is it moving fast or slow) are all processed in different areas and then it is believed that phase synchronization in the gamma frequency range is responsible for linking all of these together (Fell and Axmacher, 2011).

Because the rhythmic patterns produced by CPGs can be easily quantified and related to behavior, such systems allow for the study of the neural mechanisms leading to behavior at different levels, from the single neuron, synaptic through network activity properties. By using smaller CPGs of invertebrates such as those found in the well-characterized stomatogastric nervous system (STNS) of crustaceans, we can gain further understanding on how synaptic and intrinsic properties are regulated to produce meaningful network output. Systems such as the STNS provide an understanding of how

rhythmic and patterned output is generated through cell-to-cell synaptic connections, intrinsic neuronal properties and neuromodulation.

In order to understand how stable output is generated and maintained in an oscillatory network, we must characterize both the intrinsic and synaptic properties of all constituent network neurons. As discussed previously, phase has been shown to be maintained across different network frequencies. Goaillard et al., (2009) showed that despite differences in frequency (Figure 1.1A, Figure 1.1B), the phase of the neurons remained relatively constant across animals. They found that the mean delay of the burst onset and burst end of LP and PY with respect to the burst onset of the PD neuron, scaled as function of the pyloric frequency (Figure 1.1C). The phase of each burst event (either LP on/off, PY on/off, and PD off) was calculated as the delay divided by the period (Goaillard et al., 2009). They found that the mean phase of each burst event was maintained from animal to animal, even as the frequency changed (Goaillard et al., 2009). We define stability as the phase maintenance of the triphasic pyloric network across different frequencies. This stability seen across animals across different frequencies is important in motor behavior. However, the full extent to which the frequency-dependent properties of individual neurons and synapses lead to stability in the form of phase maintenance are not fully known. We address this topic, by taking advantage of the small, well-characterized pyloric motor network of the crab, *Cancer borealis,* to investigate the role of intrinsic and synaptic properties in maintaining stable network output. We hypothesize that the stability of an oscillatory network is
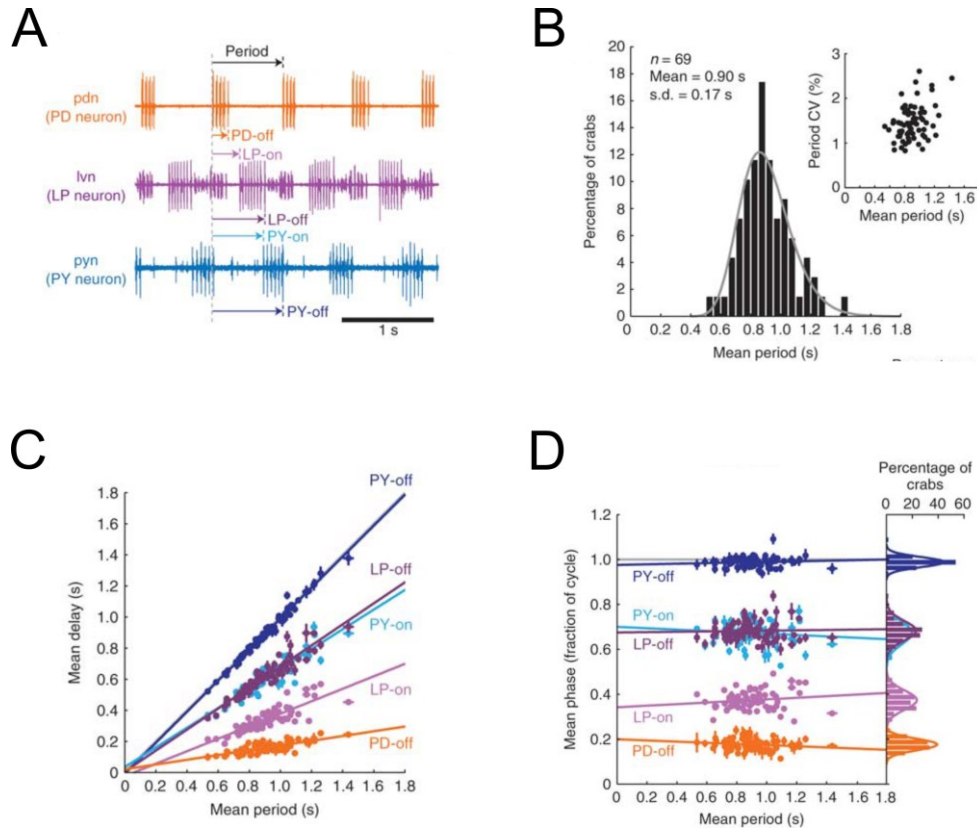
Figure 1.1 Variability of the pyloric network across different animals. **A.** Simultaneous extracellular recordings of the pyloric dilator nerve (*pdn*), the lateral pyloric nerve (*lvn*), and the pyloric nerve (*pyn*). The period (1/frequency) was measured from the burst onset of one PD neuron to the burst onset of the PD neuron in the next cycle. The delay to: PD off, LP off, LP on, PY on and PY off were also measured. **B.** The histogram showing the distribution of the mean cycle period for ganglia from 69 crabs. **C.** Mean delay versus mean period for each crab. For each burst event (delay to: PD off, LP off, LP on, PY on and PY off) was plotted for each crab. The colors match the colors of the events in *A*. **D.** The mean phase of each burst event versus the mean period was plotted for each crab. The linear regression line of each burst event passed through the origin showing that the delay for each event was proportional to the pyloric period. The mean phase of the different burst events was consistent from animal to animal. The histogram of the mean phase of each burst event type is show, and curves are the normal distribution fit for each burst event. *Adapted from Goaillard et al. (2009).*

6

inherent in the individual neurons. In other words, stability in the form of phase

maintenance arises from the properties of the individual neurons rather than the

network as a whole. We apply electrophysiological and pharmacological tools to

the pyloric motor network of the crab, to understand how stable network output

is generated (see Section 1.18). The results presented in this thesis can aid in

the general understanding of the generation of oscillations in both invertebrate

and vertebrate networks, provide insight into how stable network output is

generated, and leads to meaningful behavior.

1.2 The Stomatogastric Nervous System

The stomatogastric nervous system (STNS) of decapod crustaceans such as

crayfish, crabs and lobster is responsible for the animal's feeding behavior and

is an invaluable model system in understanding cellular and synaptic properties

found in all nervous systems (Nusbaum and Beenhakker, 2002). The STNS is

an extension of the central nervous system and controls rhythmic motor

movement of the foregut. The foregut is divided into four chambers: the

esophagus, the cardiac sac, the gastric mill and the pylorus, which produce

rhythmic motor activity through the contraction of different muscles driven by

several CPGs. Food enters the foregut through the esophagus, and is stored in

the cardiac sac region of the stomach waiting to be macerated by the gastric

mill (Figure 1.2). This food is then broken down through the movements of

three teeth (two lateral and one medial) located within the gastric mill before it

passes to the pylorus, which then filters the chewed food. In the pylorus, solid
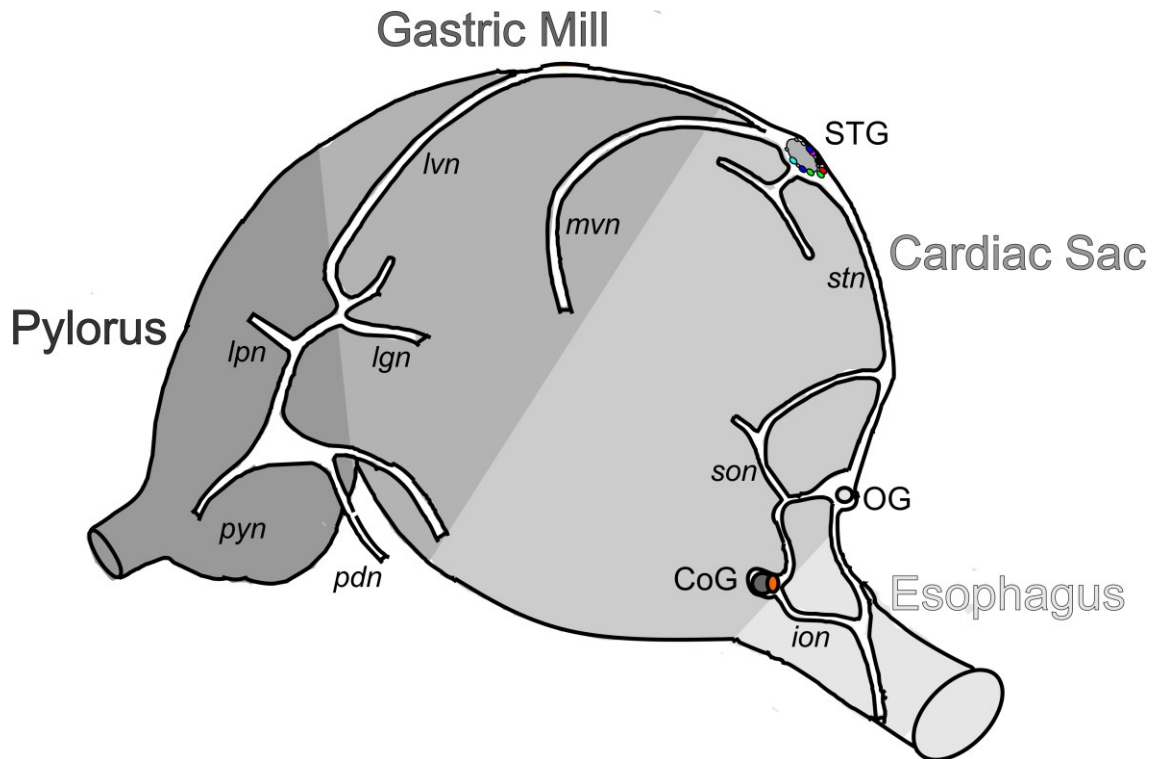
Figure 1.2 The stomatogastric nervous system lies on the dorsal surface of the foregut of Cancer borealis and other decapod crustaceans. There are four main ganglia that comprise the STNS: the oesophageal ganglion (OG), paired commissural ganglia (CoG) and the stomatogastric ganglion (STG). The CoGs are located on each side of the esophagus, the OG is found on the wall of the esophagus and is connected to the CoG through both the paired superior and inferior oesophgeal nerves (*son and ion*). The OG is connected to the STG through the stomatogastric nerve (*stn*). The foregut, midgut and hindgut comprise the intestinal tract of the crustacean. Food enters into the esophagus then passes to the stomach chamber comprised of the cardiac sac, gastric mill, and pylorus. It is stored in the cardiac sac until it reaches gastric mill. The gastric mill is a CPG whose somata are located in the STG, which produces motor activity that controls three teeth, the lateral and medial tooth. Chewed food then enters the pylorus for filtering; the muscles of the pylorus are innervated through a CPG whose somata are also found in the STG. *Adapted from Veronica Garcia (2014)*

food is separated from liquids (Stein, 2009). Fluids are absorbed through the midgut and solid particles move to the hindgut where they are excreted. The muscles are innervated through the activity of motor neurons within four different ganglia of the STNS (Selverston et al., 1976). The STG consists of two central pattern generating (CPG) networks that innervate both the gastric mill and pylorus. The gastric mill rhythm is not spontaneously active but is dependent on neuromodulatory actions of neurons that project from the paired commissural ganglion (CoG) (Blitz et al., 1999). The gastric mill rhythm is not pacemaker driven but is generated by a pair of neurons and their interactions with modulatory projection neurons. The two STG neurons are Interneuron 1 (Int1) and the lateral gastric (LG) neuron, which are coupled with reciprocal inhibition and create a biphasic rhythm. The activity of the pyloric network is driven through an intrinsically bursting (but conditional) pacemaker neuron, the Anterior Burster (AB) neuron.

Paired commissural ganglia (CoG; ~550 neurons) receive and integrate sensory input from the visual and olfactory systems, as well as the foregut and modulate the motor patterns of the STG (Selverston et al., 1976, Nusbaum and Beenhakker, 2002). The oesophageal ganglion (OG; 12-15 neurons) contains both modulatory neurons as well as motor neurons that are responsible for generation of the cardiac sac rhythm (Harris-Warrick, 1992).

1.3 The STG of the Jonah crab *Cancer borealis*

The STG lies within the ophthalmic artery, which extends from the heart to the brain on the dorsal side of the stomach. It is composed of approximately 26 neurons, 11-13 of which are part of the pyloric network and about eleven of which are part of the gastric mill network (Kilman and Marder, 1996). The gastric mill network (average freq. ~0.1 Hz) and the pyloric network (average freq. ~1 Hz) interact through both local synapses and feedback to descending modulatory projection neurons coming from the OGs and CoGs, providing both networks the ability to generate different patterns dependent on physiological conditions.

The STG receives central input via descending projection neurons only through the stomatogastric nerve (*stn*), which connects the STG to the OG and the paired CoGs (Figure 1.3). Projection neurons of the OG and CoGs release neuromodulators in the STG and modify components of both the gastric mill and pyloric networks. This will be discussed in further detail later in this introduction.

1.4 The Pyloric Network of the Crab *Cancer borealis*

The pyloric network within the STG is the motor network that governs the muscles used in filtering chewed food and its activity can be examined and recorded through both intracellular and extracellular motor nerve recordings. The 11-13 neurons of the pyloric network are grouped into 7 different neuronal types, including a pacemaker ensemble and follower neurons (Figure 1.4). The
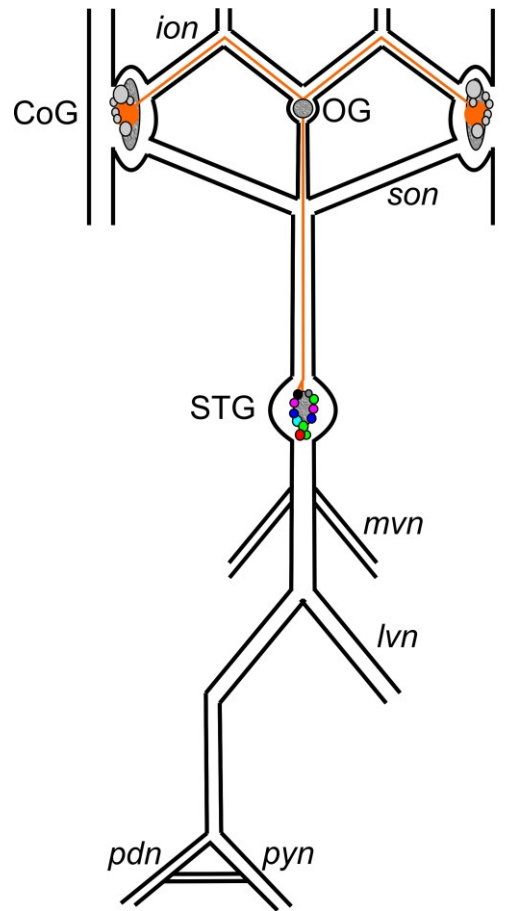
Figure 1.3 The stomatogastric nervous system is easily accessible for dissection and experimental use. The stomatogastric nervous system is comprised of four ganglia and nerves connecting the ganglia. The CoGs and OG are responsible for the release of neuromodulators onto both the pyloric and gastric mill networks located in the STG. The *stn* serves as the only source of central input to the neurons of the STG. The somata of the gastric mill and pyloric networks are located in the STG.

pacemaker ensemble consists of an anterior burster neuron (AB), two pyloric dilator neurons (PD) and two lateral posterior gastric neurons (LPG). The AB neuron is the only endogenous oscillator in the STG capable of bursting in the absence of synaptic input (Miller and Selverston, 1982b). The PD neurons are strongly electrically coupled to the AB neuron and as a result produce synchronous bursting oscillations.

In addition to the neurons of the pacemaker ensemble, there are different follower neurons that constitute the remaining neurons in the pyloric network. The lateral pyloric neuron (LP), the pyloric constrictor neuron (PY), the ventricular dilator neuron (VD), and the inferior cardiac neuron (IC) all receive inhibitory input from the pacemaker ensemble. The pyloric network contains: one AB neuron, two PD neurons, one LP neuron, one VD neuron, one IC neuron, and three to five PY neurons. With the exception of the AB neuron, all other neurons act as motor neurons in addition to their central connectivity in the STG. The follower neurons do not oscillate on their own but depend on synaptic input from the pacemaker ensemble for bursting and generation of oscillations. The LP is the sole feedback to the pacemaker ensemble. In addition to the chemical inhibitory synapses from the pacemaker ensemble the LP and PY neurons are linked by a weak electrical synapse (Mamiya et al., 2003). A weak electrical synapse also exists between the LP and IC neurons, as well as the PY and VD neurons.

The triphasic pyloric rhythm is generated by the interplay between the pacemaker ensemble and follower neurons. The endogenous oscillator AB

produces a burst that depolarizes the two PD neurons via strong gap junctions,, which causes them to burst synchronously (Maynard and Selverston, 1975). All other follower neurons receive inhibitory chemical input from the pacemaker ensemble and do not fire during the first phase of the triphasic rhythm. Upon termination of the first phase, the second phase occurs when both the LP and IC neurons depolarize on rebound with a short delay from the pacemaker ensemble inhibition (Selverston et al., 1998). The last phase occurs when the PY neurons follow with a burst of action potentials. The PY oscillations are terminated when the pacemaker ensemble (AB/PD) depolarizes again to initiate a new cycle (Maynard and Selverston, 1975). The strong inhibitory synapses from the PY to the LP neurons are responsible for allowing the PY neurons to end the LP burst (Maynard and Selverston, 1975).

1.5 Neurons of the Pyloric Network

We will outline the properties of each of the pyloric neurons to build a basis of understanding of the properties of each of these neurons in maintaining stable output in the network.

1.51 The Pyloric Pacemaker Ensemble

Pacemaker neurons control the behavior of different networks such as those involved in respiration (Pena et al., 2004). The pre-Botzinger complex which controls the inspiratory phase of breathing is comprised of two different types of pacemaker neurons, which are state-dependent (Pena et al., 2004). The

pacemaker ensemble of the pyloric network is also comprised of two different neuronal types.

The AB interneuron is the sole endogenous burster in the pyloric network (Miller and Selverston, 1982b). Its axon, interestingly, does not project to any target muscles like all other pyloric neurons, but projects to the CoGs via the *stn* (Maynard and Selverston, 1975, Selverston and Miller, 1980). The AB neuron influences the pyloric network via the chemical and electrical synapses it locally imposes onto the follower neurons within the STG.

The two electrically coupled PD neurons are strongly coupled to the AB neuron and fire in-phase with it and with each other. However, in *P. interruptus*, when isolated from the AB neuron, the two PD neurons either fire tonically or produce weak bursting oscillations (Miller and Selverston, 1982b, a, Bal et al., 1988). while the AB neuron can retain its ability to oscillate (Miller and Selverston, 1982a, Bal et al., 1988).

The synapse between the AB and PD neuron is a non-rectifying electrical synapse. The lack of rectification of the electrical coupling between the AB and PD neurons allows bi-directionality of current flow between them, allowing for in-phase oscillations.

1.52 The Lateral Pyloric Neuron

At the muscle level, the LP neuron is an excitatory motor neuron that innervates constrictor muscles of the pylorus (Hooper et al., 1986). Each STG only contains one LP neuron, which has a large cell body (70-100 µm) and

possesses an extensive dendritic tree. Even with its extensive dendritic processes, current injection into the soma of the LP neuron shows little attenuation as the current spreads into the larger branches (Golowasch and Marder, 1992a). This suggests that we can consider the soma and the major proximal neurite nearly isopotential for voltage clamping (Golowasch and Marder, 1992a).

The LP neuron makes a number of glutamatergic inhibitory connections within the neuropil of the STG, which shape the pyloric rhythm (Eisen and Marder, 1982). Importantly, the LP neuron acts as the sole chemical synaptic feedback to the pacemaker ensemble by making a graded and a spike-mediated inhibitory synapse to the PD neuron (Zhao et al., 2011). This feedback synapse is believed to stabilize the cycle period of the pyloric network (Nadim et al., 2011). Photoinactivation of the PD neurons abolished these LP-timed IPSPs. The effects of the LP synapse onto the PD neurons can be effectively blocked using 10^{-5} M picrotoxin (PTX) (Eisen and Marder, 1982, Golowasch and Marder, 1992a).

The phase at which the LP neuron fires is remarkably consistent from preparation to preparation, despite differences present in pyloric network properties such as pyloric frequency (Bucher et al., 2005, Goaillard et al., 2009). The LP neuron waveform reflects the three phases of the pyloric rhythm. During the first phase, the pacemaker ensemble is active and the LP neuron is hyperpolarized. Next, after a gap the second phase of the LP neuron fires a burst of spikes. Lastly, in the third phase the LP neuron is inhibited by
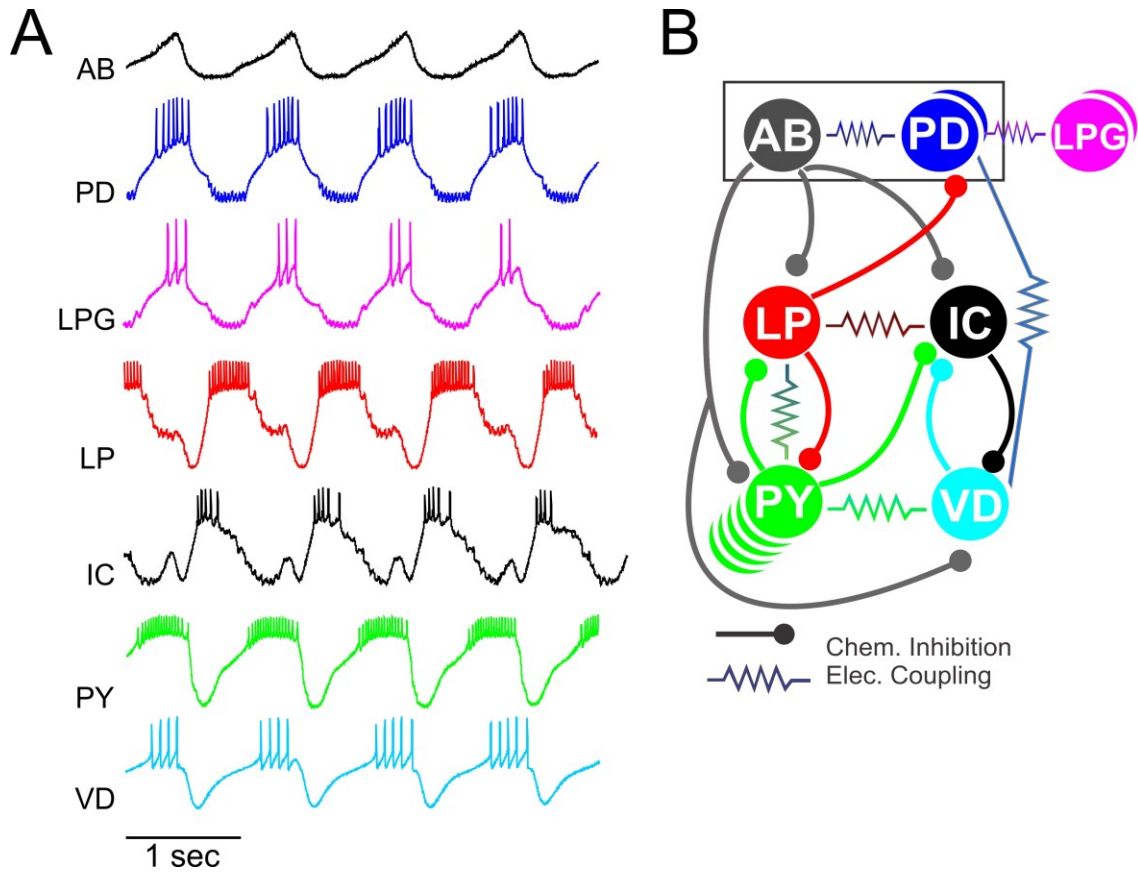
Figure 1.4 The pyloric network is comprised of seven different types of neurons. **A.** Each neuron of the pyloric network can be identified by its intracellular activity and matched to the extracellular nerve activity. The cells of the pyloric network possess both chemical inhibitory synapses and electrical coupling. This figure was made from the intracellular recordings from one preparation and then aligned to the activity of the *lvn.* **B.** The pacemaker ensemble is comprised of the Anterior burster (AB;black) interneuron and two electrically coupled pyloric dilator (PD;blue) neurons, which burst synchronously. All other follower neurons receive inhibitory chemical input from the pacemaker ensemble and do not fire during the first phase of the triphasic rhythm. Upon termination of the first phase, the second phase occurs when both the LP and IC neurons depolarize on rebound with a short delay from the pacemaker ensemble inhibition. The last phase occurs when the PY neurons follow with a burst of action potentials. The PY oscillations are terminated when the pacemaker ensemble (AB/PD) depolarizes again to initiate a new cycle.

the PY neuron but not as strongly as by the pacemaker ensemble during the first phase (Figure 1.4A). The LP neuron is also modulated differently than other pyloric neurons. For instance, in *P. interruptus* dopamine causes differential effects in the different ionic currents: an increase in I_h, and I_{Ca}, and lastly a decrease in I_A; this causes the LP neuron to fire more strongly than the PD neurons whose firing rate may be diminished or eliminated completely (Flamm and Harris-Warrick, 1986, Kloppenburg et al., 1999, Peck et al., 2006). The two neuromodulatory peptides released by MCN1, CabTRP Ia, and proctolin, both activate and excite the LP neuron (Hooper and Marder, 1987, Christie et al., 1997), by a mechanism known to involve the activation of the modulator-activated current, I_{MI} (Swensen and Marder, 2000).

1.53 The Pyloric Constrictor Neuron

In *P. interruptus*, the pyloric constrictor neuron (PY) is the second smallest neuron in the pyloric network, with a soma diameter of about 60 μm (Hooper et al., 2008). The PY neurons are weakly electrically coupled to each other and the LP neuron, and to the VD neuron.

Similar to the LP neuron, the phase of firing for the PY neuron is consistent from preparation to preparation. The synchronous burst from the pacemaker ensemble evokes an IPSP, and following the IPSP the PY neuron resumes firing. In the lobster, *P. interruptus,* the PY IPSPs have two different components: the early AB neuron component and a late PD neuron component (Eisen and Marder, 1984). In the same species, the AB-evoked IPSPs in the PY

neuron differ from those evoked by the PD neuron on the basis of reversal potential, ionic selectivity, and pharmacological sensitivity (Eisen and Marder, 1984).   Interestingly, the time at which PY stops firing is governed by the AB neuron's early component; and the point at which PY will resume firing is governed by the late PD neuron released neurotransmitter.

1.54 The Inferior Cardiac Neuron

The inferior cardiac (IC) neuron is a pyloric neuron that is the third smallest in the network averaging about 60 µm.   Usually considered part of the pyloric network, the IC neuron innervates cardiac sac, gastric mill, and pyloric muscles (Weimann et al., 1991). IC can switch between gastric and pyloric timing if the gastric mill is present (Weimann and Marder, 1994, Blitz and Nusbaum, 1997). The IC neuron is weakly-electrically coupled with the LP neuron and fires in a similar phase to it. It is also reciprocally inhibited by the VD neuron.

1.55 The Lateral Posterior Gastric Neuron

The lateral posterior gastric neuron is a pair of neurons that is electrically coupled to the pacemaker neurons (AB and PD). This set of neurons is usually active during pyloric timing but can switch to gastric mill timing depending on the state of the system, and is known as one of the gastro-pyloric neurons (Other than MG which is beyond the scope of this study) (Weimann et al., 1991).

1.56 The Ventricular Dilator Neuron

The VD neuron is the third largest neuron in the pyloric network. The single VD neuron fires in phase with the PY neurons, and is weakly electrically coupled to the PY neuron. The VD neuron, similar to the IC neuron, also can switch from firing with the pyloric network to the cardiac sac network. VD neuron fires out of phase from the IC neuron but fires in PY time (Figure 1.4A). In the lobster *P. interruptus*, synapses from the VD neuron to other neurons are cholinergic, rather than glutamatergic (Marder and Eisen, 1984b).

1.6 The Advantages of Studying the Pyloric Network

The crustacean STNS has many advantages for study as an experimental model system. First, the pyloric network within the STNS produces rhythmic patterns in the absence of sensory input and the STNS can be dissected out of the animal while maintaining pattern generation (Marder and Bucher, 2007). Second, the STG produces the same characteristic rhythmic outputs both *in vivo* and *in vitro* (Nusbaum and Beenhakker, 2002). Third, the STG is composed of a small number of neurons, which are identifiable by their firing pattern. Fourth, the neurons' somata are large, ranging from 25-120 μm, allowing for easy intracellular recordings, (Nusbaum and Beenhakker, 2002). Intracellular recordings of multiple neurons from the STG allow for prolonged recording for characterization of synapses. This has allowed for an understanding on how individual ionic currents can affect rhythmic network

output. Sixth, the electrical and chemical synaptic connections between the neurons within the STG have been well-characterized and are well-understood.

There is an increasing number of studies that shows that the values of the ionic conductances of the same cell type or identified neuron can vary two to six fold or more across cells and preparations (Golowasch et al., 1999, Marder and Goaillard, 2006, Schulz et al., 2006). Despite this variability, stable activity is maintained from animal to animal. Relative phase is maintained from preparation to preparation despite the variability shown by the ionic conductances (Goaillard et al., 2009). Understanding how phase maintenance occurs across different frequencies, despite the variability found in ionic currents is the driving force of this thesis.

1.7 Ion Channels of the Neurons in the Pyloric Network

Ionic currents within the pyloric network work in concert to determine firing characteristics of individual neurons. Three particular currents of interest are the: the hyperpolarization-activated inward current (I_h), and the transient K^+ current (I_A), and the inward modulatory current (I_{MI}). I_h, which is activated at hyperpolarized membrane potentials, acts to depolarize the neuron and determines the extent of post-inhibitory rebound following inhibition (Robinson and Siegelbaum, 2003). I_A delays the onset of bursting following strongly inhibitory input. When I_A is blocked, the cycle period is decreased due to an enhancement of pyloric neuron activity (Kloppenburg et al., 1999). I_A also plays an important role in shaping spike frequency, setting bursting rate and

modulating post-inhibitory rebound (Tierney and Harris-Warrick, 1992). In *Cancer borealis*, the high-threshold potassium current, I_{HTK} is comprised of two components: the calcium-dependent potassium current (I_{KCa}) and the delayed rectifier current (I_{Kd}). These two components can be separated by the use of blockers (Khorkova and Golowasch, 2007). I_{MI}, is a voltage-dependent nonspecific cation inward current, permeable to Na^+ and K^+, characterized by it bell-shaped current-voltage relationship (Golowasch and Marder, 1992b). It is strongly affected by extracellular Ca^{+2}, and is believed to be important in generating slow bursting oscillations. Because of their role in spike generation, it is important to understand how these currents can affect burst onset at different frequencies, and in turn phase.

1.8 Neurotransmitter Release within the Pyloric Network

Neurotransmitter release within the STG can happen in two different ways. The first type of release common in most synapses is spike-mediated, where an action potential triggers the release of neurotransmitter as a function of opening voltage gated ionic currents. The second type of neurotransmitter release is graded transmission.

Graded synaptic release is found in the retina, at the neuromuscular junction of *Caenorhabditis elegans,* in nonspiking neurons and in invertebrate systems such as the stomatogastric nervous system (Graubard et al., 1980, 1983, Heidelberger, 2007, Liu et al., 2009). During slow wave oscillations of STG neurons, neurons tonically release transmitters, as a smoothly, graded

function of the presynaptic voltage (Graubard et al., 1983). This type of transmission takes place at the synaptic locations that are found on the fine secondary processes that branch from the primary neurite of both the presynaptic and post-synaptic neurons (Graubard et al., 1983). The amplitude of release is correlated with the membrane potential of the presynaptic neuron. Graded synaptic transmission can be found in cells that also use spike mediated transmission.

The chemical synapses within the pyloric network are exclusively inhibitory synapses that can be divided into two categories based on their neurotransmitter: glutamatergic or cholinergic. According to Marder and Eisen (1984), in the lobster *P. interruptus,* the PD and VD neurons are cholinergic while the remaining neurons are glutamatergic.

1.9 Electrical and Mixed Synaptic Transmission

Electrical synapses are mediated by the passage of small molecules or ions along pores formed through gap junctional channels between adjacent neurons (Hormuzdi et al., 2004) and found between neurons of the inferior olive, thalamic reticular nucleus, and interneurons of the hippocampus (Llinas and Yarom, 1981, Fukuda and Kosaka, 2000, Landisman et al., 2002). As previously discussed, in *C. borealis* the AB neuron, the two PD neurons and the two lateral pyloric gastric neurons (LPG) are strongly electrically coupled (Weimann et al., 1991). Weak electrical coupling exists between pairs of neurons that fire in phase: the LP neuron and the IC neuron, as well as the PY

neuron and the VD neuron. All these electrical synapses are bidirectional, which allows for fast, synchronous communication between neurons (Marder, 1984, Marder and Eisen, 1984a). However, the electrical synapse between the LP and the PY neuron is rectifying (Mamiya et al., 2003).

Neurons that form chemical synapses may possess an electrical component as well (Mamiya et al., 2003, Smith and Pereda, 2003, Pereda, 2014). In the pyloric network, some synapses between neurons possess both an electrical and a chemical component. One such mixed synapse exists between the LP neuron and PY neuron, which are reciprocally chemically inhibited and possess an electrical synapse. During the ongoing rhythm, the two components of the synapse have opposing effects. During the LP neuron burst, the electrical component promotes activity of the PY neurons, while the chemical component acts to suppress it (Mamiya et al., 2003). The mixed synapse between LP and PY has been shown to be partly responsible for phase constancy (Mamiya et al., 2003).

1.10 Neuromodulation of the Pyloric Network

Neuromodulation has been studied in many oscillatory networks including, CPG networks, such as those involved in locomotion, breathing and feeding (Elliott and Vehovszky, 2000, Doi and Ramirez, 2008, Miles and Sillar, 2011). The pyloric neurons and their synapses are targets for neuromodulation. In order for rhythmic activity to be generated these neuromodulators are required; blocking

neuromodulator release either by severing the *stn* or blocking action potential generation along it eliminates rhythmic activity of the network.

Neuromodulators reach the STG in different ways: neurally, via release from the terminals of projection neurons or sensory neurons, and hormonally, via the bloodstream (Nusbaum and Beenhakker, 2002, Dickinson, 2006). The STG is ideally located to be a target of neurohormones because of its location within the ophthalmic artery. The STG is innervated by a large number of neuromodulatory projection neurons through the stomatogastric nerve (Stein, 2009). Several modulatory projection neurons have been identified by their physiological properties (Coleman and Nusbaum, 1994, Norris et al., 1994, 1996). They release a multitude of peptides, amines and classical neurotransmitters, and often a single projection neuron releases multiple modulatory neurotransmitters. The determination of the transmitters used by the projection neurons has been examined using either immunocytochemical methods or, more recently, the use of mass spectroscopy (Blitz et al., 1999, Swensen et al., 2000, Billimoria et al., 2005).

One well studied modulatory projection neuron is the Modulatory commissural neuron 1 (MCN1) that projects from the CoG onto the STG. MCN1 releases three identified neurotransmitters: *Cancer borealis* tachykinin-related peptide Ia (CabTRP Ia), γ-amintobutyric acid (GABA) and the peptide proctolin (Coleman et al., 1995, Blitz et al., 1999, Swensen et al., 2000). MCN1 uses CabTRP Ia and GABA to influence the gastric mill network (Wood et al., 2000). In contrast, proctolin and CabTRP Ia target neurons and synapses within the

pyloric network (Wood et al., 2000). CabTRP Ia causes an increase in the mean frequency of the pyloric network. Bath applied GABA, has been found to have both excitatory and inhibitory effects on pyloric neurons (Swensen et al., 2000). While bath applied GABA shuts down the activity of the pyloric network, it has differential effects on the LP and PD neuron. GABA depolarizes the LP neuron causing it to tonically fire while the pyloric network is not active, yet inhibits the PD neuron. The peptide proctolin increases the frequency of the pyloric network when it is below 1Hz. Bath applied proctolin has been found to enhance the graded component of the LP to PD synapse (Zhao et al., 2011). Additionally, in the presence of proctolin the LP to PD synapse can switch from a depressing synapse to a facilitating synapse (Zhao et al., 2011). The actions of MCN1 are gated by feedback from the pyloric network via fast inhibitory action of the ascending AB neuron axon (Wood et al., 2004).

Tonic activity of the modulatory projection neurons can initiate or alter the rhythmic outputs of CPGs. However, there is evidence that projection neurons exhibit rhythmic activity due to feedback from their target CPG networks (Coleman and Nusbaum, 1994). It is unclear what the rhythmic activity of projection neurons means for its modulatory actions. Output from MCN1 is controlled by the lateral gastric (LG) neuron which synapses onto the terminals of MCN1 within the STG and inhibits neurotransmitter release from MCN1 during LG neuron firing (Coleman et al., 1995, Nadim et al., 1998). As a result, a decay of the neurotransmitters released by MCN1 onto the gastric and pyloric networks is seen when LG is active (Coleman et al., 1995, Nadim et al.,

1998).   The decay of modulatory action is important in the transition of the gastric mill cycle from the protraction phase to the retraction phase (Coleman et al., 1995). LG is in turn inhibited by Int1, thus allowing MCN1 to release its neurotransmitters in a rhythmic fashion. When MCN1 is spontaneously active, its activity pattern is regulated through synaptic input from the AB neuron of the pyloric network (Coleman and Nusbaum, 1994, Wood et al., 2004). Subsequently, pyloric regulation of the gastric mill rhythmic is not necessary when MCN1 is spontaneously active (Wood et al., 2004).

Often, the actions of endogenously released neuromodulators can be mimicked through bath application. Zhao et al., 2011, found that proctolin can alter synaptic dynamics by shifting the direction of short-term plasticity in this synapse from depression to facilitation under certain conditions. Golowasch and Marder (1992) identified a voltage dependent inward current which is induced by proctolin, which was later to be found also elicited by other modulators such as CCAP and other neuropeptides as well as the muscarinic agonist pilocarpine (Swensen and Marder, 2000), and is now referred to as modulator activated inward current, I_{MI}. Bath application of amines, such as dopamine, excite both the LP and PY neuron and causes activity to be phase advanced (Harris-Warrick et al., 1995a, Harris-Warrick et al., 1995b). However, bath application is clearly not a perfect emulator of natural release (Wood and Nusbaum, 2002, Stein, 2009).

Neuromodulators also play an integral role in regulating additional intrinsic properties of the individual pyloric neurons.   In the lobster *P.*

interruptus, dopamine increases I_h in the LP, AB, PY and VD neurons and can alter phase of these cells as well (Kloppenburg et al., 1999, Harris-Warrick and Johnson, 2010). Dopamine also modulates the I_A current in pyloric network neurons (Kloppenburg et al., 1999, Zhang et al., 2010). In the LP neuron and PY neuron, dopamine decreases I_A, which lead to a phase advance and excitation. Similarly to dopamine, octopamine also decreases I_A in the AB neuron (Peck et al., 2001).

The release of different neuromodulators from projection neurons onto the pyloric network has provided an opportunity to study both convergence and divergence. Convergence is defined as different neuromodulators that activate the same target, while divergence is defined as one neuromodulator that may influence different target neurons. Specifically, Swensen & Marder (2000) found that peptides such as CCAP and proctolin and others, activate the same current (I_{MI}) (converge) in individual neurons while and activate different subsets of pyloric neurons. Some of these convergent neuromodulators can be co-localized in the same projection neurons (Nusbaum et al., 2001). This allows for one neuromodulator to target multiple neurons and synapses at once.

Convergence and divergence through neuromodulators allows for reconfiguration of network output without altering the hard-wire properties of the pyloric network. Neurons that are components of one network may be able to switch to another network under certain circumstances. For instance, MCN1 and MCN7 can activate different patterns of the gastric mill network, which can in turn have different effects on the timing of the pyloric neuron activity (Blitz et

27

al., 1999). Weimann et al, (1991) found that different neurons can switch between the gastric and pyloric networks, and proposed that these neurons can exist in a 'gastropyloric pool', from which different neuromodulatory inputs can select these cells to either the pyloric or the gastric mill network (Weimann et al., 1991).

1.11 Resonance in Pyloric Neurons

Neurons and synapses often show a maximal response at a preferred input frequency. This preferred or resonance frequency may be important in shaping network activity. Resonance has been implicated with low-amplitude oscillations (Llinas, 1988), and in the generation of action potentials (Engel et al., 2008). Both the neurons and the synapses of the pyloric network demonstrate preferred frequencies (Tohidi and Nadim, 2009, Tseng et al., 2014).

The AB, PD, and LP neurons each possess their own preferred frequency when driven with a sweeping-frequency sinusoidal (ZAP) function, which allows for the sampling of a variety of frequencies over time (Tohidi and Nadim, 2009, Tseng et al., 2014). Both the PD and the AB neuron resonance frequency fall within the range of the pyloric network frequency. The underlying mechanisms for the generation of the resonance frequency include I_h and I_{Ca} (Tohidi and Nadim, 2009); altering either of these causes a change in the PD neuron resonance frequency. The resonance frequency of the follower LP neuron is higher than that of the PD neuron and of the network oscillation frequency and may be due to differences in the underlying ionic currents. One

of the currents implicated in determining these resonance frequencies is I_h (Tohidi and Nadim, 2009). When I_h was added artificially using dynamic clamp, the resonance frequency could be shifted along with the suprathreshold bursting frequency (Tohidi and Nadim, 2009). This suggests that the resonance frequency of the pacemaker neurons can be correlated to the oscillation frequency of the pyloric network.

Pyloric synapses also possess their own preferred frequency. The reciprocal synapses between the PD and LP neurons, show a preferred frequency, but at a lower frequency than the intrinsic preferred frequency of the neurons of the pyloric network (Tseng et al., 2014). Additionally, the preferred frequency of the LP to the PD synapse is correlated with the presynaptic neuron's preferred frequency.

1.12 Questions Addressed in this Thesis

In this thesis, we use the pyloric network of the crab *C. borealis* to understand how stable network output in the form of phase maintenance is generated. We hypothesize that phase constancy is an inherent property of the individual neurons. The full extent to which these properties lead to stability is not known. We characterize the different components of the pyloric network: intrinsic, synaptic, and neuromodulatory properties in order to understand how stability of the pyloric network is generated and maintained. We hypothesize that the stability of an oscillatory network arises from the individual neurons.

This thesis will address four major questions. In the third chapter we identify frequency-dependent properties of the individual pyloric neurons. We characterize the frequency-dependent activity profiles of the individual neurons, to understand how the properties of individual neurons can lead to stable network output. This is accomplished by voltage clamping the pyloric neurons (except AB) using a sweeping-frequency sinusoidal input. The activity profile is defined as the following parameters: burst onset, burst end, resonance frequency and intraburst spike frequency. The fourth chapter explores the ionic current contribution to the frequency-dependent properties of the pyloric neurons. We examine how the different ionic currents can influence frequency-dependent properties of the pyloric neurons. We use the PD neuron, LP neuron and the PY neuron for this study. The fifth chapter explores the role of short-term synaptic plasticity in phase constancy. We generate different levels sets for conductance and input phase to understand how the pacemaker ensemble may alter network dynamics through changing synaptic properties. We use the LP neuron and dynamic clamp to answer this question. The sixth chapter looks to understand how the follower LP neuron to PD neuron synapse influences the pyloric network cycle period. We alter the synaptic properties from the LP to PD synapse on pyloric cycle period.

Additionally, this thesis will address two minor questions. First, we examine if PD makes a functional synapse onto the follower pyloric neurons in the crab *C. borealis.* The AB/PD neurons comprise the pacemaker ensemble which synapses onto the follower neurons. However, the role of each neuron

has only been studied in *P. interruptus* (Eisen and Marder, 1982). The second minor question explores how endogenously released neuromodulators change the network frequency and properties. We also examine the importance of the LP neuron to PD neuron synapse during neuromodulation. We stimulate MCN1 to understand the properties of the network with and without the presence of this synapse.

CHAPTER 2

GENERAL METHODS

Adult male crabs (*Cancer borealis*) were acquired from local distributors and maintained in aquaria filled with chilled artificial saline until use. Crabs were prepared for dissection by placing them on ice for thirty minutes. The dissection was performed using standard protocols as described previously (Tohidi and Nadim, 2009, Tseng and Nadim, 2010). The STNS including the four ganglia (esophageal ganglion, (2) commissural ganglia and the STG, the connecting nerves and motor nerves were dissected from the crab stomach and pinned to a saline filled, 100 mm Sylgard (Dow-Corning) lined Petri dish. The STG was then desheathed, exposing the somata of the neurons for intracellular impalement. Preparations were superfused with chilled (10-13°C) physiological *Cancer* saline comprised of: 11 mM KCl, 440 mM NaCl, 13 mM CaCl$_2$ · 2H$_2$O, 26 mM MgCl$_2$ · 6H$_2$O, 11.2 mM Trizma base, 5.1 mM maleic acid with a pH of 7.4.

Intracellular glass microelectrodes were prepared using the Flaming-Brown micropipette puller (P97; Sutter Instruments) and filled with 0.6 M K$_2$SO$_4$ and 20 mM KCl. Individual pyloric neurons were impaled and identified via their activity patterns, axonal projections in recorded motor nerves and interactions with other neurons within the network (Selverston et al., 1976, Weimann et al., 1991). Current injections were performed using microelectrodes with a resistance of 16-22 MΩ; for membrane potential measurements

32

microelectrodes with a resistance of 25-30 MΩ were used. Intracellular recordings were performed using Axoclamp 2B and 900A amplifiers (Molecular Devices) and extracellular recordings were performed using a differential AC amplifier model 1700 (A-M Systems).

CHAPTER 3

ACTIVITY PROFILES OF PYLORIC NEURONS

In this chapter, we test the hypothesis that phase maintenance in an oscillatory network is due to the intrinsic properties of isolated individual neurons. We explored frequency-dependent properties of isolated pyloric neurons to understand whether isolated neurons were sufficient in maintaining phase across different input frequencies.

3.1 Introduction

To produce meaningful behavior, oscillatory networks may require the relative activity phase of their component neurons to remain relatively constant, despite variations in the oscillation frequency. For example, the lamprey swim involves a single sinusoidal wavelength in the body, independent of the undulation frequency. The neural circuits that are located in the 100 segments of the spinal cord, fire with a one percent phase lag with respect to each other, whether the swimming oscillation is fast or slow (Grillner, 1974, Matsushima and Grillner, 1992). In many central pattern generating networks, the relative activity phase of the individual neurons in the network is maintained over these different frequencies (Bucher et al., 2005, Mullins et al., 2011).

Despite stability in phase of activity in a network, variability in conductance and ionic current levels exist. However, measurements of ionic currents in the same neuron type across animals of a given species show

variability in the conductance levels (Golowasch et al., 1992, Schulz et al., 2006). It is unclear how the varying levels of ionic currents in individual neurons can result in stable activity phases at the network level. To address this question requires a system that produces stable oscillations across a range of frequencies and allows for the comparison of multiple identified neuron types that maintain their activity phase. In this chapter we examine whether network stability in the form of phase constancy can result from the stable response of the isolated individual neurons at different sinusoidal input frequencies. We explored frequency-dependent properties of isolated pyloric neurons of the crab to understand whether isolated neurons were sufficient in maintaining phase across different input frequencies. If the synaptically-isolated neuron was able to maintain the same burst onset phase across frequencies, then stability of the network could be an inherent property of the neurons.

Given that phase is influenced by both intrinsic voltage-gated ion channels and synaptic input, there are two possible mechanisms for phase constancy: that the interplay of the voltage-gated ionic currents neuron would result in constant activity phase in response to a stable synaptic input, or that the properties of voltage-gated ionic currents in the neuron are matched to the dynamics of the synaptic inputs to that neuron to maintain activity phase. The former mechanism predicts that, if a neuron is isolated, the interactions between intrinsic voltage-gated ionic currents results in a stable activity phase when the neuron is driven by a prescribed input. This is the hypothesis that we test in this chapter.

To characterize the properties of individual neurons across different frequencies, we use sweeping-frequency sinusoidal inputs and characterize the frequency-dependent activity of individual neurons within the pyloric network. We characterize the response of an isolated neuron to inputs imposed at different frequencies using these parameters: burst onset, burst end, intraburst spike frequency and resonance frequency. We build a frequency-dependent activity profile for each neuron based on these parameters to determine its response to inputs of different frequencies. Characterization of the activity profiles is a novel method with which to examine frequency-dependent properties of an individual neuron and to show that the stability at the network level may arise from the properties of the individual neurons. The unique profile of each neuron type in isolation may potentially contribute to the stability of the intact network as a whole.

3.2 Materials and Methods

3.2.1 Determining Activity Profiles

In order to determine the activity profiles of pyloric neurons, individual pyloric neurons were identified and the preparation was decentralized, thereby removing all modulatory inputs, by severing the descending nerve *stn* (Luther et al., 2003). Individual neurons were then isolated from the network using 10^{-5} M picrotoxin (PTX) perfused for thirty minutes to block the chemical synapses (Appendix A). All experiments were conducted using two-electrode voltage clamp (TEVC), where one electrode is used for injecting current and the other

for monitoring membrane voltage. The pyloric neurons are unipolar and the axon originates from the end of the primary neurite and is distal from the somatic voltage clamp electrode. As a result, action potentials escape the somatic voltage clamp due to a lack of space clamp. We used this effect to our advantage and recorded the occurrence of action potentials in the voltage clamp current traces as described below.

In order to characterize the frequency-dependent profile, each neuron was voltage clamped with a sweeping-frequency sinusoidal (ZAP) function. The ZAP function was calculated as:

$$ZAP(t) = A\sin(2\pi f(t)) \text{ where } f(t) = F_{min}t\left(\frac{F_{max}}{F_{min}}\right)^{t/T} \qquad (2.1)$$

where A is equal to the amplitude of the injected sine wave oscillation and the frequency $f(t)$ sweeps values between F_{min} and F_{max} over a total duration of T. The ZAP function was applied for a course of $T = 100$ seconds with $F_{min}=0.1$ and $F_{max}=4.0$ Hz. In order to prevent transients, the ZAP function was preceded with 3 sinusoidal cycles applied at the minimum frequency $F_{min}=0.1$ Hz which smoothly transitioned into the ZAP function. With the addition of the three pre-cycles, the total duration of the applied waveform was 130 seconds. The first sinusoidal cycle was phase shifted by 270° in order to begin the first sine wave at its minimum. The ZAP function will henceforth refer to both the three pre-cycles and the 100-second sweeping-frequency waveform. In all experiments, the pyloric neuron tested was voltage clamped at a holding potential of -60mV and driven with a ZAP function spanning a voltage range of -60mV to -30mV.

The activity profile here is defined as the set of measureable attributes that characterize the response of an isolated neuron to inputs imposed at different frequencies.   We compared the six different pyloric neuron types: pyloric dilator (PD), lateral posterior gastric (LPG), lateral pyloric (LP), pyloric constrictor (PY), inferior cardiac (IC) and ventricular dilator (VD). In this study, We did not characterize the activity profile of the anterior burster (AB) neuron. We have excluded the AB neuron for the following reasons: (1) The AB neuron is difficult to find in many preparations, (2) it is impossible to do somatic recordings of the action potentials generated by the AB neuron; in fact, the small deflections resembling action potentials in somatic recordings are possibly reflections of action potentials generated in the electrically coupled PD neurons.

In order to build the activity profile, we measured a set of parameters that would allow me to compare the different pyloric neuron types. The activity profile was generated using scripts written in Matlab (MathWorks) and consisted of four parameters: the burst onset and end phases, the intraburst spike frequency and the membrane potential resonance frequency.

To measure the activity profile of each neuron type, the neuron was driven with the ZAP function in voltage clamp as described above (example shown for the LP neuron in Figure 3.1A). The action potentials generated in each cycle were recorded from the voltage clamp current trace and the current trace was band-pass (low cutoff 5-10 Hz; high cutoff 100-200 Hz) filtered in Matlab in order to extract the action potential times in the current trace

recording (Figure 3.1A-B). The injected ZAP waveform was divided into individual cycles with the time reference point in each cycle defined as the minimum of each sine wave and used to measure the input frequency and the phase of each spike in the cycle in the filtered current trace. We created an activity phase diagram which plotted the phase of each spike (spike time with respect to the ZAP cycle minimum multiplied by the input frequency) at all input frequencies, and then binned the data at 0.04 phase bins in order to plot the data points and facilitate analysis. In order to examine statistical significance, we then further binned the data into 8 phase bins of 0.5 Hz each. The first and last spike of the burst in each cycle were extracted for determining the phase of the burst onset and burst end.

3.2.2 Determining the Resonance Frequency

The impedance profile of each neuron was generated using a Matlab script (Tseng and Nadim, 2010). We will refer to the amplitude of the impedance profile as $Z(f)$. For each cycle, this was calculated by measuring the frequency and amplitude changes in both current and voltage. Impedance was measured as a ratio of the Fourier transforms of voltage and current (Hutcheon and Yarom, 2000). We define the preferred frequency, or resonance frequency as the frequency at which the impedance power $|Z(f)|$ was at its maximum.

3.2.3 Software

Data were acquired using both Pclamp 9.0+ (Molecular Devices) as well as Scope to record and stimulate each neuron. The software Readscope and Scope were developed and maintained by the Nadim lab and can be downloaded at http://stg.rutgers.edu/. All data were sampled at 5 kHz and saved on a PC using a Digidata 1332A (Molecular Devices) and a PCI-6070-E data acquisition board (National Instruments).

3.2.4 Statistical Analysis

Statistical analysis was performed using Sigmaplot 12.0 (Systat). Significance was evaluated at an α value of 0.05, error bars shows and error values reported denote standard error of the mean.

3.3 RESULTS

3.3.1 The Phase of the Burst Onset and End as a Function of Input Frequency is Distinct for Each Pyloric Neuron Type

We examined the phase of the burst onset and burst end for each isolated pyloric neuron type as a function of the frequency of the sinusoidal input. Each neuron type showed a distinct burst onset and burst end at different input frequencies (Figure 3.2A).

The burst onset phase of all six different pyloric neuron types was frequency-dependent and increased (phase delayed) as a function of the sinusoidal input frequency (Figure 3.2A; Two-Way ANOVA; $p < 0.001$).
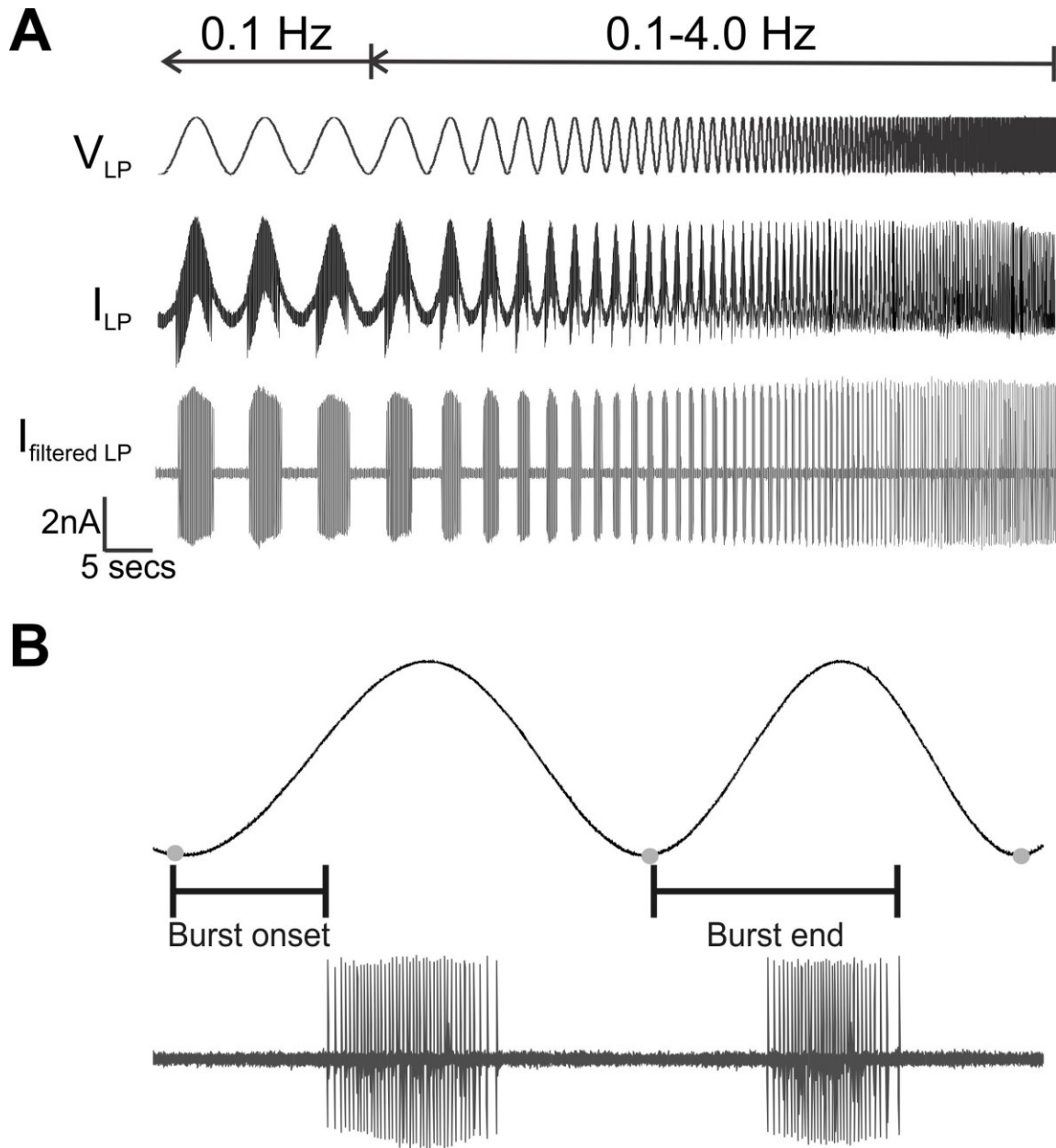
Figure 3.1 Using the ZAP function to examine different frequency-dependent parameters in the crab pyloric network neurons. **A.** Recording from a two-electrode voltage clamped LP neuron. The neuron is driven between -60 and -30 mV using a sinusoidal function from 0.1 to 4.0 Hz over a time period of 100 seconds. The pre-cycles are used at 0.1 Hz to remove transients before using the ZAP function, for a total of 130 seconds. The top trace is the voltage, the middle is the current trace and the bottom trace is the filtered trace (High-pass Filter, 50Hz) **B.** Two cycles of the ZAP function. Two of the parameters we were interested in were the burst onset and burst end, and are measured with respect to the minima of each cycle. The phase of each spike is then measured in comparison to this.

Additionally, the six neuron types were statistically distinct in their burst onset as a function of frequency (Figure 3.2A, 3.2B; Two-Way ANOVA with *post hoc* Holm Sidak test p < 0.001). In response to identical inputs, the LP neuron's burst onset was found to be earlier than the other pyloric neurons. Additionally, the LP neuron showed the greatest variability in burst onset at each frequency, when compared to the other five pyloric neurons (Table 3.1). This was determined by calculating the coefficient of variation (CV=δ(standard deviation/μ (mean)) for the burst onset of each neuron using the binned data.

Table 3.1 Coefficient of Variance (CV) for each of the Six Pyloric Neuron Types

Cell/Freq (Hz)	0-0.5	0.5-1	1-1.5	1.5-2	2-2.5	2.5-3	3-3.5	3.5-4
PD N=42	0.136	0.118	0.108	0.098	0.095	0.101	0.097	0.097
LPG N=13	0.094	0.093	0.090	0.090	0.088	0.096	0.090	0.090
IC N=11	0.082	0.074	0.071	0.073	0.075	0.083	0.086	0.088
LP N=24	0.182	0.145	0.131	0.123	0.115	0.112	0.111	0.109
VD N=6	0.077	0.081	0.075	0.066	0.063	0.058	0.058	0.065
PY N=15	0.099	0.080	0.075	0.075	0.080	0.086	0.100	0.113

CV is calculated using δ(standard deviation/μ (mean)).

When the data were shuffled across different neuron types (by choosing the same number for six different neuron groups categorized regardless of cell identity), the statistical distinction among the neurons disappeared, indicating that the distinction between the burst onset phase for the pyloric neuron types

was not due to chance. The data for the burst onset phase of all six neuron

types in different input frequency bins is summarized in Table 3.2.

Table 3.2 Phase of Burst Onset of each Pyloric Neuron Type at Different Input
Frequencies

Cell/Freq (Hz)	0-0.5	0.5-1	1-1.5	1.5-2	2-2.5	2.5-3	3-3.5	3.5-4
PD N=42	0.29 ± 0.039	0.31 ± 0.037	0.34 ± 0.036	0.36 ± 0.035	0.37 ± 0.036	0.39 ± 0.039	0.40 ± 0.039	0.41 ± 0.039
LPG N=13	0.31 ± 0.029	0.34 ± 0.031	0.36 ± 0.032	0.38 ± 0.034	0.39 ± 0.034	0.40 ± 0.039	0.41 ± 0.037	0.43 ± 0.038
IC N=11	0.29 ± 0.024	0.32 ± 0.024	0.35 ± 0.025	0.37 ± 0.027	0.39 ± 0.029	0.40 ± 0.033	0.40 ± 0.033	0.42 ± 0.036
LP N=24	0.26 ± 0.048	0.29 ± 0.042	0.31 ± 0.041	0.33 ± 0.040	0.34 ± 0.039	0.34 ± 0.039	0.35 ± 0.039	0.37 ± 0.041
VD N=6	0.31 ± 0.024	0.34 ± 0.027	0.36 ± 0.027	0.39 ± 0.025	0.40 ± 0.025	0.41 ± 0.024	0.42 ± 0.024	0.43 ± 0.028
PY N=15	0.30 ± 0.030	0.34 ± 0.027	0.37± 0.028	0.40 ± 0.030	0.41 ± 0.033	0.43± 0.037	0.45± 0.045	0.46 ± 0.052

The phase of the burst onset of all six pyloric neurons are shown for the 8 bins.
The mean phase and standard error are denoted.

The six different pyloric neuron types also showed different burst end

phases as a function of the sinusoidal input frequency: the phase of the burst

end consistently decreased with increasing input frequency up to the input

frequency of 2.5 Hz (Figure 3.2A, C; Two-Way ANOVA p < 0.001). However, at

frequencies above 2.5 Hz, the burst end phase of the neurons remained

statistically indistinguishable.

As with the burst onset phase, the burst end phase (as a function of the

sinusoidal input frequency) was also distinct for the six neuron types (Figure

3.2C; Two-Way ANOVA p < 0.001). And, as with the burst onset phase, when

the data were shuffled across different neuron types (by choosing the same

number for six different neuron groups categorized regardless of cell identity),
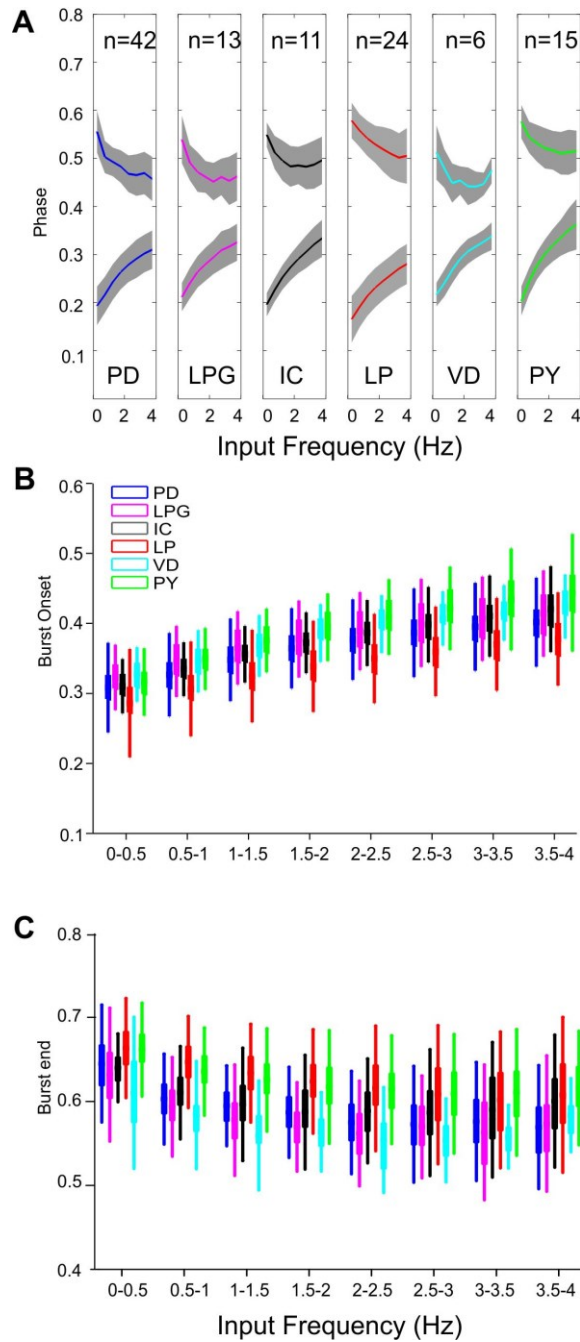
Figure 3.2 The pyloric neurons tested each had their own burst onset and burst end. **A.** Comparison of each neuron with respect to both the onset and the end of each burst across different frequencies. When comparing all neurons across all frequencies we see that each neuron's burst onset and offset is statistically different (Colored lines represent means, grey shading confidence intervals). **B.** Burst onset as a function of frequency for each neuron, binned at 0.5 Hz. **C.** Burst end as a function of frequency for each neuron, binned at 0.5 Hz.

the statistical distinction among the neurons disappeared, indicating that the distinction between the burst onset phase for the pyloric neuron types was not due to chance. The data for the burst end phase of all six neuron types in different input frequency bins is summarized in Table 3.3.

Table 3.3 Phase of Burst End of the Pyloric Neuron Type at Different Input Frequencies

Cell/Freq (Hz)	0-0.5	0.5-1	1-1.5	1.5-2	2-2.5	2.5-3	3-3.5	3.5-4
PD N=42	0.65 ± 0.043	0.60 ± 0.036	0.59 ± 0.031	0.58 ± 0.035	0.56 ± 0.038	0.56 ± 0.041	0.57 ± 0.044	0.55 ± 0.045
LPG N=13	0.63 ± 0.049	0.59 ± 0.036	0.57 ± 0.041	0.56 ± 0.032	0.55 ± 0.038	0.56 ± 0.037	0.55 ± 0.050	0.56 ± 0.050
IC N=11	0.64 ± 0.025	0.61 ± 0.034	0.59 ± 0.041	0.57 ± 0.042	0.58 ± 0.038	0.58 ± 0.046	0.59 ± 0.049	0.59 ± 0.048
LP N=24	0.67 ± 0.036	0.65 ± 0.034	0.64 ± 0.036	0.62 ± 0.038	0.61 ± 0.046	0.60 ± 0.051	0.60 ± 0.053	0.60 ± 0.058
VD N=6	0.61 ± 0.055	0.57 ± 0.03	0.54 ± 0.040	0.55 ± 0.030	0.54 ± 0.038	0.54 ± 0.030	0.54± 0.023	0.57 ± 0.027
PY N=15	0.67 ± 0.034	0.64 ± 0.032	0.63 ± 0.038	0.62 ± 0.041	0.61 ± 0.040	0.61 ± 0.040	0.61 ± 0.044	0.61 ± 0.046

The phase of the burst end of all six pyloric neurons is shown for binned data. The data was binned into 0.5 Hz bins in order to facilitate analysis. The mean phase and standard error are denoted.

3.3.2 Intraburst Spike Frequency Varies Amongst Different Neurons

Previous work in the pyloric network has suggested that different pyloric neurons express characteristic cell-specific intra-burst spike frequencies (Szucs et al., 2003). The intra-burst spike frequency of the PD neuron, for example, was found to be regulated by the inhibition it receives from the LP neuron in the intact network (Szucs et al., 2003). The intra-burst spike frequency of the
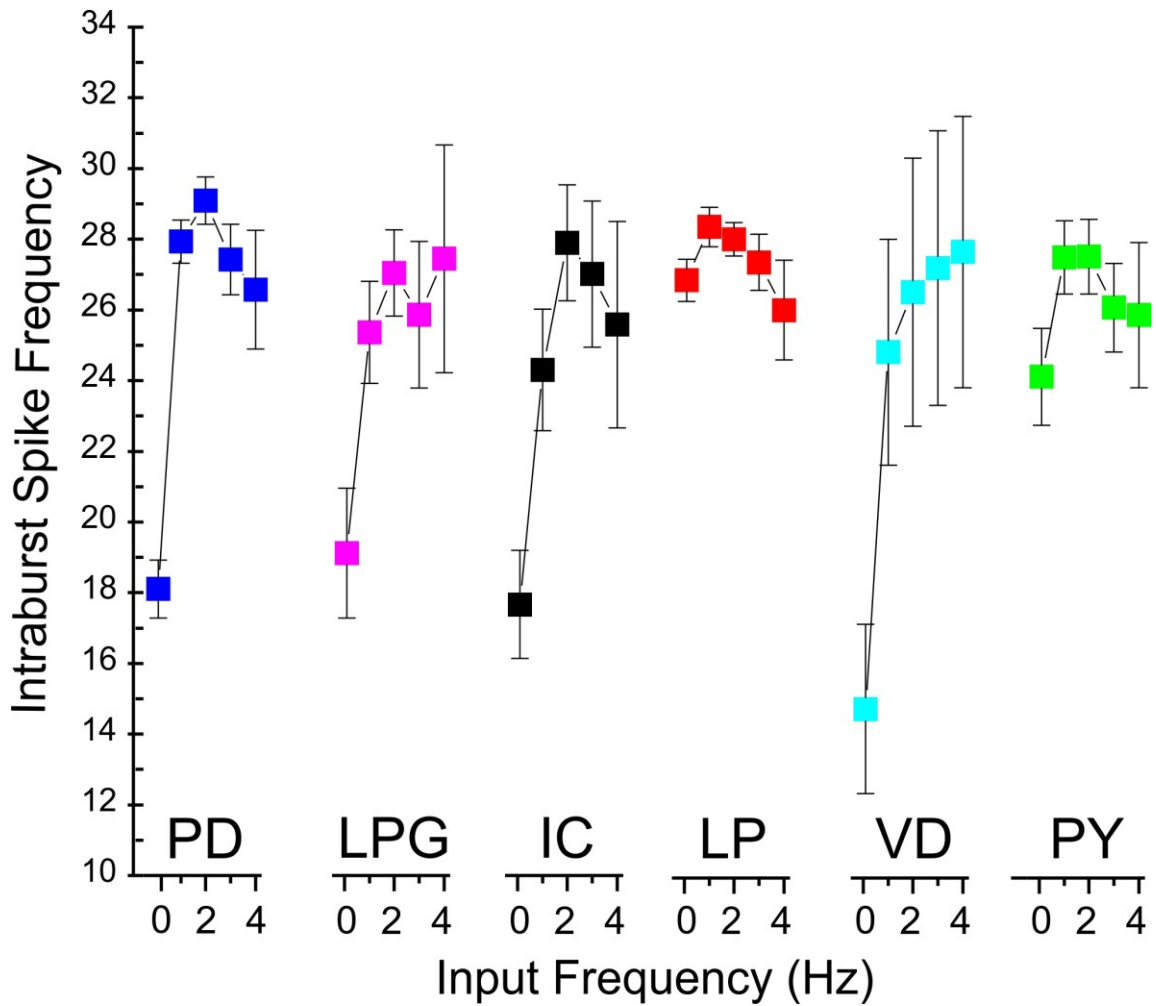
Figure 3.3 Comparison of the intraburst frequencies of the different pyloric neurons. When comparing the six pyloric neurons, the different neurons each possess very different IBSF below a frequency of 1 Hz. LP notably had the largest intraburst spike frequency below 1 Hz of all of the neurons tested. Mean and standard error are shown for each frequency and each neuron.

pyloric neurons is also important for their influence on the muscles that control the movements of the pylorus (Morris and Hooper, 1997).

We examined how the intra-burst spike frequency of different isolated pyloric neuron types varied as a function of sinusoidal input frequency. We` calculated this attribute in bins of 0.5 Hz input frequency (0-0.5 Hz, 0.5-1 Hz, etc.) using the data obtained through the ZAP function. We found that each pyloric neuron type had a distinct intra-burst frequency at input frequencies below 1 Hz. However, at input frequencies above 1 Hz, there was no difference among the different neuron types (Two-way ANOVA, $p < 0.115$). The LP neuron's intra-burst spike frequency was higher than those of the other pyloric neurons at input frequencies below 0.5 Hz (Figure 3.3; Two-Way ANOVA with *post hoc Holm-Sidak method*, $p < 0.001$). When the data were scrambled as previously described (see section 3.2.1 burst onset) across neuron types, the statistical distinction among the neurons disappeared, demonstrating that the distinct intra-burst spike frequency of each pyloric neuron type was not due to chance.

3.3.4 Membrane Potential Resonance Frequency

Previous studies examining the membrane potential resonance of pyloric neurons focused on subthreshold membrane potential resonance and were therefore performed in TTX to block spiking activity (Tohidi and Nadim, 2009, Tseng and Nadim, 2010). Our current study did not block voltage-gated sodium channels but did block synaptic inputs among the neurons. We were interested
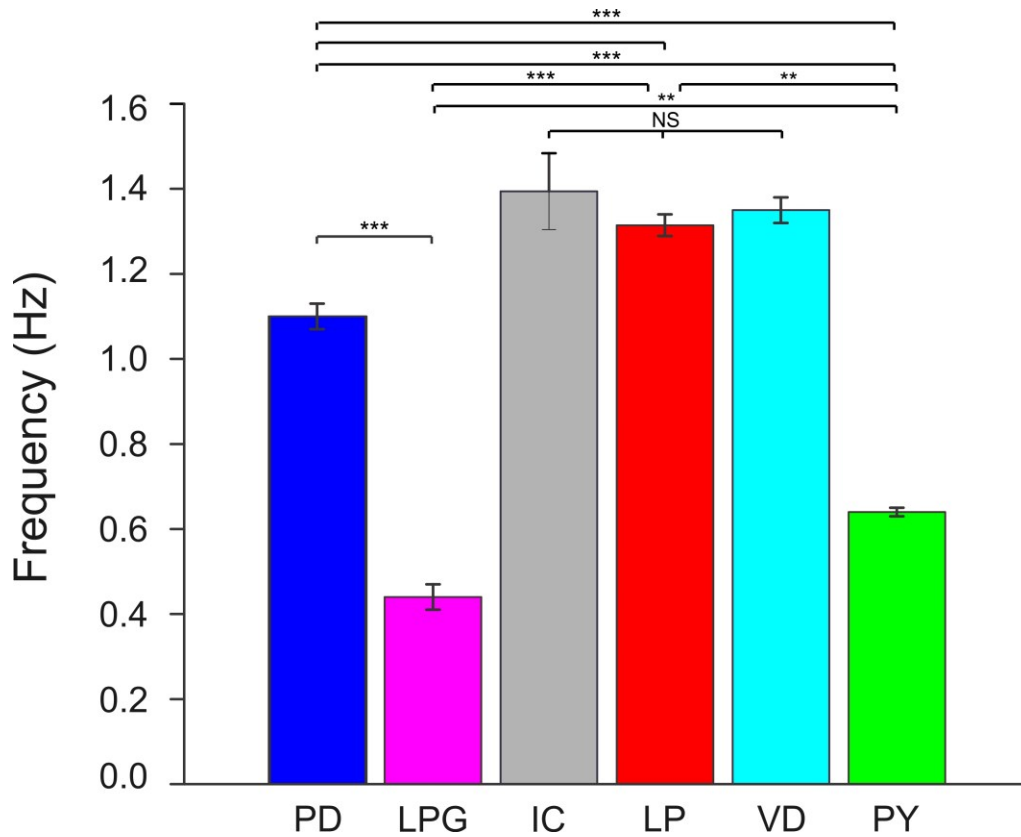
Figure 3.4 Each of the pyloric neurons possesses their own resonance frequency. Each neuron type had a characteristic resonance frequency we determined resonance frequency by low pass filtering the output of our ZAP function to remove spikes. We compared the frequency of each of the different neurons and found that each neuron possesses. However, the IC, LP and VD resonance frequencies are not unique. While the PD, LPG and PY possess unique resonance frequencies. (NS=non-significant, *p<0.05, **p<0.01, ***p<0.001)

in determining if the pyloric neurons possessed distinct resonance frequencies. We determined the resonance frequency for each of the six pyloric neurons and found that they were statistically different ($p < 0.001$; Figure 3.4). Pairwise comparisons, did not show the same level of significance (Table 3.3). LPG had the lowest resonance frequency at 0.44 ± 0.03 Hz, while IC had the highest at 1.39 ± 0.09 Hz. PD and PY also had distinct resonance frequency, while the IC neuron, the LP neuron and the VD neuron did not (Table 3.3).

Table 3.3 Resonance Frequencies of Pyloric Network Neurons

Cell	F_{res} (SEM)	PD	LPG	IC	LP	VD	PY
PD (N=7)	1.1 ± 0.03		<0.001	<0.001	0.003	0.002	<0.001
LPG (N=7)	0.44 ± 0.03			<0.001	<0.001	<0.001	0.003
IC (N= 5)	1.39 ± 0.02				**0.492**	**0.783**	<0.001
LP (N=7)	1.31 ± 0.02					**0.623**	<0.001
VD (N=5)	1.35 ± 0.03						<0.001
PY (N=7)	0.64 ± 0.01						

Resonance frequencies for each of the 6 neurons are shown. The F_{res} mean and standard error are shown, in addition to pairwise comparisons to the p values.

3.3.5 Do Neurons that Have Similar Burst Phase in the Intact Network also Possess Similar Frequency-Dependent Burst Onsets when Driven in Isolation?

Now that we have shown that each neuron possesses its own frequency-dependent activity profile, we were interested in determining if pairs of neurons which usually fire approximately in phase in the intact pyloric network also do so when compared in isolation.

During the ongoing pyloric rhythm, certain neurons in the pyloric network fire approximately in phase with respect to each other. In the intact network, IC

overlaps in phase with but leads LP, and PY overlaps in phase with but slightly leads VD (Figure 3.5). We were interested in knowing if this phenomenon was a frequency dependent property of these neurons and if neurons that fired in phase in the intact network would behave similarly in isolation.

The phase of the burst onset was compared between pairs of neurons that normally fire in phase, by subtracting the phase of the first neuron to that of the second neuron at the same input frequency. Using this method, we examined the frequency-dependent phase characteristics between the follower neurons: PY/VD and IC/LP. We binned the data in bins of 0.5 Hz (input frequency) in order to easily compare the data across frequencies (Figure 3.5). At input frequencies below 2.5 Hz, we found that LP (N=24) and IC (N=11) did not show a significant difference in their phase relationship. However, at frequencies above 2.5 Hz, IC always lagged in phase when compared to LP (One-Way ANOVA; $p < 0.001$). The phase of VD (N=6) and PY (N=15) was not significantly different in phase at all input frequencies examined (One Way ANOVA; $p = 0.154$).

3.4 Discussion

We explored frequency-dependent properties of isolated neurons of the crab pyloric network to understand whether isolated neurons within a network
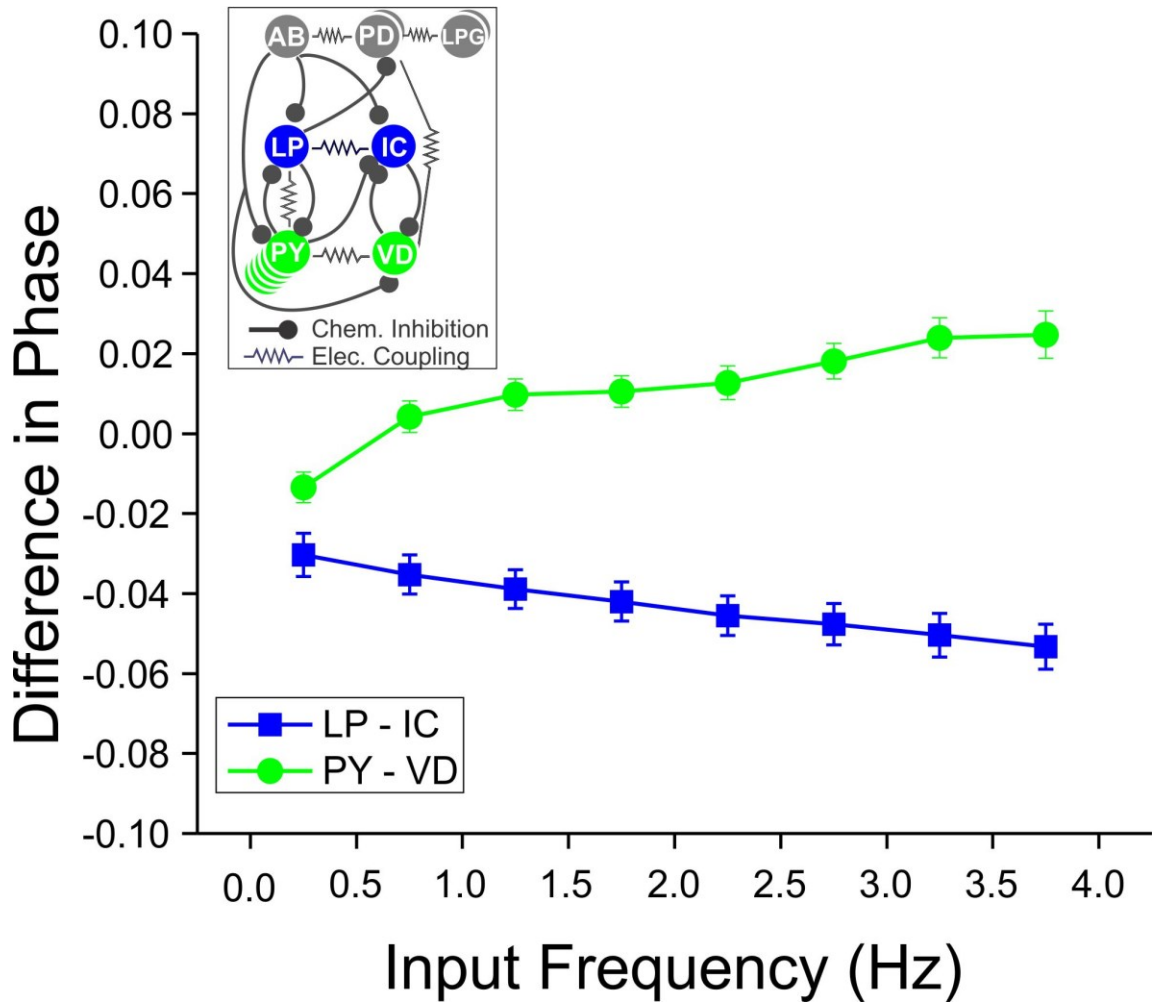
Figure 3.5 The phase difference of LP/IC and PY/VD in the isolated neurons. During the ongoing rhythm, IC leads LP in firing, however, we do not see that same trend here (blue line). The burst onset of the LP neuron occurs earlier in phase than that of the IC neuron, in the isolated neurons. In contrast, during the ongoing rhythm PY leads IC in firing, and that trend continues in the isolated neurons as well (green line).

possess unique activity profiles and, if so, whether these profiles predict the activity properties of these neurons in the intact network. Specifically, we examined whether the properties of the individual neurons are enough to explain phase constancy in the pyloric network. We established that each pyloric neuron type is unique in the parameters we tested: burst onset, burst end, resonance frequency and intra-burst spike frequency.

We also found that, when driven with a sinusoidal input, the LP neuron fired at an earlier phase than the other five pyloric neuron types tested. Additionally, the LP neuron showed the greatest variability in its burst onset across all input frequencies. The variability calculated with the CV in the burst onset of the LP neuron may have important ramifications for interactions within the network. The ability for the LP neuron to vary its burst onset, indicates that it possesses the ability to respond to different inputs with greater flexibility. Because the synapse from the pacemakers can change in response to the LP neuron's synapse, the LP neuron can alter its burst onset and then feedback onto the PD neuron to compensate for any changes.

The pyloric network has been shown to operate at a variety of frequencies (0.5 – 6.0 Hz) and maintain phase constancy between network neurons throughout. Using our current study, we show that there is a link between frequency and the onset/end of a burst. If the synaptically-isolated neuron was able to maintain the same burst onset phase across frequencies, then stability of the network could be an inherent property of the neurons.

However, as frequency is increased, the onset of the burst was phase delayed, while the burst end becomes more phase advanced.

3.4.1 The Effect of Frequency on Spike Timing

Recent studies in the lateral line of larval zebrafish, showed that the afferent neurons could maintain their firing activity for a much longer period of time at lower input frequencies than at higher input frequencies, using sine waves (Levi et al., 2015). This ability to identify differences in frequency may indicate an ability of larval zebrafish to distinguish biologically relevant signals in their environment such as larger predatory fish and smaller conspecifics (Levi et al., 2015). In that way, the neurons may effectively tune their activity dependent on signals received. In our data, we see that the neurons tuned their parameters based on the input frequency.

The pyloric network of *C. borealis* can maintain stable function at frequencies of up to 6Hz (Tang et al., 2010). Despite the higher frequencies, phase of the individual neurons was found to be maintained, when examined both in vivo and in vitro. The robust nature of the pyloric network is inherently a consequence of the intrinsic cellular properties as well as the synaptic connections within the network. The ability for each of these neurons to possess their own burst onset and burst end properties, contributes to the network as a whole to maintain stability. If all of the neurons within the network possess similar properties, then we may argue that the stability of the network arises exclusively due to synaptic interactions. However, the distinct frequency-

dependent properties in each pyloric neuron type demonstrates that the robustness of the network may arise in large part from a mixture of both synaptic and intrinsic properties.

Rabbah and Nadim (2005) showed that when the LP and PY neurons received identical input, both neurons maintained relative phase of activity. Their results suggested that the relative phase of the activity among the follower neurons is dictated solely by their intrinsic properties. We show here that each pyloric neuron possessed frequency-dependent properties that made them unique in their characteristics. Our findings provide support for the predictions of Rabbah and Nadim (2005), showing that the intrinsic properties dictate relative phase among the follower neurons. Additionally, whereas Rabbah and Nadim only examined the relative phase of LP and PY neurons at one frequency, our results indicate that the intrinsic properties of these two neurons contribute to their phase difference at all pyloric frequencies.

Intrinsic membrane properties have been shown to play a role in setting relative phase in the pyloric network. In the pyloric network, two ionic conductances have been found to participate in postinhibitory rebound in the follower neurons: I_A and I_h (Golowasch and Marder, 1992a, Tierney and Harris-Warrick, 1992). I_A delays the onset of the burst and I_h advances burst onset (Tierney and Harris-Warrick, 1992, Harris-Warrick et al., 1995a). I_A is larger in the PY neuron and smaller in the LP neuron, whereas I_h is larger in LP and almost undetectable in the PY neuron. The larger quantity of I_h in the LP neuron may be a reason that the LP burst onset is earlier than compared to the

other follower neurons. When the pacemaker neurons burst, the LP and PY receive inhibition with similar strengths and dynamics as shown in Rabbah and Nadim (2005). The additional I_h allows the LP neuron to escape inhibition first, and the increased I_A in the PY neuron delays the burst onset. As discussed previously, each neuron type demonstrates variability in these ionic currents. However, despite this, the different neuron types are able to maintain phase within the intact network. These intrinsic properties may combine with synaptic currents in order to maintain phase, and there individual current differences may be primarily enough to maintain it.

3.4.2 The Functional Implications of Phase

The maintenance of phase within the pyloric network is important to maintain coherent functional activity However, the importance of phase maintenance is not seen only in this CPG. The well-studied swimming behavior of the lamprey, is due to the fixed phase lags between consecutive segments which ensures that they will swimming is possible at all speeds (Mullins et al., 2011). The results of my study may provide insight into the phase maintenance in lamprey circuits. We show that phase constancy cannot be explained solely on the properties of the individual neurons. This result may be also applicable to understanding the role of individual neurons and synapses in the segments of the lamprey and the phase lags present between consecutive segments. The reticulospinal glutamatergic neurons, become excited and activated the first segment network in the spinal cord. These excite motorneurons (M), excitatory

(E) segmental neurons and inhibitory (I) segmental neurons on the active side. The I neurons cross the midline and inhibit all neurons on the other side , making it inactive and the M neurons contract swimming muscle. The initiation of activity on the side opposite the active side is a result of disinhibition. The lamprey swim CPG is an example of a network, similar to the pyloric network, whose activity is determined through interactions of both synaptic and intrinsic properties. By understanding the role of individual neurons in a network, such as the study we present here, the principles of the system can be applied to larger networks.

Phase, therefore, can be important in maintaining meaningful behavior in an intact animal. However, the question arises, what percentage can neurons be 'off-phase' and still maintain rhythmic circuit dynamics, i.e. how far off phase can these neurons be and still continue to maintain proper timing within the network.   In this study, we see that the difference in phase is small between isolated pair of neurons (LP/IC and VD/PY). We do not know the full effects of the phase maintenance of these pairs of neurons, the question is therefore: does the local in-phase activity of two follower neurons create a subnetwork that promotes phase? The phase difference between the LP and IC neurons, was considered small, but present. However, is this difference large enough to affect system dynamics? The pyloric frequency can increase to 6Hz without 'crashing,' in other words, the frequency can increase while still maintaining the stable triphasic rhythm. The difference that we find in our LP and IC can be explained by understanding the firing order of these neurons. IC leads LP in

firing during the normal ongoing rhythm, which would give us a positive phase difference. However, in the results we see a negative phase difference, because we see that LP's burst onset with our ZAP function occurs before that of IC across all frequencies. In addition to the synapses from the pacemaker, IC and LP receive inhibition from both PY and VD. Perhaps, this inhibition helps to maintain the LP and IC phase difference in the intact network. In the lobster, *Panilirus vulgaris,* the VD to IC synapse can possibly play two roles: (1) during VD neuron bursting it serves to inhibit the IC neuron, (2) because the AB/PD inhibition is relatively weak onto the IC neuron, the VD neuron provides additional inhibition to prevent the IC neuron from firing out of phase (Hooper and Moulins, 1990). Additionally, the LP to PY synapse is believed to be important in controlling the phase of the postsynaptic PY neuron (Mamiya and Nadim, 2005). In another species of lobster, *Panilirus interruptus*, the LP to PY synapse delays bursting in the PY neuron and this delay has been found to increase with increasing cycle period (Mamiya and Nadim, 2005). Even though these mechanisms were described in other species of crustaceans, this can be applied to our study as well. While these synapses may be weak compared to the synapse from the pacemaker ensemble, they act to support the inhibition from the pacemaker ensemble and maintain phase of these pairs of neurons.

3.4.3 Intra-burst Spike Frequency and the Activity Profile

Previous work in the intact network, shows that the intra-burst spike frequency (IBSF), showed that PD, LP and VD each possessed a distinct IBSF (Szucs et

al., 2003). Additionally, manipulations of synaptic currents have been found to also result in characteristic changes in the IBSF of these pyloric neurons (Szucs et al., 2003). Our question was whether these findings also correlated with changes in input frequency, a proxy for the network cycle frequency. As a parameter in the activity profile, we see that, similar to the results of Szucs et al., (2003), our pyloric neurons had different IBSFs. Interestingly, our result that the difference was specifically found at input frequencies below 1Hz, could mean that at higher frequencies, the differences do not make much of an impact. Previous work from Morris and Hooper (1997) in the lobster *Panulirus interruptus*, investigated the relationship of spike frequency and muscle response. Their study showed that IBSF may be a parameter that determines slow muscle output in cells and muscles that comprise the gastric mill network (Morris and Hooper, 1997). This may be a way for other neurons to use IBSF to control muscle contraction amplitude, such as found in their study (Morris and Hooper, 1997). Subsequently, perhaps the stabilization of the IBSF at higher frequencies occurs when synaptic connections are present, as seen in the Szucs et al., (2003) study.

Information about network dynamics can also be expressed through IBSF. One such study on *Callinectes sapidus,* demonstrated that the informational content of IBSPs of the LP neuron appears in the activity of the inferior ventricular nerve (*ivn*), which connects the brain and the STNS, is due the IBSF of the LP neuron. Additionally, the same study claimed that the PD neuron dynamics is in part due to the informational content of the IBSF of the

LP neuron, specifically that in the previous burst (Brochini et al., 2011). The use of the LP neuron IBSF may be a method in which, the information of the state of the network can be transmitted to the PD neuron, so that it may alter its firing pattern in an appropriate matter. This may be a method in which spike patterns of motor neurons can not only transmit information to other networks but can also be a method to control higher levels of motor output.

3.4.4 Preferred Frequency and Active Properties

Previous work from our lab had demonstrated that the neurons that comprise the pyloric pacemaker ensemble (AB/PD) and that the follower LP neuron show membrane potential resonance (Tohidi and Nadim, 2009, Tseng et al., 2014). In the current study, we examined the follower neurons and the PD neurons resonance without blocking voltage gated Na^+ channels.

As previously reported (Tseng et al., 2014), we have also found that the LP neuron possesses a resonance frequency that is different than that of the pacemaker neurons. We have shown that the resonance frequency of the IC, VD and LP neuron are similar. Our expectation was that each neuron has its own resonance frequency, however, this is not the case. The three neurons PD, LP and PY that comprise the triphasic characteristic patterning of the pyloric neuron each possess their own resonance frequencies.

Our belief is that the LP, PY and PD are the three neurons that contribute most greatly to the preferred frequency of the network. Studies have shown that the resonance frequency of network neurons are correlated to the

network oscillation frequency (Lampl and Yarom, 1997, D'Angelo et al., 2001, Tohidi and Nadim, 2009). Additionally, Pike et al., (2000) reported that different neuron types of the hippocampus possess different resonance properties. We have previously shown that the network frequency of the pyloric network, falls between the resonance frequency of the pacemaker and LP neuron (Tseng et al., 2014). The belief is that the range of resonance frequencies, contributes to the network's ability to also produce stable activity over a range of frequencies.

We were interested in examining the resonance frequency as another parameter that would create the activity profile of each neuron. The goal of this study was not to solely examine resonance, however, to describe a phenomenon which may be different in each of the pyloric neurons. Therefore, we did not perform a full examination on the resonance of each of the pyloric neurons, and only examined resonance as a feature of the activity profile. Further studies are needed to understand the implications of the follower neurons resonance properties in this network.

Resonance properties are not exclusive to the neurons of the pyloric network. But because of the ease of determining the resonance profiles of these neuron types, the principles garnered from this study can be applied to support other networks. A theoretical study, shows that resonance is believed to promote synchronous activity of both inhibitory and excitatory neurons in networks of the cortex (Hahn et al., 2014). The role of resonance in these networks may be to amplify weak signals in the neurons that would otherwise fail to propagate. Other studies, both experimental and theoretical, show the

ability of excitatory and inhibitory neurons to resonate at different frequencies during light stimulation of the barrel cortex (Cardin et al., 2009, Tchumatchenko and Clopath, 2014). Excitatory neurons amplify low frequencies at the network level, however, inhibitory neurons can resonate at the gamma frequency range. Perhaps, in the data presented in this chapter, similar to studies in the barrel cortex, the resonance frequency of a subpopulation of neurons may define the pyloric network frequency. The results we have presented show that only a subpopulation of pyloric neurons possess a resonance frequency that is close to the pyloric network frequency.

3.4.5 Conclusion

We have shown that each neuron in the pyloric network possesses its own frequency-dependent activity profile. And that network stability is in part due to inherent stability within the neuron itself. However based on our results, it does not fully explain network stability. In the intact network, IC overlaps in phase with but leads LP; however, we show that in the isolated neurons at frequencies below 2.5 Hz IC and LP did not show phase differences, but above 2.5 Hz, IC lagged LP. Therefore, other mechanisms must be involved in maintaining network stability.

What then does stability mean of the network in the presence of variability of ion channel expression levels in individual neurons? As frequency increases, a neuron's intrinsic properties should compensate for this change in frequency. For instance, I_h and I_A, are compensatory in the pyloric network and

are correlated within different neurons in the system (MacLean et al., 2003). This type of correlation could lead to the stability that we see in each of the different neurons of the pyloric network. Understanding the contributions of ionic currents, should warrant further investigation as in which mechanisms can possibly be responsible for the frequency-dependence seen in the isolated pyloric neurons.

CHAPTER 4

FREQUENCY DEPENDENCE OF CURRENTS

In Chapter 3, we show that the intrinsic properties of an isolated pyloric neuron are not enough to explain phase maintenance in the pyloric network. We also showed that as input frequency increased the burst onset phase of the isolated neurons was delayed. In this chapter, we are interested in determining if I_h contributes to the burst onset phase in a frequency-dependent manner.

4.1 Introduction

Rhythmic activity in CPGs relies on the properties of the voltage gated ion channels that govern the activity of individual neurons within the oscillatory network. Variability of these ionic channels has been found to exist across the same neuron type across animals (Golowasch et al., 1999). Different ionic currents need to adjust their amplitude according the input frequency in order to stable activity i.e. phase constancy. Therefore, understanding how intrinsic cellular properties contribute to phase constancy at different frequencies is important.

The hyperpolarization-activated mixed-cation current (I_h), is activated by hyperpolarization, possesses slow kinetics of activation and inactivation, contributes to the baseline membrane potential, and determines the extent of post-inhibitory rebound (Harris-Warrick et al., 1995b, Pape, 1996). The role of I_h

in generation of rhythmic activity is the subject of many studies. I_h modulates the rhythmic activity of different systems including the pre-Bötzinger complex, mammalian hindlimb movement, the inferior olive and the hippocampus (Bal and McCormick, 1997, Magee, 1999, Butt et al., 2002). In the leech heartbeat CPG, I_h determines the period of the bursting of the heart interneurons and balances the activity of the right and left side of the interconnected ganglia (Olsen and Calabrese, 1996, Hill et al., 2002). I_h can depolarize the membrane to threshold, so that activation of non-inactivating currents can occur. I_h can have an effect on the activity phase of pyloric neurons (Harris-Warrick et al., 1995b, Kloppenburg et al., 1999, Zhao and Golowasch, 2012). Both the LP neuron and the PY neuron possess distinct expression patterns of I_h, which is demonstrated through their differences in ion channel expression (Harris-Warrick et al., 1995b). The PD neuron also possesses different levels of I_h, , which is implicated in phase maintenance and pacemaker activities (Tierney and Harris-Warrick, 1992).

However, these studies in pyloric neurons have used pulses and not sinusoidal inputs at different frequencies. To understand the contribution of currents to phase at different frequencies, we used a sweeping sinusoidal input (ZAP) to examine the currents at different frequencies. Because we are interested in understanding the contribution of the currents to burst onset using a sinusoidal input allows for an examination of how these currents modify bursting properties across different frequencies. The advantage of using a ZAP

function is that while it sweeps across a predetermined range of frequencies, its amplitude is fixed.

My previous chapter establishes the presence of different activity frequency dependent profiles in the neurons of the pyloric network. In this chapter, the focus is on the LP, PY, and PD neurons because their ionic channel and ionic current composition has been extensively studied (Schulz et al., 2006). Specifically, we focus on how I_h determines the burst onset across different frequencies.

4.2 Materials and Methods

4.2.1 Current Measurement and Blocking

We measured I_h in LP, PD and PY to determine the dynamics for our dynamic clamp experiments (see below). We placed two electrodes into each neuron and used two-electrode voltage clamp to measure the currents in each neuron. I_h was activated with 5s hyperpolarizing pulses from a holding potential of -40mV. The maximum amplitude was measured at the end of the 5 second pulse at -120 mV (Figure 4.1A). Since I_h is a hyperpolarization activated current, its amplitude is larger with stronger hyperpolarization. These measurements were taken in normal saline. Previous studies have shownthat taking these measurements in the presence of activity blockers (Tetrodotoxin (TTX)) is consistent with measurements in control saline (Zhao and Golowasch, 2012).

4.2.2 Determining Burst Activity

In order to determine bursting activity at different frequencies, individual neurons were identified and isolated by severing the *stn* and the preparation was superfused with 10^{-5}M picrotoxin (PTX) for 30 minutes to block chemical synapses (Appendix A). In the voltage clamp experiments, the neuron was driven with a sweeping frequency sinusoidal input. The axons of the unipolar pyloric neurons originate from the end of the primary neurite and are distal to the somatic current clamp electrode. This allows for recording the occurrence of action potentials in voltage clamp.

In order to determine the burst phase as a function of frequency, the neuron received a sweeping frequency sinusoidal (ZAP) input. The ZAP function was calculated as:

$$ZAP(t) = A\sin(2\pi f(t)) \text{ where } f(t) = F_{min}t\left(\frac{F_{max}}{F_{min}}\right)^{t/T} \tag{4.1}$$

where A is equal to the amplitude of the injected sine wave oscillation and the frequency $f(t)$ sweeps values between F_{min} and F_{max} over a total duration of T. The ZAP function was applied for a course of T = 100 seconds with F_{min}=0.1 and F_{max}=4.0 Hz. In order to prevent transients, the ZAP function was preceded with 3 sinusoidal cycles applied at the minimum frequency of F_{min}=0.1 Hz. With the addition of the three pre-cycles, the total duration of the applied waveform was 130 seconds. The first sinusoidal cycle was phase shifted by 270° in order to initiate the first sine wave at its minimum. The ZAP function will henceforth refer to both the three pre-cycles and the 100-second sweeping-frequency waveform. In all experiments, the pyloric neuron tested was held at a holding

potential of -60mV and driven with a ZAP function spanning a voltage range of -60 to -30mV.

The burst phase was compared in control and when I_h was blocked. We blocked I_h using 5 mM of CsCl (Sigma Aldrich) (Peck et al., 2006). Although ZD7288 has been found to be an effective blocker of I_h, CsCl is effective and channel specific in the STG and its effects rapidly reverse (Peck et al., 2006). CsCl was superfused for 30 minutes in 10^{-5}M PTX. We measured the burst onset (first spike) within each cycle. We reported the spike time with respect to the minima of each cycle of the ZAP input.

4.2.3 Software

Data were acquired using both pClamp 9.0+ (Axon Instruments) as well as Scope to record and stimulate each neuron. The software Readscope and Scope were developed and maintained by the Nadim lab and can be downloaded at http://stg.rutgers.edu/. All data were sampled at 5 kHz and saved on a PC using a Digidata 1332A (Molecular Devices) and a PCI-6070-E data acquisition board (National Instruments). Matlab scripts were developed in order to calculate the burst onset.

4.2.4 Statistical Analysis

Statistical analysis was performed using Sigmaplot 12.0 (Systat). Significance was evaluated at an α value of 0.05, error bars show and error values reported denote standard deviation.

4.3 Results

Our experiments were done in three parts: (1) we first determined if the PD, LP and PY neurons each possessed different levels of I_h, (2) we then used a sweeping sinusoidal function to examine the frequency dependence of I_h, (3) we examined how removal of I_h from three neuron types affected the burst onset.

4.3.1 Do the Pyloric Neurons Express Different Levels of I_h?

We were interested in understanding if each of the three neurons possessed different levels of I_h. The currents of the LP and PY neuron have been previously studied in detail (Harris-Warrick et al., 1995b). However, the ionic currents of the three neurons have not been fully compared. Here we used square pulses to measure the levels of I_h in the PD, LP, and PY neurons. The maximum amplitude was measured at the end of the 5 second pulse at -120 mV (Figure 4.1A). We find that the PD, LP and PY neurons each possess their own levels of the I_h current (One-way ANOVA, $p < 0.001$; Figure 4.1B). PY (1.96 ±0.11nA, N=5) has the highest amount of I_h, LP had the second (1.57 ± 0.09 nA, N=6), and PD (1.19 ± 0.11 nA, N=7) the lowest quantity of I_h.

We found that 5 mM CsCl effectively blocked I_h in the PD, LP, and PY neuron (Table 4.1). A pairwise comparison of each of the control and the CsCl conditions showed that between CTL and CsCl for each neuron, there was a significant decrease and difference in the levels of I_h (Table 4.1).
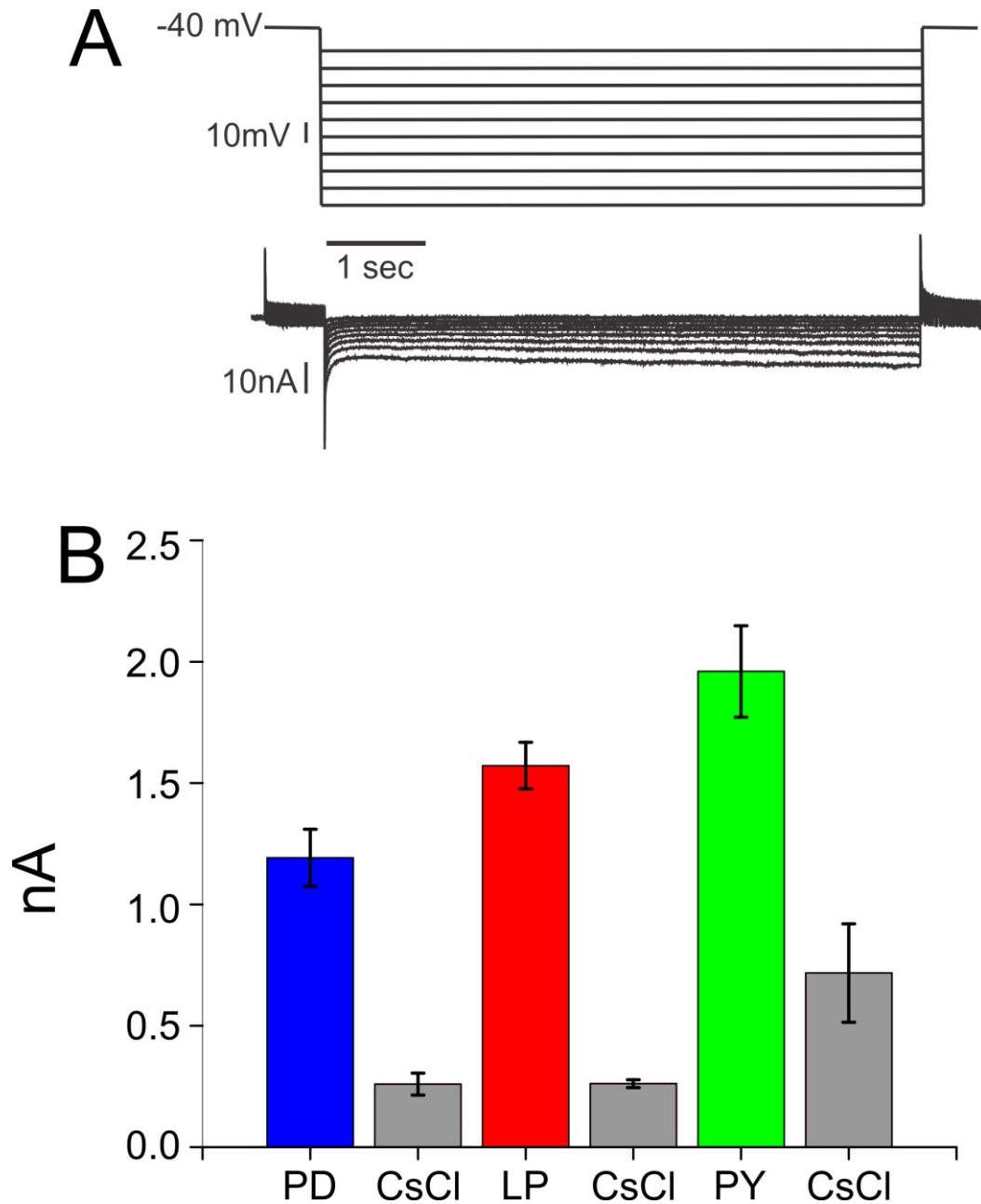
Figure 4.1 Measurement of I_h using the Pulse Protocol at 120mV. **A.** I_h was measured using a 5 second hyperpolarizing pulse with a holding voltage of -40mV and change of -10mV per step. **B.** Each of the different neurons possess a different level of I_h. PY had the highest quantity of I_h and PD the lowest. Each of the three neurons had a significant decrease in I_h in the presence of 10^{-5} M CsCl.

Table 4.1 Pairwise Comparisons of Levels of I_h in the PD, LP and PY Neurons in CTL and CsCl

	PD	PD CsCl	LP	LP CsCl	PY	PY CsCl
PD		<0.001	0.041	<0.001	<0.001	0.042
PD CsCl			<0.001	**0.991**	<0.001	0.037
LP				<0.001	0.043	<0.001
LP CsCl					<0.001	0.039
PY						<0.001
PY CsCl						

P values for pairwise comparison of CTL and CsCl in PD, LP and PY using One- way ANOVA with *post hoc* Holm-Sidak method.

4.3.2 Effect of Currents on Burst Onset in Pyloric Neurons

In the presence of constant synaptic input, blocking I_h causes a delay in the firing of pyloric neurons (PY and LP) while blocking I_A causes a phase advance in those same neurons (Harris-Warrick et al., 1995b). We were interested in understanding how I_h affects burst onset.

To measure the effects of blocking I_h in LP, PY and PD, we measured each neuron in control and in the presence of CsCl. We voltage clamped each neuron at a resting potential of -60mV and drove each neuron to -30mV using the ZAP function. When we blocked I_h we saw a statistically significant phase delay of the burst onset across all frequencies of LP (P<0.001; N=7, Figure 4.2A). This result is expected as I_h is an inward current activated by hyperpolarization, and blocking it should cause a phase delay on the burst onset.

The effect of I_h on the PD neuron was found to be different than on the LP neuron. In the presence of CsCl, at the lower frequencies 0.1 – 1.0Hz there was a delay of burst onset. Removing I_h did not have a significant change on

the phase of the burst onset (Two Way ANOVA with *post hoc* Holm Sidak; p=0.868; p=4; Figure 4.2B).

Previous work on PY found that when the neuron was hyperpolarized in dopamine, which causing an increase in I_h, the cell would fire earlier from rebound (Harris-Warrick et al., 1998). Surprisingly, we found that across all frequencies there was a phase advance in the burst onset in PY when I_h was blocked (Two way ANOVA; p<0.001; N=4; Figure 4.2C).

4.4 Discussion

Oscillatory networks are composed of a variety of neuron types, each possessing their own ionic current configuration. In many systems, individual neurons have been shown to express ionic currents at highly variable levels. This variability allows for plasticity in the individual neurons, which translates to flexibility in the network, all while still maintaining stable network output. This network output -specifically the phase of the neurons- is possibly influenced by both synaptic and voltage-gated currents; however, the challenge is to explain how this interaction is possible. In this study, we start to dissect the effects of altering these ionic currents at different input frequencies. By doing this, we garner a further understanding of how variability leads to stability in a neural network. A decrease in I_h can cause a phase advance across frequencies in the LP neuron, but also causes a phase delay across the PY neuron. Perhaps
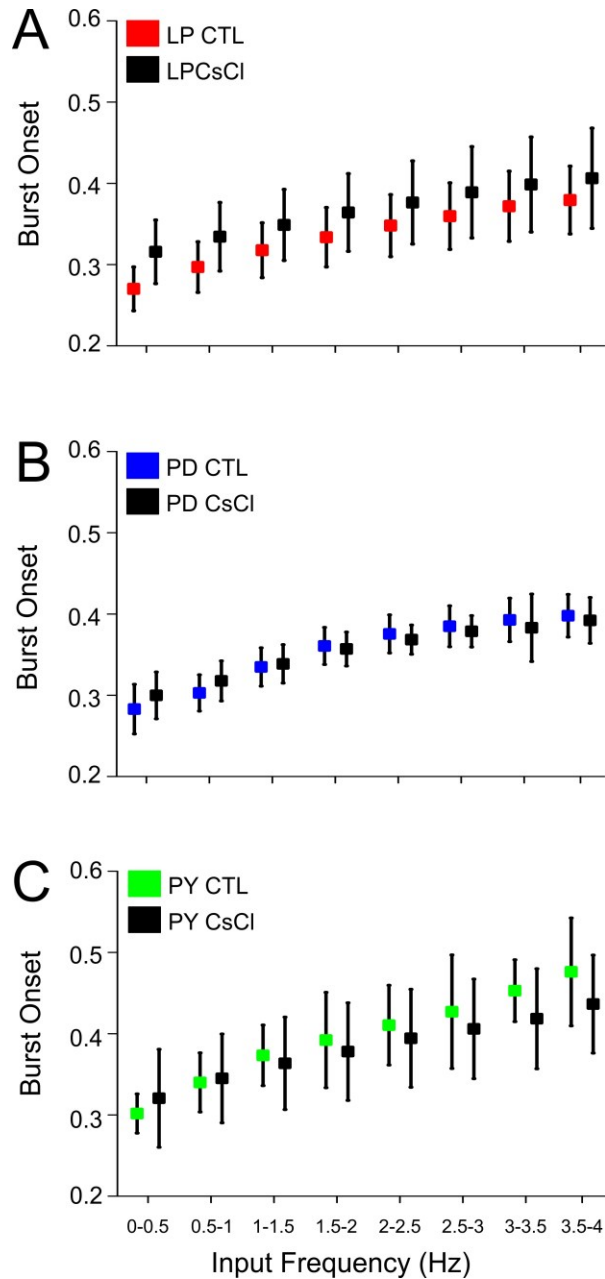
Figure 4.2 Effect of I_h on the Burst Onset on PD, PY and LP. **A.** At all input frequencies in the presence of I_h, there is a phase delay for the burst onset of LP. **B.** In CsCl, there is not a significant difference in burst onset phase across input frequencies. **C.** In the presence of CsCl there is a phase delay at low frequencies in PY. As input frequency increased however, we see significant phase advance.

this decrease in I_h seen in the pyloric neuron is a compensatory mechanism by which to maintain phase In order to maintain stable output across frequencies.

The compensatory mechanism we observe in this system is through the interaction of I_h is different at lower and higher frequencies. At lower frequencies, the quantity of I_h is larger than at higher frequencies; at higher frequencies the current does not have enough time to fully activate. This is one possible reason that the phase of burst onset delays with higher frequencies (Figure 2A).

Previous work in the PD neuron showed that in the intact network, removing I_A caused an increase in spike frequency per burst, an increase in the burst duration and an increase in the pyloric frequency. We show that removing I_h with CsCl does not have an effect on the burst onset phase in the PD neuron.

4.4.1 Interplay of Synapses and Currents Leads to Stability in the Network

I_h has been proposed to be involved in synaptic transmission, long-term facilitation, shaping of temporal summation, contribution to membrane potential and integration of synaptic input to neurons (Harris-Warrick et al., 1995b, Beaumont and Zucker, 2000, Migliore et al., 2004, Migliore et al., 2005). I_h has been found in presynaptic terminals such as: the crayfish neuromuscular junction, basket cells, and the calyx of Held (Beaumont and Zucker, 2000, Southan et al., 2000, Cuttle et al., 2001). I_h is believed to mediate LTP at the mossy fiber synapse to pyramidal cells of the CA3 region (Fan et al., 2005). In pyramidal neurons, HCN channels are believed to dampen postsynaptic

potentials that may generate synaptic plasticity. Deletion of the gene for I_h channels is enhances LTP and hippocampal-dependent learning and memory (Nolan et al., 2004). We have shown that the levels of I_h differ between pyloric neuron types but have not correlated those levels with levels of synaptic current.

Since both the LP neuron and PY neuron each possess their own ionic conductances of I_A and I_h, their levels may in turn help maintain their phase maintenance as frequencies increase. Specifically, the LP neuron possesses a higher level of I_h which may allow the LP neuron to escape inhibition first. The LP neuron still maintains a higher level of I_h allowing it to still escape inhibition from the pacemakers first, rather than the PY.

In the pyloric neurons of the lobster *P. interruptus*, I_h channels are not uniformly distributed, but there is low level of staining in the stomata and higher levels in the fine neuropil (Goeritz et al., 2011). The fine neuropil is the location of synaptic transmission within the pyloric network, and I_h channels are believed to be close to the site of synaptic contact. However, the location of the I_h channels are not fully clear, it is not clear whether they are located on the pre or postsynaptic side of the synapse. The question remains then about the role of I_h in synaptic transmission. Activation of I_h was found to dramatically reduce the amplitude of the postsynaptic response; this effect was abolished in the presence of Cs^+ or ZD7288. When I_h channels are activated the effective length constant is reduced, membrane resistance is decreased, and in turn shunt synaptic events are shunted (Magee, 1998, Berger et al., 2003).

Therefore, an increase in I_h at synaptic locations in the pyloric network could reduce the synaptic amplitude by reducing the postsynaptic input near the synapse and providing an inward current to shunt inhibitory IPSPs.

CHAPTER 5

PHASE CONSTANCY IN OSCILLATORY NEURONS

Thus far, we have shown that the intrinsic properties of the individual neurons are not enough to explain phase constancy at different frequencies in the pyloric network. Therefore, phase maintenance must be explained through other mechanisms. Here we explore the contribution of short-term synaptic plasticity to phase maintenance in an oscillatory network.

5.1 Introduction

In this chapter, we examine the mechanisms through which phase is maintained across different network cycle periods. Prior theoretical work suggests that short-term synaptic depression of inhibitory synapses can promote phase constancy between neurons and across oscillation frequencies (Manor et al., 2003). Manor et al. showed that the mechanism for short-term depression is frequency dependent: the longer the period, the stronger the synapse and the more effective the synapse becomes. The shorter the period the less effective the synapse becomes and the greater role of the neuron's intrinsic properties, such as the ionic channel composition, in phase constancy. In sum, these results indicate that synaptic dynamics along with intrinsic properties can extend the range of periods for which phase can be maintained.

We examined the contribution of short-term synaptic dynamics to phase constancy. An important property of the pyloric network of the crab *Cancer*

borealis is that follower neurons' relative phase of activity is adjusted depending on the cycle frequency in order to maintain a stable triphasic rhythm (Bucher et al., 2005). Here we test the idea that phase constancy across frequencies is achieved via short-term synaptic plasticity. Specifically, we use the lateral pyloric neuron (LP), a follower neuron that acts as the sole transmitter mediated feedback to the pacemaker neuron (PD) that exhibits short-term synaptic plasticity.

When the presynaptic neuron (PD) was driven using the ZAP function, the synaptic phase and amplitude of the postsynaptic current was found to be frequency-dependent (Tseng et al., 2014). As frequency increased, the synaptic amplitude from the PD to LP neuron peaked and then decreased (Tseng et al., 2014). When the PD neuron was driven at lower frequencies, the synaptic current in the LP neuron peaked before the presynaptic membrane voltage. At higher frequencies, the synaptic current peaked after the presynaptic membrane voltage (Tseng et al., 2014). When the presynaptic neuron was driven with a sinusoidal function, the synaptic current was triangle-shaped across all frequencies tested.

We blocked these synapses to the LP neuron and used the dynamic clamp technique to introduce artificial periodic synaptic conductances into these neurons. Using dynamic clamp to introduce an artificial synapse, from the pacemaker ensemble to the LP. We examine the effects of changing the following properties of the PD to LP synapse:

1) synaptic amplitude (G_{max}),

2) peak phase, and

3) duty cycle (either 0.3 duty cycle at each period, or a constant duration of 300 ms) of the synapse to the LP neuron.

These parameters, with the exception of peak phase, are similar to those studied in prior theoretical work (Manor et al., 2003). We make two predictions based on the results of the prior theoretical work. The first prediction is that a decrease in synaptic strength as a function of frequency (short-term depression) promotes phase maintenance. The second, a decrease in synaptic peak phase as a function of frequency promotes phase maintenance. We have found that phase constancy can be achieved through short-term depression. This is accomplished through changing synaptic strength, peak phase or duration, as well as by changing a combination of these three parameters.

5.2 Materials and Methods

5.2.1 Driving the Neuron with Periodic Triangular Synaptic Conductances

In order to measure the effects of synaptic inputs on the phase of the follower LP neuron, we mimicked the biological synapse from the pacemaker neurons to the LP neuron. We used the Netclamp software (Gotham Scientific) using a dynamic clamp conductance. We used a periodically injected triangle-shaped waveform conductance to replace the synapse from the AB/PD pacemaker ensemble (blocked by PTX). The reversal potential of the current was set to -80 mV (Zhao et al., 2011). A periodic triangle waveform of different parameters

was applied to mimic the synaptic current from the pacemaker neurons in order to drive the LP neuron with an inhibitory input in an open-loop fashion.

We used a brute-force method to test four different parameters in our triangle conductance injections: triangle peak phase (TP), duration, period, and maximal conductance or G_{max}. This type of method allows us to test different possibilities of each of the different parameters in order to determine how phase is maintained. The triangle shape was chosen because it mimics the observed natural shape of the synapse (Tseng et al., 2014). The value of TP was varied to cover the whole range: 0, 0.25, 0.5, 0.75 and 1 (Figure 5.1A). Three values for G_{max} were used: 0.1, 0.2 and 0.4 µS (Figure 5.1B), consistent with previous measurements (Zhao et al., 2011, Tseng et al., 2014). The period (P: time between onsets of dynamic clamp synaptic injection; Figure 5.1C) and the duration (length of triangle; Figure 5.1D) were also varied. Five values for P were used: 500, 750, 1000, 1500, and 2000 ms which cover the typical range of pyloric cycle periods. The duration of the synapse was either kept constant (at 300 ms) for all values of P or changed according to the P value to keep a constant duty cycle (fraction of the cycle that the synapse was active) of 0.3.

We recorded a minimum of ten cycles per experiment and used the average of the last three cycles to calculate both burst onset (Δt calculated in reference to the onset of the synaptic input) and number of spikes per burst
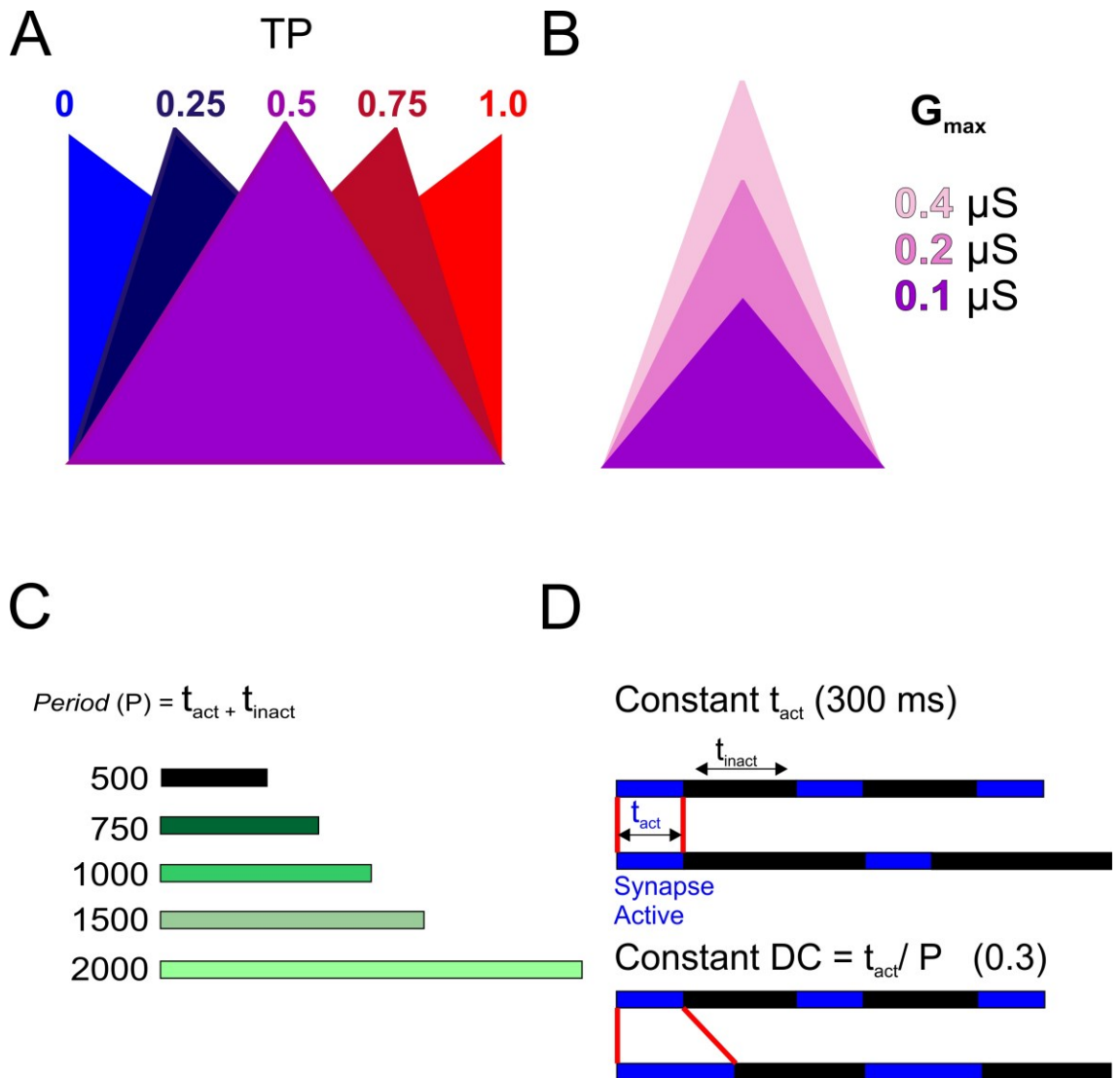
Figure 5.1 Four parameters of the synapse were varied in the experimental paradigm. **A**. The triangle peak phase (TP) of the synaptic conductance was varied to mimic the shape of the synapse and cover the range from 0 to 1 (0.00, 0.25, 0.50, 0.75, 1.00). **B**. Three values of G_{max} were chosen: 0.1, 0.2, and 0.4 µS. **C**. The period (P) was varied to mimic the typical range of pyloric cycle periods: 500, 750, 1000, 1500, and 2000 ms. **D**. The duration of the synapse was either a constant 300 ms or maintained at a constant duty cycle of 0.3 across all values of P. One example at 500 ms the synaptic duration could either be 300 ms or 150 ms (if using a duty cycle of 0.30).

(Figure 5.2). The burst onset was used to calculate the activity phase ($\varphi = \Delta t / P$) of the LP neuron in response to the dynamic clamp synaptic injection.

5.2.2 Data Sampling

The data points were measured at only five different P values. We estimated the value of φ at other periods P by fitting the data using the hyperbolic function c/P (Manor et al., 2003) and then used the fit function to resample our data at 100 ms intervals for P and extrapolated the samples to the range of P between 400 and 2100 ms (Figure 5.4).

5.2.3 Software

Data were acquired using Pclamp 10.1 software (Molecular Devices) and the Netclamp software (Gotham Scientific), sampled at 4-5 kHz and saved on a PC using a Digidata 1332A (Molecular Devices) or PCI-6070-E data acquisition board (National Instruments). The realistic waveform data were acquired using the software Scope (Nadim lab; stg.rutgers.edu) at 4 kHz on the National Instruments board.

5.2.4 Analysis and Statistics

Data were analyzed using a Matlab script to calculate both spike number and time of burst onset. Statistical analysis was performed using Sigmaplot 12.0 (Systat). Significance was evaluated with an α value of 0.05, error bars and error values reported denote standard error of the mean.
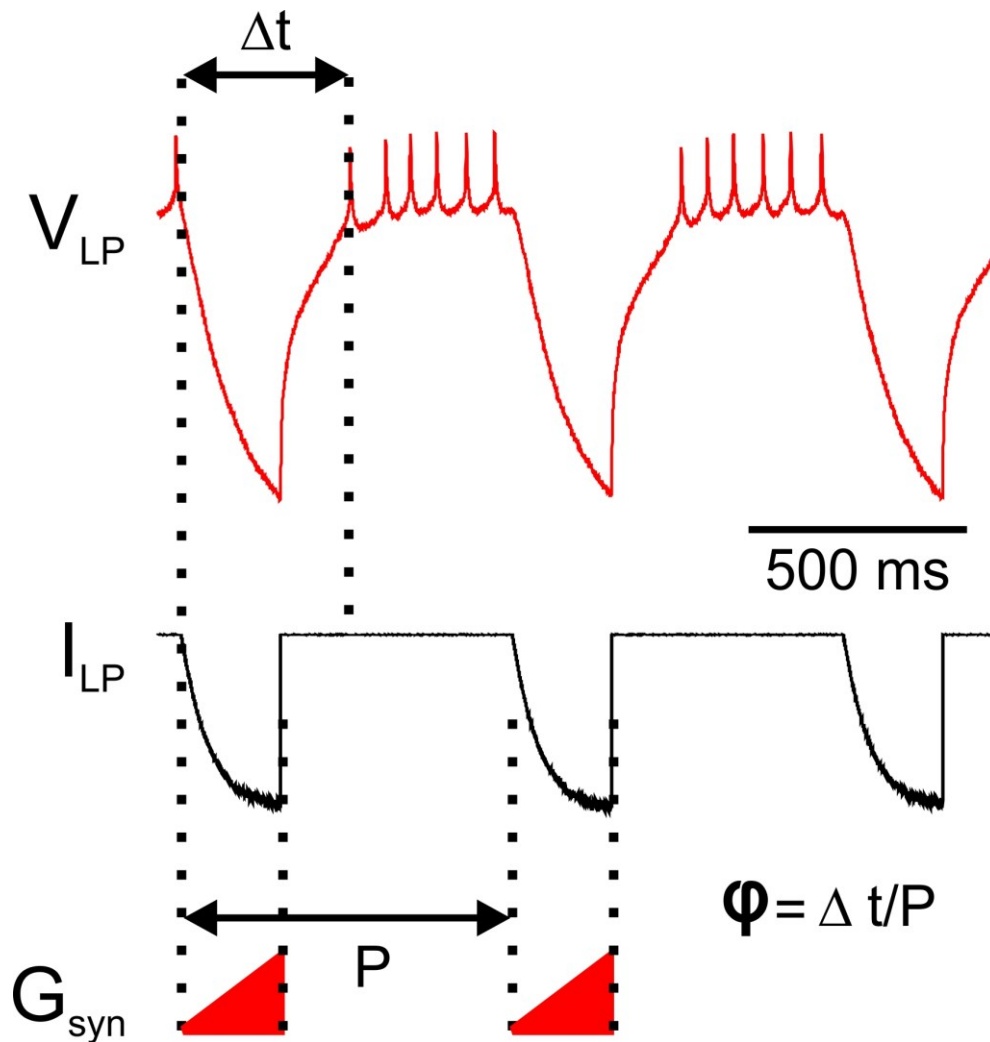
Figure 5.2 Determining the activity phase (φ) of the LP neuron. Intracellular voltage recording of the isolated LP neuron is shown during dynamic clamp stimulation using the triangle conductance (red trace). The current of each LP neuron is recorded as a minimum of ten cycles for each combination of parameters (Figure 5.1). The average of the last three cycles were taken to calculate the burst onset (Δt calculated in reference to the onset of the synaptic input; G_{syn} (red solid triangle). The period (P) is determined from the onset of the triangle conductance to the onset of the next triangle conductance stimulus. The burst onset was used to calculated the activity phase (φ = Δt/P) in response to the dynamic clamp synaptic injection.

5.3 Results

5.3.1 What Effect does Synaptic Amplitude, TP and Constant Duty Cycle have on the φ of the LP neuron?

We confirmed that the synaptic peak phase and synaptic amplitude changes as a function of presynaptic period. While maintaining a constant duty cycle, we were interested in understanding how varying G_{max}, and TP, would shift the φ of the LP neuron across different periods.   With a constant duty cycle of 0.3, the effect of TP and G_{max} on φ was statistically significant across all periods (Three-way ANOVA; $p<0.001$, N=6).

We examined how φ changed as a function of TP across the different periods and at different G_{max} values.   φ was calculated as time to burst onset from the initiation of the stimulus divided by the period (P) (Figure 5.2, Figure 5.3).   In order to determine φ, we fixed the TP at each of the five values (0, 0.25, 0.5, 0.75 and 1.0) (Figure 5.5).   At a particular TP, as period increased (500 to 2000ms), φ decreased.   This trend in the φ of the LP neuron was seen across all values of TP.   At each TP value, we used three different conductance. As a function of TP and as period increased, φ decreased for all of the G_{max} values (0.1, 0.2, 0.4 µS). With a constant duty cycle of 0.3, the φ values had a range of 0.26 to 0.54 for periods of 500ms to 2000ms (N=6).

We then examined how at different periods, the φ of the LP neuron, changed with G_{max} across the different TP values (Figure 5.6A1-3). We fixed the G_{max} values and examined the average φ across the five different TP values at all periods.   Across all TP values, at 0.1 (Figure 5.6A1), 0.2 (Figure 5.6A2)

and 0.4 (Figure 5.6A3) µS, φ decreased as period increased. At 0.4 µS, φ was greater than at 0.1 µS across all periods and TP values tested.

We determined the effect of G_{max}, and period had on φ, at each of the different TP values. When the values of φ versus TP were compared, as TP increased so did φ. Interestingly, at all of the G_{max} values, the smallest period (500ms) had the highest φ across all values of TP (Figure 5.6B).

5.3.2 What Effect does Synaptic Amplitude, TP and ConstantDuration have on the φ of the LP neuron?

We have shown that a constant duty cycle of 0.3 produces a range (0.26 to 0.54) of φ across all periods regardless of TP and G_{max} values. While maintaining a constant duration of 300ms we now examine how φ depends on G_{max}, and TP across all periods. Using a constant duration of 300 ms, all three G_{max} values, and TP values had a significant influence on φ across all periods.

Similar to previous results, while maintaining a constant duration, we determined the effect of G_{max}, and period on φ at each of the different TP values. Not surprisingly, at all G_{max} values, the smallest period produced the highest φ value across all TP (Figure 5.8B). Using a constant duration of 300 ms, all three G_{max} values, and TP values had a significant influence on φ across all periods.
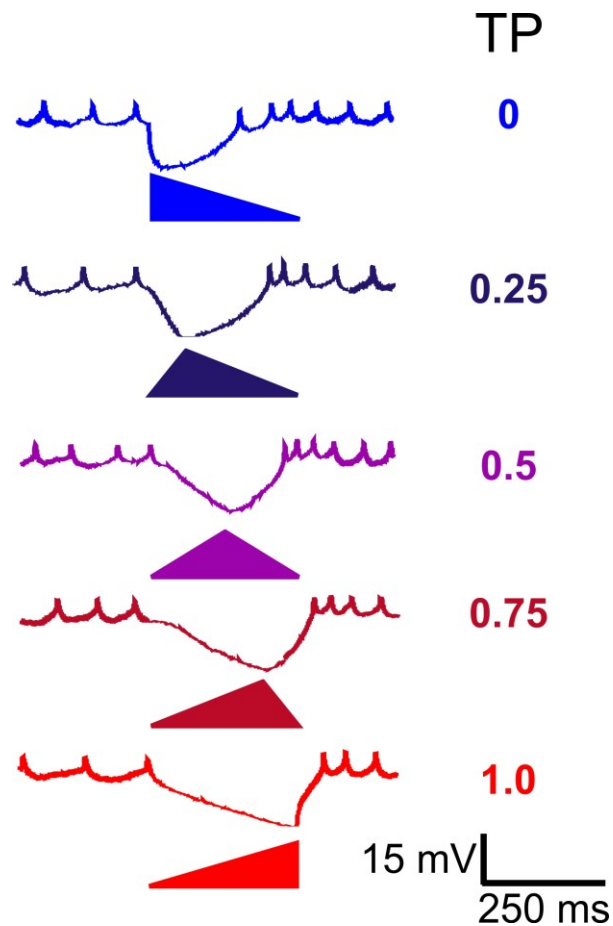
Figure 5.3 Recordings from one LP neuron during dynamic clamp injections across the five different TP values. An example of the voltage recordings from a single LP neuron across the five different TP values (Gmax = 0.2 µS, duration = 300ms). The burst onset is calculated as the time that the LP neuron begins to fire after the onset of the stimulus. As the TP increased, the delay of the burst onset was increased in this example.

Similar to the constant duty cycle results, we examined how φ changed as a function of TP across the different periods and at different G_{max} values. To determine φ at a constant duration as period increased, we fixed the TP at each of the five values (0, 0.25, 0.5, 0.75 and 1.0) (Figure 5.5). We observed that as TP increased, φ decreased as a function of period. Additionally, for each TP value, three different conductance values were used. As a function of TP and as period increased, φ decreased for all of the G_{max} values (0.1, 0.2, 0.4 µS). While maintaining a constant duration, the φ values had a range of 0.19-0.94 for periods (N=6).

5.3.3 How Should G_{max} Change with Period to Produce φ Constancy?

We have shown that φ decreases with increasing period while maintaining either a constant duration or a constant duty cycle. We then interpolated and extrapolated sampled data to predict the values of G_{max} at each TP needed to maintain φ at a pre-determined constant value (see Methods). These predictions will serve to understand the synaptic input necessary to maintain a particular phase across all periods.

The average has of the LP neuron in the intact network was calculated to be 0.34(0.34 ± 0.01; N=6). The sampled data, for both the constant duty cycle and constant duration, was used to determine which values of G_{max} will give the best phase constancy (at 0.34) at each TP value (Figure 5.9, Figure 5.10).
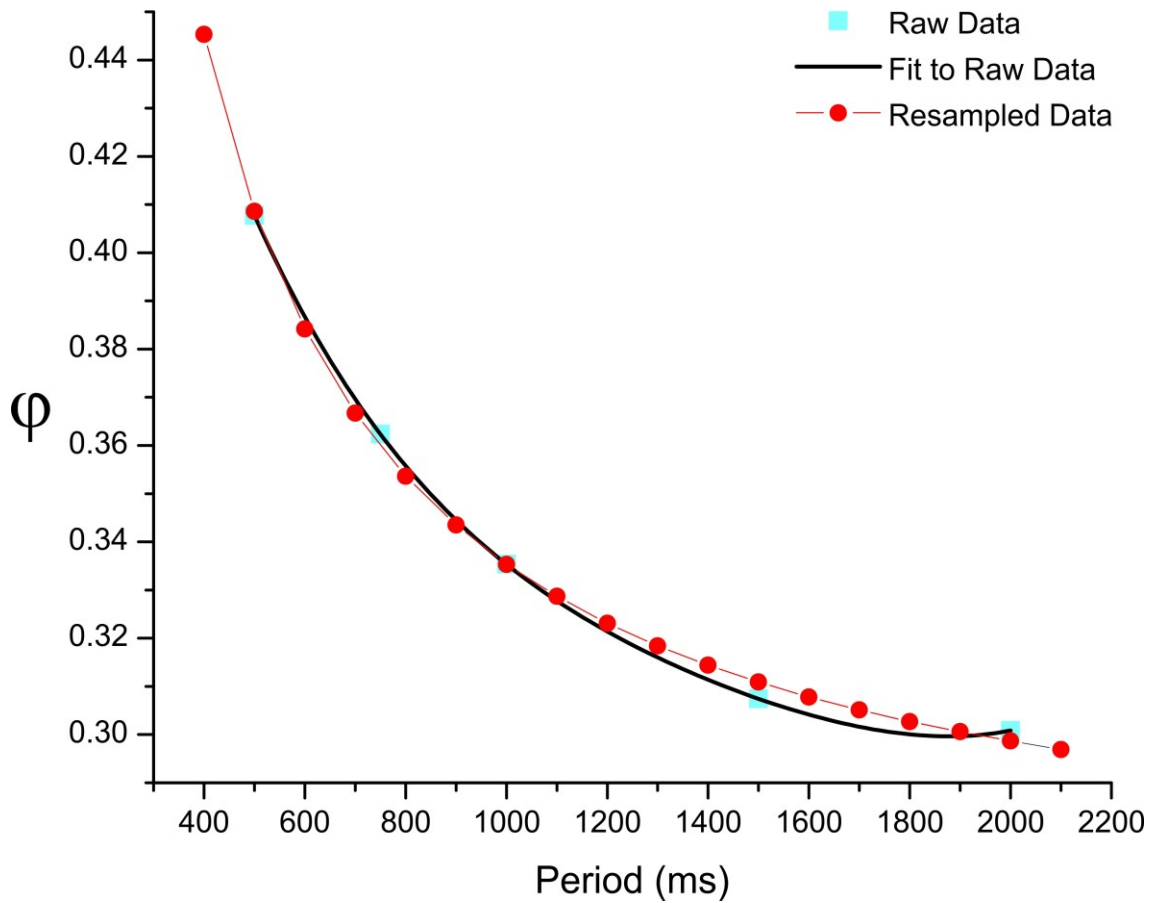
Figure 5.4 Extrapolation of Data. The data obtained was only measured at five different values of P (500, 750, 1000, 1500, and 2000) (N=6). The pyloric network does not operate just as these periods, however, examining all combinations will make experiments time consuming. Therefore, the raw data (aquamarine) was sampled by first fitting the experimental data using a hyperbolic function (black line; see methods). The fit from the hyperbolic function was then sampled at 100 ms intervals for P, and extrapolated to include 400 and 2100 ms (red circles).
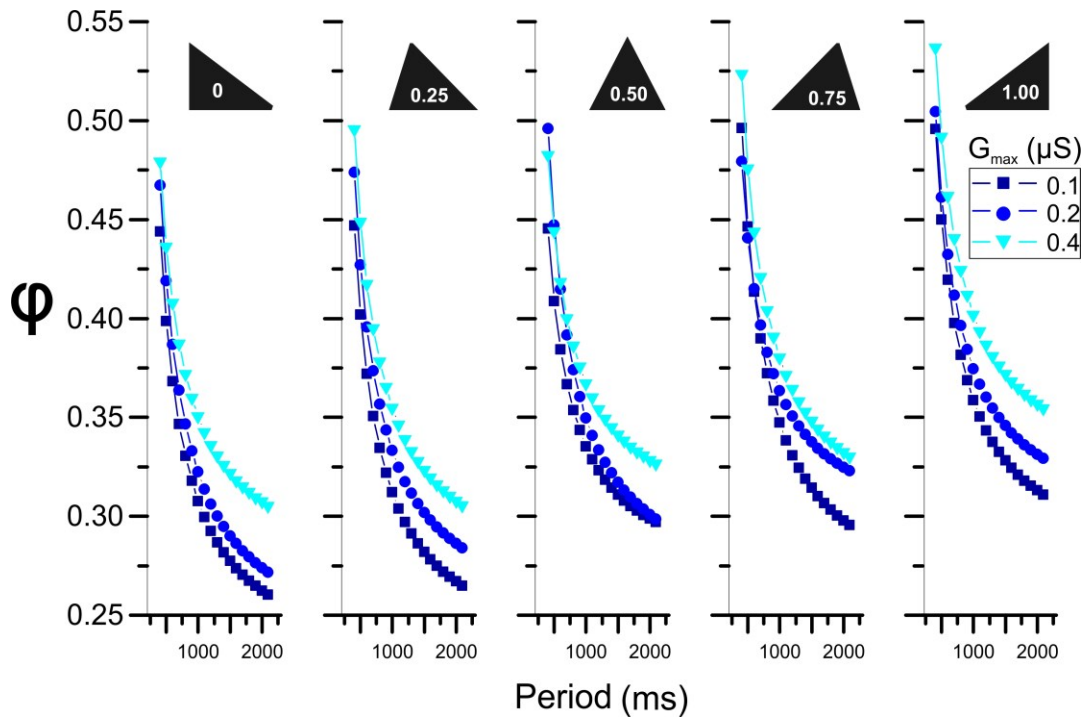
Figure 5.5 Effect of period, waveform and conductance on LP burst onset φ with a constant duty cycle of 0.3. Using the sampled data, TP was fixed at each of the five different values (0, 0.25, 0.50, 0.75 and 1.00 – left to right panels). At each TP value, the effect of changing G_{max} to three different values 0.1 µS (navy blue squares), 0.2 µS (royal blue circles) and 0.4 µS (aquamarine triangles). At the first TP value of 0.00, as period increased so the LP φ decreased. This trend was seen across all values of G_{max} with a TP value of 0.00. At all values of TP and at each G_{max} value, as P increased a decrease in φ was seen.
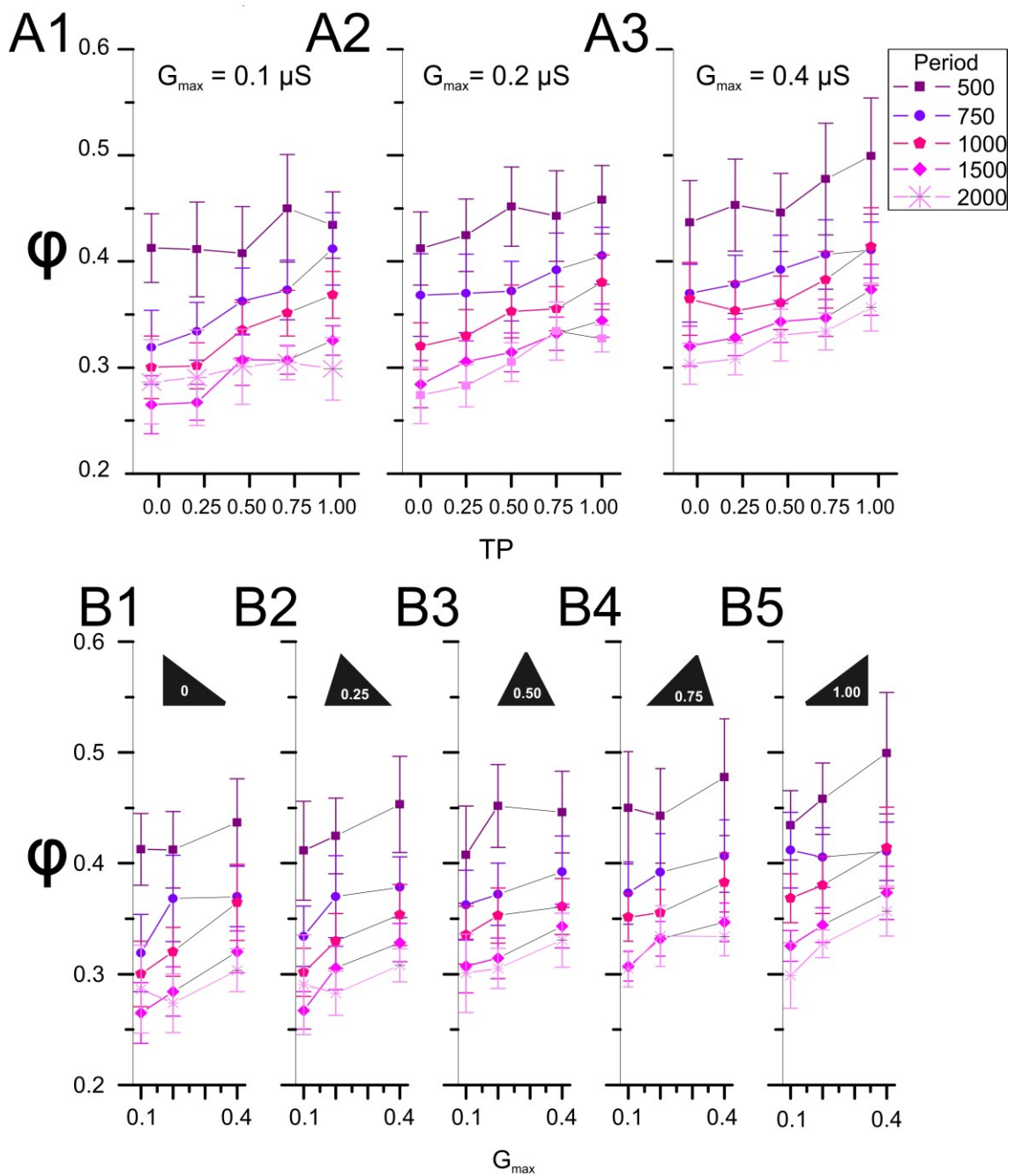
Figure 5.6 Determining φ to synaptic input of constant duty cycle of 0.3 at fixed G_{max}. Panel A1-A3 Using the raw data, at fixed G_{max}, we determined how φ changed across the different values of TP, at each of the values of TP. At each fixed G_{max}, the φ of LP neuron increased with TP and period (different shades of purple, N=6). Panel B1-B5 Using the raw data and fixed TP values, the φ of the LP neuron was determined to increase with both G_{max} and period. With smaller values of period (500ms) , φ increased as a functions of G_{max} across al TP values.
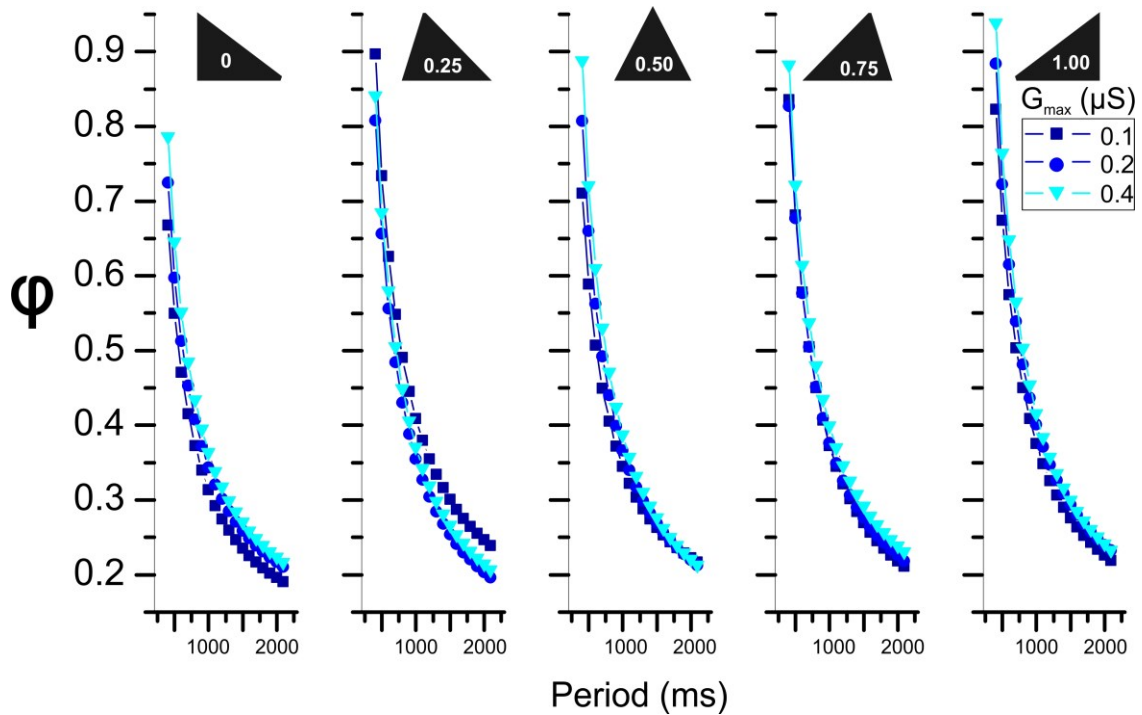
Figure 5.7 Determining activity phase ($\varphi = \Delta t / P$) to synaptic input of constant duration of 300ms at fixed TP. The sampled data was used to determine φ, TP was fixed at five different values (0, 0.25, 0.5, 0.75 and 1.0, left to right panels). The same trend was seen at the three different values of G_{max} were used at each TP, 0.1 (navy blue squares), 0.2 (royal blue circles) and 0.4 (aquamarine triangles) μS. At each of the different TP values. As period increased, the φ of LP decreased greatly across all values of TP. The values for G_{max} across each of the different the different TP is seen to not be different. With a duration of 300ms, the φ values had a large value range for periods of 500ms to 2000ms (N=6).
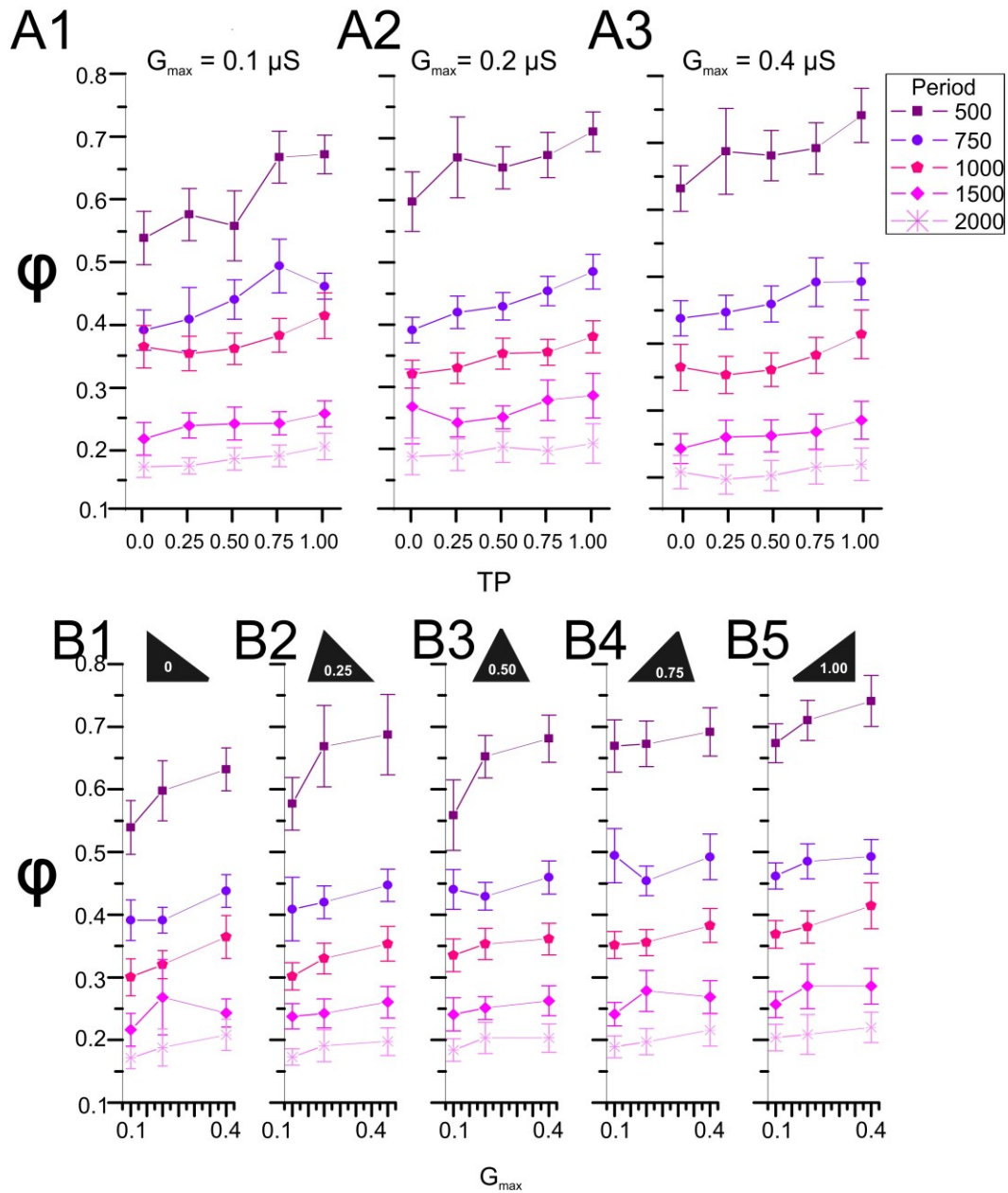
Figure 5.8 Determining activity phase (φ= Δt / P) to synaptic input of constant duration of 300ms at fixed G_{max}. **Panel A1-A3** At fixed G_{max} values, φ changed across period (denoted as different shapes with shades of purple) and different values of TP. As period and G_{max} increased there was an increase in the LP φ. A period of 500ms had the highest level of φ, when compared across the different G_{max} values. **Panel B1-B5** Determining φ to synaptic phase of constant duty cycle (0.3) as a function of conductance. Similar to the previous figure, the TP was kept constant for each panel and determined the effect of G_{max} across the different values of period and TP. With smaller values of period (500 ms) at each TP φ increased as a function of G_{max}.

At each of the five different TP values (Figure 5.9A), changing the G_{max} value is insufficient to maintain φ constant at 0.34 (Figure 5.9B). For example, with a TP of 0.25, conductance values were negative for periods below 600ms. Therefore, it is not possible to maintain φ at those periods. With a constant duty cycle the predicted values of G_{max} required to maintain phase, closely matched the experimental values used for this study. To maintain a constant phase of 0.34 at a constant duration and a TP value of 0.25, the predicted G_{max} values required were not biologically feasible across a majority of the periods.

In the pyloric network despite the mean φ of the LP neuron is consistent across animals, the φ of the LP neuron in a single animal is not always constant. The color map is used to plot the predicted the values of G_{max} and TP required to maintain a particular φ across different periods (Figure 5.9C). Using this map, a particular φ for the LP neuron can be chosen at each of the three different values of G_{max}. For a constant duty cycle, the color map demonstrates that at small periods (i.e. 500) there is a narrow region at each G_{max} where the neuron could possibly maintain φ of 0.32. The color map shows that using a constant duration, the regions where a particular φ to be maintained can extend a wide range of TP and periods. At a particular φ and a synapse of a constant duration, it is difficult to maintain that φ across a wide range of frequencies and periods. The range both TP and periods is smaller when compared to the ranges in the constant duty cycle case. This predicts that with a synapse of a constant duration it is difficult to maintain φ across all values for period.

5.3.4 What Values of TP will give the Best φ Constancy at Different Periods?

The predictions have shown that, for a constant TP, only certain values of G_{max}, at both constant duration and constant duty cycle, can maintain a φ of 0.34 (dotted line, Figure 5.11A, Figure 5.12A). If G_{max} is fixed and TP varied, we examine if the LP neuron could maintain a φ of 0.34 across different periods.

Maintaining a constant duty cycle of 0.3 while increasing G_{max}, there is a shift in the periods that can maintain φ at certain TP values (Figure 11B). Using the specific limits for TP between 0 and 1, the range for which the neuron can maintain φ, changed with each G_{max} value. For instance, φ of the LP neuron was maintained, when G_{max} was set at 0.1 μS and for periods of 800 to 1200 ms (Figure 5.9). At G_{max} of 0.2 μS, φ can be maintained between 900 and 1500 ms, while changing TP between 0 and 1. Finally, at the highest G_{max} value of 0.4 μS, TP can be varied to maintain phase for a period of 1100 to 2100 ms. It is noteworthy that with G_{max} = 0.4 μS , a TP value of 1.00 cannot maintain a φ of 0.34 at any period.

In contrast with a constant duration of 300 ms, maintaining a φ of 0.34 could be achieved in only a narrow range of TP values across all periods (Figure 5.12B). When G_{max} was set at 0.1, there was only a narrow range of periods and TP where φ of 0.34 can be maintained. Similarly, with G_{max} at 0.2, φ can only maintained at periods of 1100 and 1200ms, and with TP values of 0.5 and 1.0. Therefore, a constant duration of 300 ms severely limited the range at which φ of 0.34 could be maintained by varying only TP.
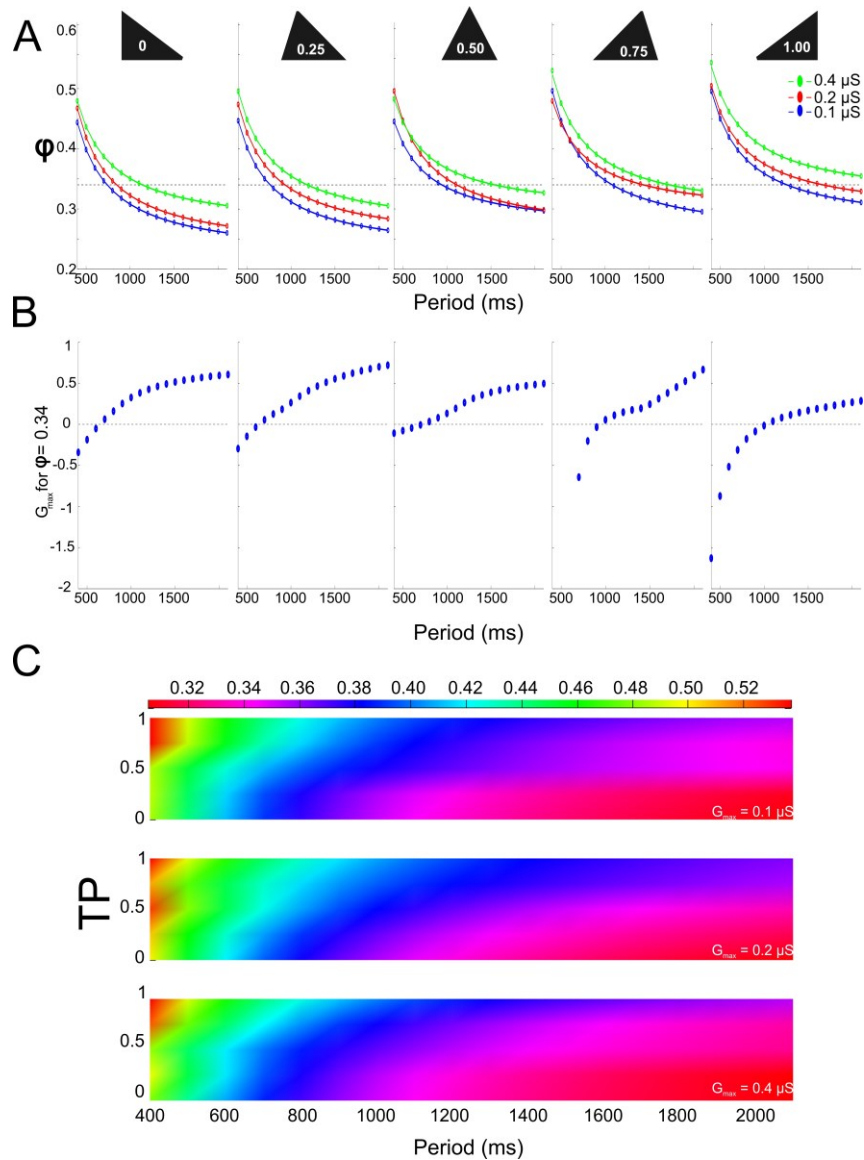
Figure 5.9 Predicting conductance required to maintain a specific (0.34) φ constancy at constant duty cycle and fixed TP. **A.** Using the sampled data, the values for LP φ constancy was fixed to 0.34, which matches the average LP phase in the intact network (0.34 ± 0.02; N=6; grey dotted line). The sampled data was plotted at fixed TP values, and with changing G_{max} values, 0.1 (blue) , 0.2 (red) and 0.4 (green) μS. **B.** Using the sampled data plotted (400-2100ms) in A, the values of G_{max} required to maintain LP φ constancy to 0.34 across all periods and TP values. For example, the left most panel, for frequencies 500-700ms (blue circles) and a TP of 0, it would be impossible to maintain LP φ constancy of 0.34.   Any period across the different values where the G_{max} drops below 0 would be impossible to maintain the LP φ constancy of 0.34. **C.** The color map shown is an interpolated representation of how at each G_{max} and TP value, how period is changed to obtain a particular φ constancy. A particular φ can be chosen and the TP and period needed to achieve that φ at each of the different G_{max} values can be predicted.
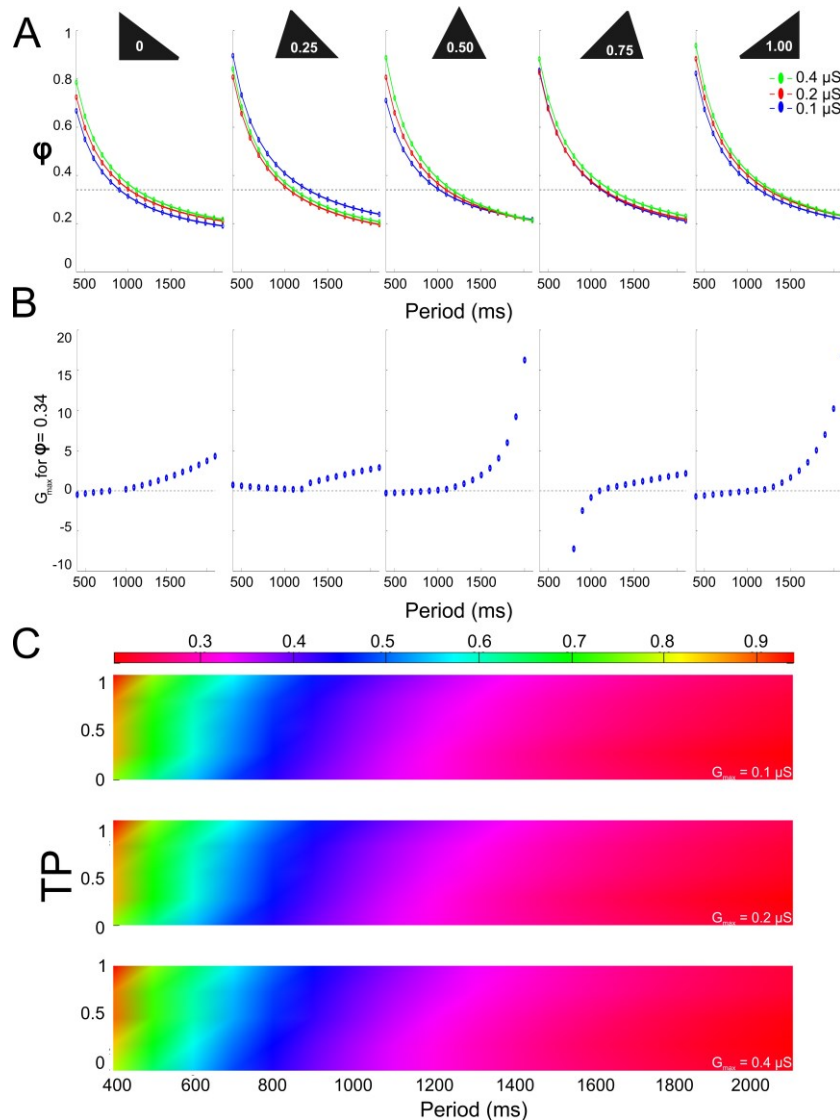
Figure 5.10 Predicting conductance required to maintain a specific (0.34) φ constancy at constant duration of 300ms and fixed TP. **A.** Using the sampled data, the LP φ constancy value was fixed to 0.34, which matches the average LP phase in the intact network (as described in 5.9; grey dotted line). The averaged data was plotted at fixed TP values, and with changing G_{max} values, 0.1 (blue), 0.2 (red) and 0.4 (green) μS. **B.** Using the sampled data plotted (400-2100ms) in A, the predicted values of G_{max} required to maintain LP φ constancy to 0.34 across all periods and TP values. For example, the fourth panel, for frequencies 500-700ms (blue circles) and a TP of 0, it would be impossible to maintain LP φ constancy of 0.34. Any period across the different values where the G_{max} drops below 0 would be impossible to maintain the LP φ constancy of 0.34. **C.** The color map shown are an interpolated representation of how at each G_{max} and TP value, how period is changed to obtain a particular φ constancy. A particular φ can be chosen and the TP and period needed to achieve that φ at each of the different G_{max} values can be predicted.
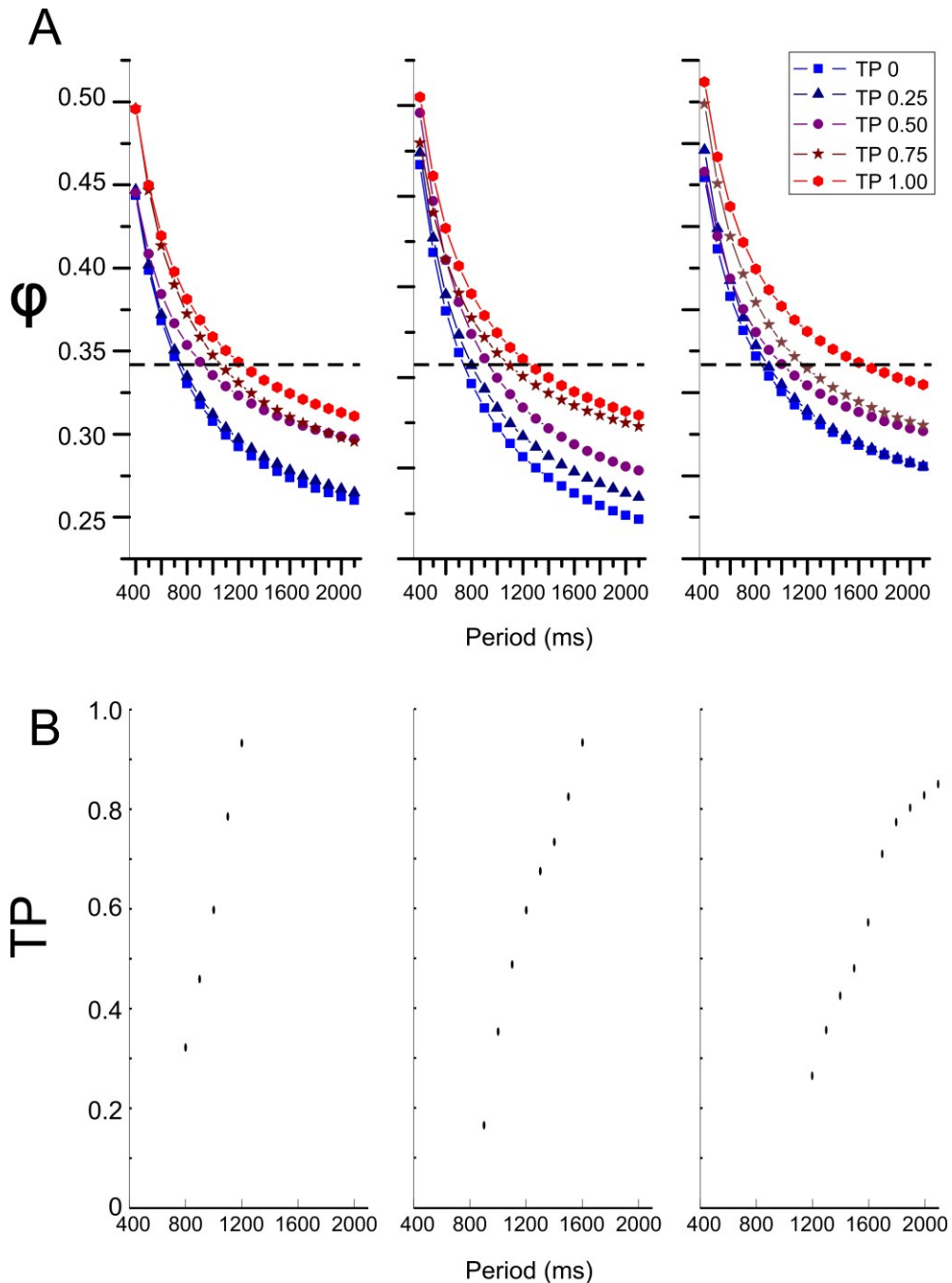
Figure 5.11 Predicting TP value required to maintain a specific (0.34) φ constancy at constant duty cycle and fixed G_{max}. **A**. Using the sampled data, the LP φ constancy was fixed to 0.34 (grey dotted line) and fixed G_{max} , and plotted each of the five different TP values: 0 (royal blue), 0.25 (dark blue), 0.50 (purple), 0.75 (burgundy) and 1.00 (red). **B.** Using the data plotted in A, the values of TP were predicted (black dots) at each period required to maintain a LP φ constancy of 0.34.   At each of the different values of G_{max}, across certain periods it would be impossible given the range of TP value to maintain a LP φ constancy to 0.34.
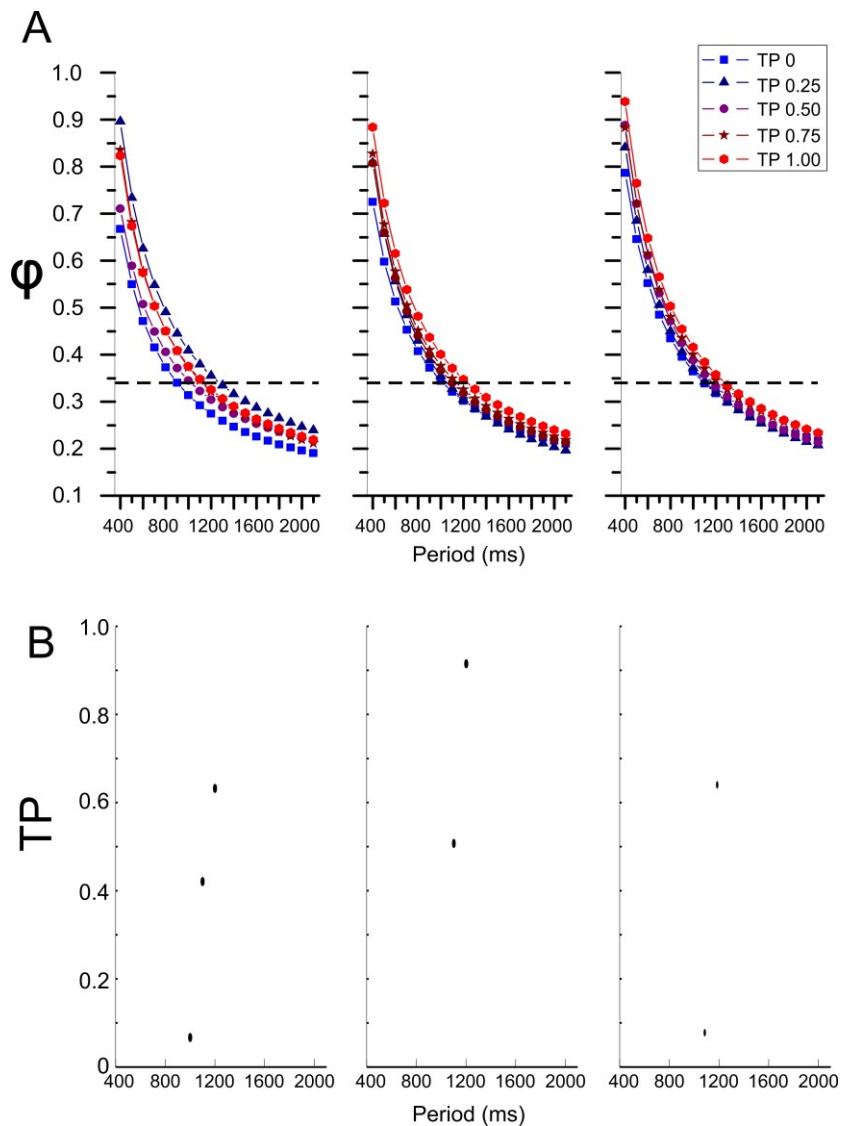
Figure 5.12 Predicting TP value required to maintain a specific (0.34) φ constancy at duration of 300ms and fixed $G_{max.}$ **A**. The sampled data was plotted, and the LP φ constancy was fixed to 0.34 (grey dotted line) and fixed G_{max}, and plotted each of the five different TP values: 0 (royal blue), 0.25 (dark blue), 0.50 (purple), 0.75 (burgundy) and 1.00 (red). **B.** Using the data plotted in A, the values of TP predicted (black dots) at each period to maintain a LP φ constancy of 0.34. With a constant duration of 300ms across all periods, it is very difficult at each period with a fixed a LP φ constancy to 0.34. At each of the different values of G_{max}, across certain periods it would be impossible given the range of TP value to maintain a LP φ constancy to 0.34.

5.4 Discussion

This chapter shows that there are different ways in which cycle period of an oscillatory network can change while maintaining phase. We used a brute-force method to test short-term synaptic plasticity by TP, G_{max} and duration to determine how φ can be maintained for different parameters. This type of method allows us to test different possibilities of each of the different parameters in order to determine how phase is maintained. First, we found that phase changes with period, G_{max}, and TP. Second, we found level sets of TP and G_{max}, that would maintain φ at 0.34. Third, we found that it is difficult for a synapse of a constant duration to maintain φ just by changing the properties of the synapse.

We have shown how short-term depression can coordinate network output despite changes in frequencies. Synapses change their properties depending on the frequency of the network. In order to maintain phase at lower frequencies either: synaptic strength must increase or the TP is delayed. At lower frequencies, the synapse strengthens because longer periods of inactivity in the presynaptic neuron allows for a recovery of the depressing synapse. To maintain phase at higher frequencies either: synaptic strength must decrease or the TP is advanced. At higher frequencies, the synapse interval is shorter, not allowing for the synapse to fully recover.

5.4.1 Constant Duration or Constant Duty Cycle: one better than the other.

Previous modeling studies have suggested that synaptic depression in inhibitory synapses promotes phase maintenance by delaying neuronal firing as synapses recover with longer cycle periods (Manor et al., 2003, Bose et al., 2004). Depressing synapses in particular, are found to be frequency-dependent; longer intervals of inactivity from the presynaptic neuron will allow for a faster, stronger recovery of the synapse. Non-depressing synapses, however, do not have frequency dependence, making it difficult to maintain phase (Manor et al., 2003).

As shown in this study, a synapse with constant duty cycle of 0.3 was able to maintain φ when compared to a synapse of constant duration across all frequencies. The longer the duration that the postsynaptic cell was allowed to remain active, the harder it was to maintain phase. One example of this is with a period of 2000 ms and synapse of 300ms, allowed the postsynaptic neuron to be active for a longer period of time than compared to a period of 2000 ms and a synapse with a constant duty cycle of 0.3 (600 ms). However, across all periods it was difficult to maintain phase using a synapse of constant duration. In this case, the intrinsic properties of the LP neuron most likely had a greater influence in determining phase. Using the interpolation data, a synapse of a constant duration and setting the LP phase to 0.34, the values obtained for G_{max}, are not biologically plausible in the synapses in this system. Therefore, with high values of $G_{max,}$ it is not possible for φ to remain constant.

We show that a synapse with a constant duty cycle maintains phase better than a synapse with a constant duration. Short-term synaptic plasticity is ubiquitous in neural circuits (Fortune and Rose, 2002, Carver et al., 2008). At some ranges of the cycle periods tested, the synapse determines phase, where in others the postsynaptic neuron's intrinsic properties determine phase. This interplay between the dependence on intrinsic properties and synaptic depression allows for a greater range of periods where phase can be maintained when the synapse has a constant duty cycle. At lower periods, with a synapse of constant duration, the synapse is characterized as strong and maintains phase. However, as period increased the synapse becomes weaker and therefore less effective in maintaining phase.

5.4.2 How would TP affect the φ of the Neuron?

The results from this study show TP is effective at maintaining a particular φ across different periods. The effect of changing TP values works in concert with the constant duration and constant duty cycle of the synapse. Changing the TP of the synapse, creates a way with which to limit the φ maintenance to a particular range. The effectiveness of TP is dependent on the period, the G_{max} and the duration (constant duty cycle or duration) of the synapse.

There are marked differences with which TP can maintain φ in both the constant duration and constant duty cycle cases. We show that with a constant duty cycle, a wider range of TP can be used to maintain φ but only within particular ranges of cycle period. Changing TP and G_{max} to a smaller value, we

show that phase is maintained at faster periods. When the duration is constant, changing TP allows for a very limited range of phase maintenance, at periods between 1000 and 1200 ms. These results indicate that in combination with a constant synaptic duration, this method is an ineffective method with which to maintain phase biologically.

The results indicate that there are different methods in which to effectively maintain phase in a biological network. This phase maintenance is state dependent and may depend on 417004114the current network needs, in which to adjust the phase of follower neurons.

5.4.3 Neuromodulators

Our results show the effects of a compound synapse onto the LP follower neuron. However, we have shown that the contribution of each of the pacemaker ensemble neurons is different, with the main contributor being the AB neuron (glutamatergic), while the contribution of the PD neuron (cholinergic) is relatively small (Appendix A).

One way that the network may use this to its advantage is to use neuromodulators to change the effect of one pacemaker neuron over the other. By doing so, a completely different functional output can arise. Changes in pyloric frequency are induced through the use of network neuromodulators (Ayali and Harris-Warrick, 1999, Zhao et al., 2011). .

5.4.4 The Importance of Phase Maintenance in Oscillatory Networks

The results strongly suggest an important role for short-term synaptic depression to produce phase maintenance in oscillatory networks as predicted by Manor et al (2003). Additionally, the effectiveness of short-term depression in oscillatory networks can possess both a frequency and time dependent modality as shown here.

Phase maintenance is important in producing and maintaining rhythmic neural output across different frequencies. Locomotion in organisms such as leeches and lamprey swim be organizing left-right alternation in each body segment and produce a wave that propels them (Marder et al., 2005). Behaviors such as locomotion, respiration, heartbeat generation, and feeding do not occur at one frequency, but the networks that control these behaviors must be adjusted depending on organismal needs (Sillar, 1996, Feldman and Del Negro, 2006). Therefore, it is reasonable that the properties of the synapses must adjust dynamically as a function of network frequency to meet network demands. We show that networks can find different solutions in order to promote phase maintenance. Networks most likely use a combination of these two parameters (synaptic peak phase or synaptic strength) to promote phase maintenance. The data from this study shows that synaptic strength can change across different periods, to maintain a specific phase. Differences in synaptic strength, have been shown in the leech heartbeat central pattern generator. The synaptic strength of the synapses in the core CPG of the leech heartbeat, can vary three to seven fold. Yet despite these differences, the

characteristic output is maintained, showing that wide variability in connections strengths occur despite the neuron pair type. At higher pyloric network frequencies, for example, the synapse may not largely contribute to phase but may be regulated by the intrinsic properties of the postsynaptic neuron; the opposite at low frequencies. This study mimicked the varying of these parameters to acquire the best solution for maintaining a specific phase.

CHAPTER 6

ALTERING THE PARAMETERS THAT DETERMINE THE EFFECT OF THE INHIBITORY FEEDBACK SYNAPSE ON THE PYLORIC CYCLE PERIOD

So far, we have shown that phase maintenance cannot be solely determined by the intrinsic properties of the isolated individual neuron. We have also shown that short-term synaptic depression of a feedforward synapse is plays a role in phase maintenance. However, this also is not solely responsible for phase maintenance in the pyloric network. In this chapter, we investigate the dynamics of a feedback synapse and determine how the phase of the synapse can induce changes in pyloric cycle period.

6.1 Introduction

The strength, temporal dynamics, duration, and timing of the activation of synaptic currents can have profound effects on the performance of neural circuits. In oscillatory circuits, such as CPGs, the parameters that define the properties of synapses can determine the oscillation frequency (Prinz et al., 2003, Mamiya and Nadim, 2004, Nadim et al., 2011). In this chapter, we describe how the amplitude, dynamics, duration and phase of synaptic inputs to pacemaker neurons in an oscillatory network affect the cycle period of oscillations.

In the crab pyloric network, the synapse from the lateral pyloric (LP) neuron to the pyloric dilator (PD) neuron represents the sole chemical feedback from the follower neurons. This inhibitory feedback synapse has complex

dynamics exhibits short-term synaptic depression (Zhao et al., 2011) and is believed to stabilize the pyloric network frequency (Nadim et al., 2011). Additionally, the LP neuron is inhibited by the pacemaker neurons (feedforward inhibition) as well as from other follower neurons such as the PY neuron.

Changes in the dynamics of the LP to PD synapse can regulate the pyloric cycle period (Mamiya and Nadim, 2004, Nadim et al., 2011). When the LP neuron is active in the early part of the pacemaker cycle, it speeds up the rhythm, whereas when the synapse is active in the middle or late phases of the pyloric rhythm, the synapse acts to slow down the oscillations (Nadim et al., 2011). Furthermore, functionally removing the LP to PD synapse during the ongoing rhythm increases pyloric network cycle variability (Nadim et al., 2011, Nadim et al., 2012). Mamiya and Nadim (2004) used dynamic clamp in order to mimic the change in the peak of the biological synapse and found that the peak time of the synapse may be important in determining the cycle period (Mamiya and Nadim, 2004). Prinz et al., (2003) examined the effect of both duration and synaptic strength on the cycle period. They found that duration of the synapse could act to increase the cycle period; strength did not have an effect. Ayali and Harris-Warrick (1999) provided the relationship between synaptic phase and cycle period, showing that a synapse later in the synaptic phase caused an increase in the cycle period. However, these studies did not examine the effects of changing all four of the above parameters simultaneously on the pyloric cycle period.

We were interested in building on the previous studies listed above and understanding how the pyloric cycle period is affected by a combination of the following parameters: synaptic phase (φ_{syn}), duration of the synapse (Dur), triangle peak phase (TP), and synaptic strength (G_{max}). These parameters define the shape and timing of the synaptic conductance waveform. To examine the effect of the altering the synaptic conductance waveform, we blocked the LP to PD chemical synapse pharmacologically and added a simulated version of this synapse using the dynamic clamp technique. We varied all four parameters through several values and injected the synaptic input through all combinations, thus exploring the role of each parameter and the combination of all four parameters on the network cycle period.

6.2 Materials and Methods

6.2.1 Activation of the Artificial Synapse

To study how the LP to PD feedback synapse (Figure 6.1) affects the pyloric cycle period, we replaced the biological synapse with an artificial synapse implemented using the dynamic clamp technique. The artificial synapse was activated using the PhaseResponse program (version 2.1; maintained by the Nadim Lab). PhaseResponse controls the injection of different waveforms at a fixed phase or time delay into an oscillating neuron. The PD neuron was impaled with two electrodes, one for reading membrane potential and the other for injecting current. We recorded 5 seconds of control activity, 20 seconds during
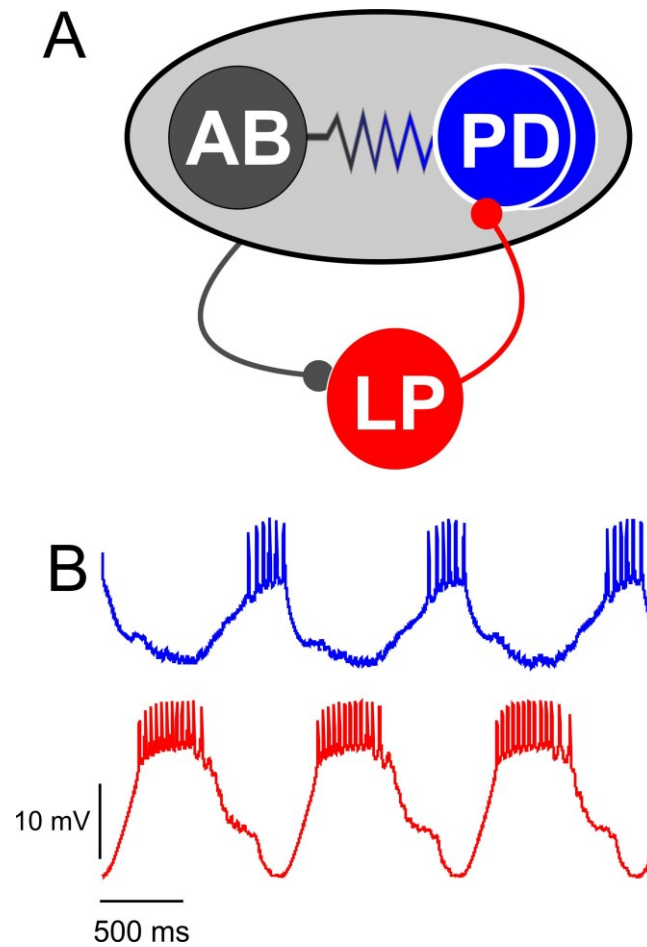
Figure 6.1 The pacemaker ensemble (AB and two PD) neurons and the follower LP neuron are connected through a reciprocally inhibitory synapse. **A.** Schematic diagram of the pyloric subnetwork, consisting of the pacemaker ensemble (the electrically coupled PD and AB neurons), which is connected to the follower LP neuron via inhibitory synapses. The LP neuron, the sole chemical feedback from the follower neurons to the pacemaker, inhibits the PD neuron. **B.** Simultaneous intracellular voltage recordings of the PD and LP neurons. The PD neurons oscillate antiphase with the LP neuron.

the synaptic injections and 5 seconds after the artificial synaptic input. We measured the pyloric cycle period for different combinations of the following synaptic parameters: synaptic onset phase, duration, TP, and synaptic strength.

The synaptic onset phase (φ_{syn}) was defined as the time between the onset of the PD neuron burst and the onset of the synapse, normalized by the period of the previous cycle (PD neuron burst onset to burst onset duration). Four values of φ_{syn} were used: 0, 0.15, 0.35 and 0.50 (Figure 6.2A). We used three values for the duration of the synaptic injection (Dur): 250, 300 and 500 ms (Figure 6.2B). The injected synaptic conductance in each cycle had a triangular shape: the conductance ramped up to the maximal value and then ramped down back to 0. The peak phase (TP) of the triangular conductance was varied over five values: 0, 0.25, 0.5, 0.75, and 1.00 (Figure 6.2C). For example, the value TP=0 indicates that the conductance was immediately set to its maximum and then ramped down to 0 whereas TP=1 means that the conductance ramped to its maximum and then immediately set to 0. We used three different maximal synaptic conductances (G_{max}): 0.1, 0.2, and 0.4 µS (Figure 6.2D). With this combination of parameters, in each experiment the triangular conductance was injected over 180 runs (4 φ_{syn} x 3 G_{max} x 5 TP x 3 Dur). Lastly, the reversal potential of the artificial synapse was set to a fixed value of -80 mV as reported previously (Zhao et al., 2011).

The artificial current was activated periodically (once for each cycle of the PD neuron oscillation). The synapse was activated at a prescribed phase φ_{syn} as defined above for a preset duration (Dur). The cycle period of the pyloric
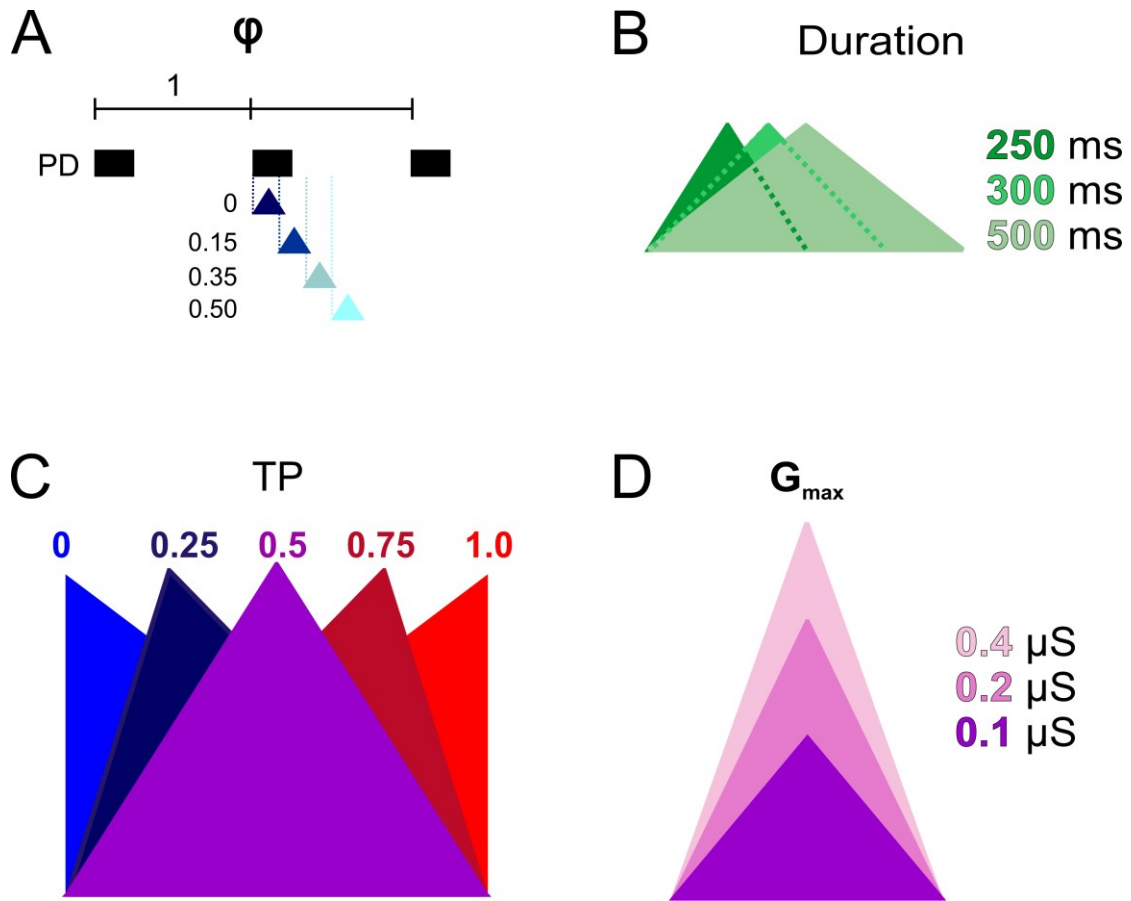
Figure 6.2 Four parameters were varied in the experimental paradigm. **A.** The synaptic onset phase (φ_{syn}) was defined as the time between the onset of the PD neuron burst and the onset of the synapse, normalized by the cycle period (PD neuron burst onset to burst onset duration). Four values of φ_{syn} were used: 0, 0.15, 0.35 and 0.50 (denoted through blue triangles). The PD burst is denoted by each black square, the point at which the triangle stimulus is applied is calculated from the prior cycle. **B.** The conductance had three different durations: 250ms, 300ms, and 500ms. **C.** Triangle peak phase (TP) was varied to mimic and cover the whole range: 0, 0.25, 0.5, 0.75, and 1.00. **D.** Three values were chosen for G_{max}: 0.1, 0.2 and 0.4 µS.

network is not known at the initial time of the synaptic injection, the Phase Response software automatically calculates the delay, using the previous cycle period, to the selected value of φ_{syn}. For example, if φ_{syn} was set to 0.15, Dur to 300 ms, TP to 0.5, G_{max} to 0.4 µS, and the previous cycle period was 1000 ms, the synapse was activated at 150 ms (following the onset of the PD burst), peaked at 300 ms and at 0.4 µS, and then decayed linearly (in conductance) to end at 450 ms. Because the PD cycle period could vary, the Phase Response program adapted the onset time of the synapse on a cycle-to-cycle basis to maintain a constant φ_{syn} value. This produces a closed-loop stimulation protocol. This protocol was chosen to mimic the activation of the biological LP to PD feedback synapse.

6.2.2 Software

Data were acquired using both pClamp 9.0+ (Axon Instruments) and PhaseResponse. All data were sampled at 5 kHz and saved on a PC using a Digidata 1332A (Molecular Devices) and a PCI-6070-E data acquisition board (National Instruments). Matlab (MathWorks) scripts were developed in order to calculate the burst onset and cycle period.

6.2.3 Analysis and Statistics

Data were analyzed using both Readscope and a Matlab script to calculate changes in cycle period. Statistical analysis was performed using Sigmaplot

12.0 (Systat). Significance was evaluated with an α value of 0.05, error bars and error values reported denote standard error of the mean.

All quantitative measurements in this chapter were done on the PD neuron cycle period while changing four different parameters, synaptic phase (φ_{syn}), duration (Dur), maximal conductance (G_{max}) and peak phase (TP), across a number of values (Figure 6.2, as described earlier in this section). All parameter values were measured in every preparation (N=3) and there were no missing data points. The only statistical analysis performed, therefore, was a four-way ANOVA which indicated which of the parameters produced a significant change in the cycle period. A *post hoc* Tukey analysis was then performed to determine the statistical significance of the effects of individual parameters and to do pairwise comparisons.

6.3 Results

In order to understand how synaptic phase (φ_{syn}), duration (Dur), maximal conductance (G_{max}) and peak phase (TP) alter the pyloric cycle period, we pharmacologically blocked the biological synapse and used the dynamic clamp technique to periodically apply an artificial LP to PD synapse (Figure 6.1). In each run, a synaptic conductance of specific G_{max}, Dur, and TP was applied periodically, starting at a constant φ_{syn} in the PD cycle. The shape of this conductance was triangular, which approximated the shape of the PSP recorded in the PD neuron (Mamiya and Nadim, 2004). The different TP values were used because the peak time of this synapse is known to vary as a function

of cycle period (Mamiya and Nadim, 2004). First we examined the result of varying each single parameter individually and then the result from all four parameters combined.

6.3.1 How does the synaptic phase φ_{syn} affect the pyloric network period?

φ_{syn} was calculated from the PD burst onset, and applied at four different values (Figure 6.2A): 0.00 (the onset of the PD burst) 0.15, 0.35, and 0.50. These data show that the cycle period can either decrease or increase depending on the value of φ_{syn}. For φ_{syn} at either 0 or 0.15, the cycle period decreased when compared to control (Figure 6.3). There was not a significant difference between φ_{syn} =0.00 and 0.15. At the higher value of φ=0.5, the period increased greatly when compared to control (110 – 140%). However, with φ_{syn} =0.35, the pyloric period did not differ much from control. Therefore, we found that the artificial LP to PD synapse shortened the cycle period when applied at an early phase (*post hoc* Tukey Test F=623.369, p<0.001) and increased the cycle period when applied at the later phase. This result is consistent with previously reported findings (Ayali and Harris-Warrick, 1999, Mamiya and Nadim, 2004, Nadim et al., 2011).

6.3.2 How does synaptic duration (Dur) affect the pyloric network period?

The average duration of the LP to PD synapse is approximately 200 ms. However, the duration of the synaptic current may vary depending on the cycle period of the network (Mamiya and Nadim, 2004). Previous studies have

indicated that this parameter may have a large influence on the rhythm cycle period (Prinz et al., 2003). Therefore, we examined how cycle period is changed by altering the duration of the synaptic input (Figure 6.2B) for a decreased cycle period (φ_{syn} = 0.0, 0.15) and increased cycle period (φ_{syn} = 0.35 and 0.50). As synaptic Dur increased, we found that for φ_{syn} values of 0.35 and 0.50 and for all G_{max} and TP values that the cycle period increased from the original control values (*post hoc* Tukey Test, F=64.573 p<0.001). The greatest difference in cycle period was found with Dur=500 ms and φ=0.50, where the cycle period increased to 1.5x that of control.   For φ=0 and 0.15, the cycle period increase was greater with increasing Dur values (Figure 6.3).

6.3.3 How does the synaptic peak phase (TP) affect the pyloric network period?

Now that we have determined that synaptic duration and φ_{syn} can change cycle period, we examined the effect of the different TP (triangle phase) on the pyloric cycle period. The TP values that we used were 0, 0.25, 0.50, 0.75 and 1.00, covering the entire possible range (Figure 6.2C & Figure 6.4), and each

TP value was applied at all Dur (250, 300, 500ms) and φ_{syn} (0, 0.15, 0.35, 0.50) values. Across all values of φ_{syn} and Dur, TP had a great influence on the cycle period. In general, increasing TP (0 to 1) always led to longer cycle periods 15 (*post hoc* Tukey Test F=28.106, p<0.001; Figure 6.3).
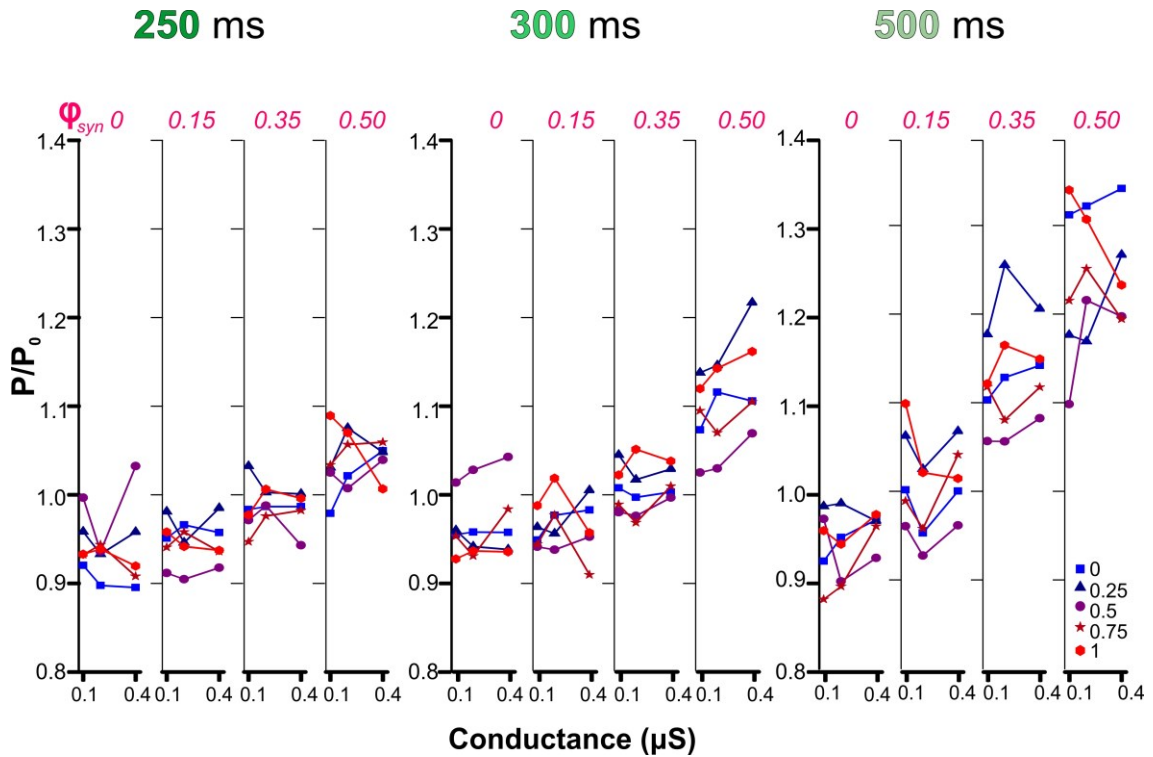
Figure 6.3 The effects of duration, G_{max}, φ_{syn}, and TP on the cycle period of the PD neuron. Each panel represents one of the three different durations (Dur) of 250ms, 300ms, and 500 ms. At each Dur, we calculated the normalized cycle period at the three values of G_{max} (0.1, 0.2, and 0.4 µS), five values of TP (0, 0.25, 0.5, 0.75 and 1.00) and the four values for φ_{syn} (0, 0.15, 0.35 and 0.50). When the duration was at 250ms, and with φ_{syn} at 0, 0.15, 0.35, the cycle period decreases. However, at φ_{syn} 0.5, the cycle period increases with the stimulus in comparison to control. At 500ms, with a φ_{syn} of 0.15, 0.35 and 0.50 the period increases in comparison to control.

6.3.4 Does synaptic strength G_{max} affect the pyloric period?

Thus far, we have shown that synaptic phase, duration and TP can affect the pyloric cycle period. We were also interested in determining if G_{max} could also alter cycle period. We used three values of synaptic amplitude: 0.100, 0.200 and 0.400 µS (Figure 6.2D). Across all φ_{syn}, Dur and TP values, G_{max} did have a significant effect on cycle period (*post hoc* Tukey Test, F=10.203 p<0.001; Figure 6.3).

6.4 Discussion

we used the pyloric network of the crab (*Cancer borealis*), to explore the feedback synapse from a follower neuron to pacemaker. We determined the response of the pacemaker neuron to the synaptic input of the follower neuron depends on the synaptic phase, and this feedback synapse may be responsible for stabilizing the rhythm period of the network.

If the synapse is active earlier in the PD phase, it acts to decrease the cycle period. Comparatively, if the synapse arrives late in the PD phase, then it acts to increase the pyloric network cycle period. We speculate that the changes initiated by the LP to PD synapse, therefore, not only change the cycle period but can also promote changes in the follower neurons. These changes in the follower neurons, including the LP neuron, may include changes in burst duration, amplitude and spike rate. The PD neuron receives inhibition from the LP neuron, and the AB/PD inhibits the LP neuron. There is also a reciprocal

115
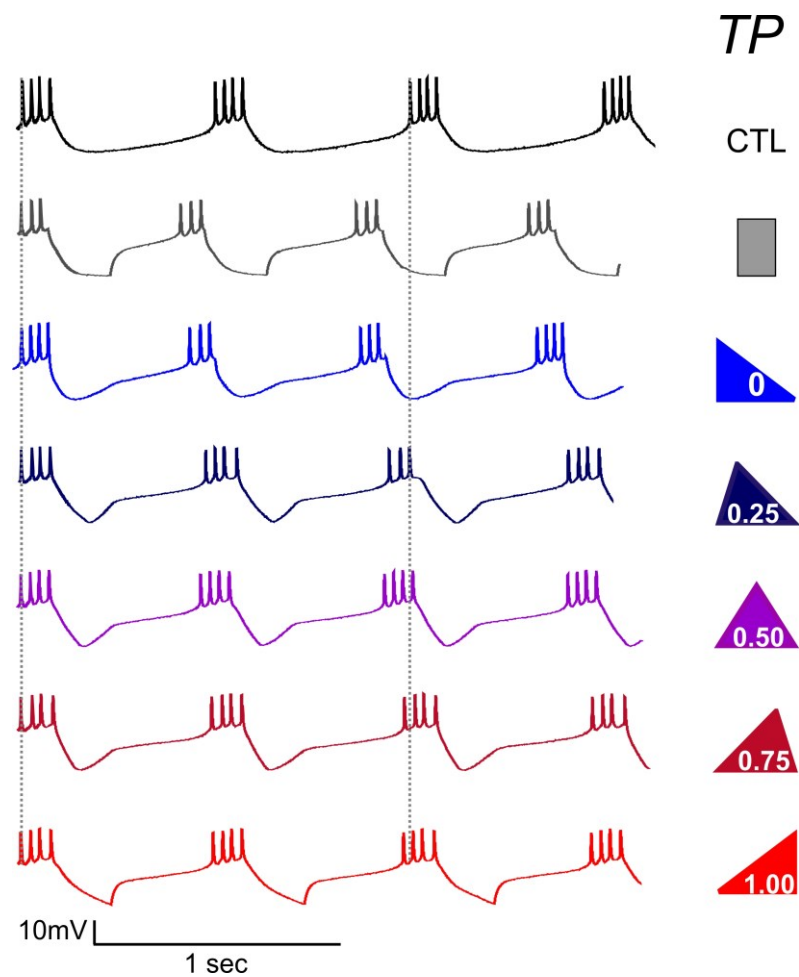
Figure 6.4 Recordings from the PD neuron during different TP stimuli. The PD neuron was recorded in control conditions, in the presence of PTX without inhibition from the LP neuron. All traces are lined up from the beginning of each PD burst at each TP. As the TP is varied from 0 to 1, we see that there was a delay of the onset of the burst when compared to control (denoted as difference from grey vertical line). The duration (Dur) was 500 ms for each trace. The square pulse had a duration of 250ms, equivalent to the same area of the 500ms TP.

synapse between the LP and PY neuron, this synapse can change the bursting properties of the PY neuron. If the cycle period is increased, then the LP burst becomes longer, and in that manner the LP to PY synapse acts to shorten the burst duration of the PY neuron and still maintain relative phase in the network. The PY neuron then synapses onto the LP neuron, which then synapses onto the PD neuron providing details on the bursting properties of the follower neurons. The interaction of these two feedback loops, demonstrates how two feedback loops can maintain phase constancy in an oscillatory network. This closing of the feedback loop (between the LP and PD) allows for phase constancy across the pyloric network. As changes are detected in the network and imposed onto the follower neurons, phase can therefore be maintained by promoting changes in the properties of each neuron.

This study builds on the concepts previously explored by Ayali and Harris-Warrick (1999), Mamiya and Nadim (2004) and Prinz et al (2003). Ayali and Harris-Warrick only examined the effect of φ_{syn} and in their study they did not change φ but only provided a correlative relationship between φ and cycle period, showing that a synapse occurring later in synaptic phase caused an increase in the cycle period. Mamiya and Nadim (2004) only explored the effect of TP on cycle period, showing that at an earlier TP shortened the rhythm period and a later TP increased the cycle period when compared to control. Whereas Prinz et al. (2003) only examined the effect of G_{max} and Dur on the cycle period. They found that G_{max} did not have an effect on the cycle period, however, synaptic duration did act to increase the cycle period. None of these

117

studies explored the combined effect of all four synaptic parameters on cycle period as we have done here.   By varying duration, G_{max}, φ_{syn}, TP, and duration, we set out to find how the combinations of these four parameters interact to either shorten or lengthen cycle period.   However, we have found that G_{max} does have an effect on cycle period, which differs from findings from Prinz et al. (2003). We propose that the synapse adjusts these properties when the cycle period becomes too long or too short, in order to compensate and oppose these changes, therefore, stabilizing the cycle period.

6.4.1 Feedback Inhibition in Other Networks

Feedback is an important feature in many neural networks such as those responsible for heartbeat generation, and sensory transmission at the thalamocortical level (Norris et al., 2007a, Wright and Calabrese, 2011, Suzuki and Bekkers, 2012).   In order to understand how differences in synaptic strength are compensated for in an oscillatory network, Norris et al., (2011) examined the synapses of the leech heartbeat CPG. The leech heartbeat CPG differs from the pyloric network. While both the leech heartbeat CPG and the pyloric network are centrally located, the leech heartbeat CPG is distributed among multiple interconnected ganglia which possess phase relationships with respect to each segment. Phase progression in four of these segments (H8-H12) arises because the relative synaptic strength of four inputs varied across the segmental motor neurons. In a motor neuron that receives multiple inputs, they found that not only was the synaptic strength variable from all of the inputs,

but that this synaptic strength varied greatly from animal to animal (Norris et al., 2007a). In order to compensate for this variation in synaptic strength, they found that the temporal patterns of the presynaptic neurons in fact also possessed wide variation. The changes in synaptic strength and temporal firing patterns were found to determine different firing patterns of the leech heartbeat CPG. Consequently, in the peristaltic motor patterns, the temporal patterns of the neurons determined the phase with which the motor neurons fired, while synaptic strength defined intersegmental motor phase progression (Wright and Calabrese, 2011). An assumption is that changes in synaptic strength will have functional consequences for the circuit. In the pyloric network, we see that within the same animal, changes in synaptic strength of the feedback synapse altered the cycle period. The ability for synaptic strength vary across animals may be a way in which cycle period changes can occur despite variable synaptic strengths across different animals.

Feedback inhibition is a property of not only the pyloric network but larger networks as well. The piriform cortex (PC) located in the ventral forebrain and the first cortical recipient of the information from the olfactory bulb, exhibits both feedforward and feedback inhibition (Suzuki and Bekkers, 2012). The properties of feedback inhibition in the PC, mostly accomplished via fast-spiking multipolar cells, are of interest in understanding olfactory coding and oscillations. Dynamic clamp experiments in this system have shown that feedback inhibition is provided mainly by one class of interneuron, similar to the role of the LP neuron in the pyloric network. This feedback inhibition is driven by

two types of layer II neurons, cells from the neurogliaform and the horizontal cells of the superficial layer of the PC.   This microcircuit is similar to the feedforward and feedback relationship in the pyloric network.   As we had previously shown, feedforward inhibition is responsible for changing properties of the follower neurons; here, we present that feedback inhibition is important in altering cycle period and therefore neuronal properties.   In the PC, these two processes are believed to be responsible for processing of olfactory information, however, the mechanism is not fully known. My work here can give insight on the interaction of feedback and feedforward networks such as the in the PC. We have proposed how a feedback and feedforward work in concert to maintain stable activity in a network.   The same mechanism may be present between the interneuron of layer II that drives the feedback inhibition to horizontal cells of the PC. It would be interesting to apply some of the same mechanisms we have presented for changing synaptic parameters of the LP to PD synapse, to the interconnected neurons of the PC.

6.4.2 Changing the Cycle Period via Synaptic Phase

We found that when the synaptic phase is early, the cycle period is slowed and when the synaptic phase is late, the cycle period increases (Mamiya and Nadim, 2004).   The LP to PD synapse therefore provides a method in which to control the pyloric network speed. This negative feedback closed loop system stabilizes the cycle period after a perturbation and allows for flexibility in network output (Nadim et al., 2011).

Of all parameters examined, the φ_{syn} had the second largest effect on the pyloric cycle period. This result was consistent across all TP and G_{max} values. The shortening of the pyloric period for small φ_{syn} could be due to the early termination of the PD burst by the synapse. This decrease in the pyloric period could result in an earlier post-inhibitory rebound and a faster cycle period. For larger φ_{syn} values the cycle period increased. This increase in cycle period is primarily due to the fact that late inhibition delays the next PD neuron burst..

In the crayfish swimmeret system four segmental oscillators are interconnected by coordinating neurons. Synaptic strength between the segmental oscillators decreases as a function of distance (Smarandache et al., 2009). However, due to a phase difference of 0.25 between each segmental oscillatory, inputs of different strengths arrive at different phases of the cycle, or as we refer to here φ_{syn}. While this shows a manner in which φ_{syn} promotes phase maintenance in other systems, synaptic strength seems to vary with the presence of multiple oscillators, similar to the leech heartbeat CPG.

6.4.3 The Role of Synaptic Duration

When the duration of the synapse was increased, we saw an increase in the effect of changing synaptic phase. An increase in duration of the synapse only served to further decrease the cycle period at the lower synaptic phases, and further increase it at higher synaptic phases. Changing the synaptic duration may allow for the altering of the synapse at either faster or slower cycle periods without having to change the synaptic phase in the process.

The duration of the inhibitory pulses determines the time delay of the next burst. The PD neuron remains hyperpolarized during the duration of the or through the stimulus of different TPs. Therefore, the longer the duration of the synapse the longer the delay the onset of the next burst. This method may be a way in which to increase or decrease the period of the network.

6.4.4 Neuromodulation of Feedback Inhibition

Within the pyloric network there are neuromodulators that change the dynamics of the synapse from the LP neuron to the PD (Zhao et al., 2011). This may be one of the ways in which the network's feedback through the LP to PD neuron synapse can influence the AB neuron and therefore change the release of neuromodulators from projection neurons. The actions of the modulatory commissural neuron 1 (MCN1) are gated through the feedback from the pyloric network. Specifically, spontaneous MCN1 activity occurs in pyloric timing, via inhibitory action of the ascending AB neuron (Coleman and Nusbaum, 1994). Comparatively, RPCH causes a several-fold increase in synaptic strength in the LP to PD synapse, but does not cause a change in pyloric cycle period (Thirumalai et al., 2006).

In the CA1 area of the hippocampus, cell-type-specific modulation of the feedback inhibition by serotonin is prominent. Serotonin exerts many modulatory functions in the CNS in physiological and disease conditions (Barnes and Sharp, 1999). The regulation of serotonin release is attributed to presynaptic serotonin 1A (5-HT_{1B}) and serotonin 1B (5-HT_{1B}) receptors

(Boschert et al., 1994, Sari, 2004, Fink and Gothert, 2007). Serotonin activates presynaptic 5-HT$_{1B}$ receptors in the CA1 region of the hippocampus, which therefore regulated glutamate released from the CA1 pyramidal neurons onto interneurons in a target-cell specific manner (Winterer et al., 2011). This activity then acts as a selective modulator of feedback inhibition. First, activation of 5-HT$_{1B}$ heteroreceptors reduces synaptic excitation of cholecystokinin-expressing interneurons. This activation is specific to the input, affecting only glutamate transmission from CA1 pyramidal cells. This glutamate release from CA1 pyramidal cells causes a demonstrable reduction in spike probability in serotonin-sensitive interneurons (Winterer et al., 2011). Perhaps, neuromodulation of specific cells as seen in the pyloric network, can be a method with which changes of the properties of the feedback synapse can be accomplished. Neuromodulation of CA1 pyramidal cells, similar to the pyloric network, can change the properties of the feedback inhibition. Cell-specific modulation of the pyloric network is also present, affecting the properties of the network (Swensen and Marder, 2001). While not having a direct impact on the synapses, changing different parameters of the neurons, such as activating inward currents, could in turn change the properties of the feedback inhibition and in turn the network. For example, CCAP targets both the LP and AB neurons however, does not target the PD neuron directly. However, even though the PD neuron may not be a direct target of CCAP, PD can possibly change its activity pattern as a consequence of circuit interactions. Phaseresponse studies such as the ones we have performed here can provide

a tool by which to assess the role of neuromodulators while changing the parameters of the synaptic conductance waveform on cycle period.

6.4.5 Individual Solutions for the Same Problem

We have shown four different ways in which the feedback synapse from the LP to PD neuron can alter cycle period. The combination of G_{max}, φ_{syn}, TP, and duration may be a way for the system to maintain stable output. While a general conclusion cannot be applied wholly across the board, each animal can adapt a method of these three parameters or all of them to meet system needs. The temporal pattern of output of each neuron may be different, and compensating for these changes and promoting phase maintenance would be an essential task of the feedback synapse.

CHAPTER 7

DISCUSSION/CONCLUSION

7.1 General Discussion

The primary purpose of this thesis is to understand at what level stability, defined as phase constancy, arises in an oscillatory network. In order to determine the source of this stability, the aims of this thesis were divided into two main goals. The first goal was to understand the frequency-dependent biophysical properties of synaptically-isolated neurons which are components of an oscillatory network and whether these properties were sufficient to enable phase constancy. The second goal was to understand how synapses can promote phase constancy and set the relative phase of neurons in an oscillatory network. As a model system, we used the pyloric network of the crab *Cancer borealis*, and applied pharmacological and neurophysiological tools to accomplish the goals we have outlined. Based on the results outlined in this thesis, we conclude phase constancy arises through the interaction of intrinsic properties of neurons and synapses.

The first goal of the thesis (i.e. understanding the frequency-dependent biophysical properties of the synaptically-isolated neurons) was accomplished in two ways. Specifically, we asked (1) if each synaptically-isolated pyloric network neuron possessed distinct frequency-dependent biophysical properties, and if these properties gave each neuron an inherent stability, and (2) what ionic currents underlie these frequency-dependent properties as well as the

burst onset and burst end of each neuron (Chapters 3 and 4). My second goal was also accomplished in two ways. We used (1) the dynamic clamp to investigate the effects of particular parameters (G_{max}, peak phase, cycle period and duty cycle) on phase maintenance on the follower neuron LP, and (2) phase response to determine how the synapse from a follower (LP neuron) to a pacemaker neuron (PD) can alter the cycle period and network properties (Chapter 5 and Chapter 6).

7.2 Main Results of the Thesis

To understand at which level (i.e. individual neurons vs. synaptically-connected neurons) stability arises in a motor network, we examined four main questions relating to the properties of the individual pyloric network neurons and synapses. In this section, we explore the general findings of the question addressed in each chapter.

7.2.1 Chapter 3: Activity Profiles of Pyloric Neurons

In this chapter, we proposed that network stability is captured as inherent properties of the individual neuron types. We were interested in determining if each pyloric neuron type had a unique frequency-dependent activity profile.

The activity profiles surveyed the following properties of each synaptically-isolated neuron as a function of frequency: burst onset phase, burst end phase, resonance frequency and intraburst spike frequency. My results indicate that each isolated pyloric neuron type possesses a unique frequency-

dependent activity profile. One of the key findings in this chapter is that burst onset phase changed as a function of the sinusoidal input frequency that was used to drive each pyloric neuron type tested. This provides evidence that the pyloric neurons are not intrinsically phase-constant, and are therefore not the source of phase maintenance in the pyloric network.

7.2.2 Chapter 4: Frequency Dependence of Currents

In this chapter, we were interested in determining the contribution of one particular intrinsic ionic current, I_h on one activity profile parameter, burst onset. we suppressed I_h, using extracellular CsCl, in the LP, PY and PD neurons and examined the consequences for their burst onset. We found that I_h contributes to the burst onset in a frequency-dependent manner in these three neurons.

7.2.3 Chapter 5: Phase Constancy in Oscillatory Neurons

After showing that phase constancy was not a property of the individual neurons, we were interested in determining the contribution made by synapses to promote phase constancy in the follower pyloric neurons. We hypothesized that phase maintenance across frequencies is achieved via short-term synaptic plasticity.

Previous theoretical work showed that short-term plasticity, specifically short-term depression (STD), and inhibitory synapses, can promote phase constancy (Manor et al., 2003). Therefore, we used a brute-force method to confirm the results of these previous theoretical studies. Specifically, we used

the dynamic clamp to mimic short-term synaptic plasticity in a synaptically-isolated neuron and manipulate the associated synaptic parameters (G_{max}, duration, and peak phase (Δt/period)) to understand which parameter(s) promoted phase constancy. We focused on the feedforward inhibitory synapse from the pyloric pacemaker group (AB/PD) onto the LP neuron, and found that phase constancy was produced by changing synaptic strength, peak phase or duration, as well as by changing a combination of these three parameters.

7.2.4 Chapter 6: Altering the Parameters that Determine the Effect of the Inhibitory Feedback Synapse on the Pyloric Cycle Period

In Chapter 5, we investigated the effect of changing synaptic parameters of a feed-forward synapse (AB/PD to LP). Now, in Chapter 6, we proposed to understand how feedback inhibition (LP to PD) promotes cycle period change in the pyloric network. We used the dynamic clamp to mimic the LP to PD synapse and implement a brute force method by simultaneously changing four parameters of this synapse (synaptic phase, peak phase, amplitude and duration). We were interested in determining what combination of these parameters was most effective in setting the pyloric cycle period. It was previously proposed that synapse duration, but not amplitude, was important for promoting changes in cycle period (Prinz et al., 2003). This thesis builds on work previously explored by Ayali and Harris-Warrick (1999), Prinz et al. (2003), and Mamiya and Nadim (2004). We studied the effect of simultaneously varying all four parameters rather than individual parameters. We found that

peak phase, synaptic phase and duration, G_{max} were the most influential parameters in changing cycle period.

7.3 The Role of Intrinsic and Synaptic Properties in Setting Phase in the Pyloric Network

We showed that a combination of intrinsic neuron properties and synaptic input can contribute to maintaining stable pyloric network activity. Each pyloric neuron possesses a distinct set of electrophysiological properties that determines their bursting across different input frequencies. However, these properties are not enough to explain phase constancy (Chapter 3). The activity profiles, as we have deemed them, give these neurons the ability to fire uniquely at different frequencies. Additionally, the intrinsic current levels and their frequency dependence add further to the flexibility possessed by each neuron. These frequency-dependent properties, including that of the intrinsic currents (Chapter 4), may work in conjunction to set the stable temporal characteristics of the pyloric network.

In the intact network, the neurons of the pyloric network maintain phase quite well across many different frequencies (Bucher et al., 2005). As shown by my results, as the frequency of our input increased so did the phase of each neuron. If the intrinsic properties of the neurons were sufficient to maintain phase, then at all input frequencies we would not have seen a change in the phase of the burst onset. My results clearly indicate that the properties of the individual neurons are not sufficient to explain phase constancy in this oscillatory network. This finding shows that, in order to maintain phase, there

must be synaptic interactions that promote phase constancy, enabling the neurons to maintain relative phase.

Previous work in *P. interruptus* indicated that the relative activity phase of the LP and PY neurons was independent of the compound synapse they receive from the pacemaker ensemble (Rabbah and Nadim, 2007). This suggests that the intrinsic properties of the individual neuron types are also responsible for maintaining phase. As we show here, the frequency-dependence of the burst onset of neurons in the pyloric network may be a way in which the intrinsic properties of the neurons set phase. The synapse from the pacemaker ensemble is responsible for setting phase of the network by recruiting the intrinsic currents of the LP and PY neurons: e.g. I_h, which contributes to the LP neuron burst onset; I_A, which was previously shown to delay the PY neuron burst onset. Hyperpolarization acts to activate I_h and de-inactivate I_A. We show, for the first time experimentally, that by mimicking the AB/PD to LP synapse, and using the same synaptic periodic input, a specific activity phase can be set for the LP neuron.

7.4 Implications for Oscillatory Networks

The general lessons learned from the study of invertebrate oscillatory neural networks can be applied to the study of larger vertebrate networks. Invertebrate systems such as *Tritonia* swimming, leech heartbeat, insect walking and the decapod crustacean stomatogastric nervous system have been invaluable for understanding the neuronal basis of motor pattern generation

(Getting, 1983, 1989, Calabrese, 1995, Marder and Calabrese, 1996, Marder, 2012). One such lesson is that, despite the presence of noise and variability intrinsic to network neurons, oscillatory network output must remain stable. The findings in this thesis underline the synergistic relationship that synapses and neurons have in promoting this stability in network output.

Many of the principles present in the STNS are also found in other networks, such as the mammalian respiratory CPG (Ramirez et al., 2004, Ramirez et al., 2011). Some of these principles include (1) utilizing pacemaker neurons to synchronize other networks neurons, (2) modifying intrinsic and synaptic properties with neuromodulators, (3) having various network properties (e.g. cycle frequency) be state-dependent. The mammalian respiratory network, for example, can be reconfigured from generating an inspiratory motor pattern to a gasping motor pattern. Gasping is an auto-resuscitation mechanism which can fail in infants, leading to death via sudden infant death syndrome (SIDS) (Ramirez et al., 2004). To generate multiple behaviorally-relevant motor patterns, such a network needs to have many mechanisms for producing stable temporal output. Failure in such a network could have grave consequences. We demonstrated the importance of feedback inhibition for stabilizing cycle period, by changing parameters such as synaptic phase and onset in the follower to pacemaker neuron. Comparable mechanisms may be employed by other networks to maintain stable output, such as those involved in the aforementioned auto-resuscitation mechanisms.

Feedback inhibition, such as that found between the follower and pacemaker neurons of the pyloric network, also occurs in larger networks. For example, feedback inhibition regulates and stabilizes neural networks in the mammalian brain (Tepper et al., 2004). One example of this is found in the GABA-mediated inhibitory postsynaptic currents (IPSC) recorded in rodent cortical neurons that promote stable oscillations in the hippocampus. In pyramidal neurons, feedback inhibition resulting from the activation of interneurons limits sustained pyramidal neuron firing (Pouille and Scanziani, 2004). This feedback inhibition is accomplished in two ways, either by responding quickly to the firing of the CA1 neurons or through sustained inhibition which takes time to develop (Pouille and Scanziani, 2004). These two methods of feedback inhibition extract timing details to act as both a coincidence detector and an integrator. This type of feedback inhibition is also found through the LP to PD synapse of the pyloric network. The LP neuron is well-positioned to act as both a coincidence detector and integrator in the pyloric network. In *P. interruptus*, the LP neuron receives synaptic input either directly or indirectly from the IC, PY and VD neurons (Marder and Eisen, 1984b). The LP neuron can integrate these signals and produce one single coherent feedback onto the PD neuron. This process eliminates the necessity of the PD neuron receiving multiple synapses from the different follower neurons.

The phase in which LP fires ensures the activity of the pacemakers remains stable. For example, if there is a phase shift in LP activity, that may

influence pacemaker neuron activity. If cycle frequency changes, then the LP neuron adjusts its activity to maintain phase in the network, and once this adjustment occurs LP's influence is removed. We propose that the LP neuron acts as both a coincidence detector and an integrator. Because the LP neuron receives synaptic input from all of the follower neurons, and acts as the sole feedback to the pacemaker neurons, it acts as a target of convergence of all of the synapses from the follower neurons. This signal is integrated and then the LP synapses onto the pacemaker neurons. Without this, the pacemaker neurons would receive feedback from all of the follower neurons, rather than one single synapse. By mimicking the LP to PD synapse, and changing different parameters, we showed a possible mechanism by which this integration and coincidence detection can maintain and counteract change in the cycle period – either by changing synaptic phase, peak phase or duration.

Feedback inhibition can also occur between two different networks, as seen in sound localization in birds (Monsivais et al., 2000). The primary cue that animals use to localize low-frequency sounds are Interaural time differences (ITD) that vary with the position of the sound source in space (Burger et al., 2011). The nucleus laminaris (NL) of birds leads to calculation of the ITDs. binaural centers located in the superior olivary nucleus in birds (Burger et al., 2011). This allows for many properties which are geared to enhance the processing of temporal information. This system the provides inhibitory feedback to monaural and binaural systems in the superior olivary complex (SON) in birds and the superior olivary complex in mammals (Burger

et al., 2005). The inhibition allows for neural computation at the synaptic, cellular and system level, including extending the range of responses to sound and enhancing temporal coding by restricting the time window for integration of sound (Burger et al., 2011). This feedback inhibition leads to changes in spike rate, spike timing and frequency tuning, that maintain stable output and achieves sound localization in both humans and birds (Yang et al., 1999, Burger et al., 2011). The work in this thesis, allows for us to further understand how networks can inhibit one another. The same concepts discussed earlier can also be applied here to understand the mechanisms of feedback inhibition between multiple neural networks. The understanding of the feedback synapse from the LP to PD neuron allows us to understand the functional consequences of altering the feedback from one network to another.

Neural networks can adapt to constantly changing environments by modifying circuit configurations and producing several different functional outputs. Our understanding of these properties are not only applicable to the CPG we study here, but also to understanding the maintenance of stable activity in systems we have outlined such as the respiratory network and on a larger scale the interaction of many brain regions for maintenance of sound localization.

7.5 Future Directions

To understand the means by which a CPG can promote stability, the projects outlined in this thesis can be developed further. Some of these directions have been outlined above.

We studied the mechanisms by which short-term depression can promote phase constancy in an oscillatory network (Chapter 5). Additional work can be done to determine if any differences exist in the role(s) and effectiveness of the same properties in other pyloric network neurons (e.g. PY neuron). For example, we showed that the PY neuron possesses a different level of I_h than the LP neuron (Chapter 3). It remains to be determined, however, whether this distinct level of I_h has a different consequence for PY. The impact of I_h will result not only from its amplitude but from the amplitude of the other currents co-expressed in PY (which will often be distinct from LP). We propose that because the PY neuron possesses different levels of I_h, differences should be seen in the activity that is generated by the PY neuron to these experiments. If these experiments are repeated in the PY neuron, this will give further credence to our belief that both intrinsic and synaptic properties are responsible for maintaining a stable output.

Additionally, to understand the frequency-dependent properties of the network and the individual neurons (Chapter 3), the same manipulations can be repeated in the intact network. Specifically, driving the pacemaker neurons in the intact network with a sinusoidal stimulus (ZAP) can provide results on how the neurons adapt their firing properties to maintain phase constancy. As

frequency increases, the pyloric neurons would need to adjust in order to maintain phase. These additional data will also provide insight into the mechanisms by which the synapses also change their peak phase. Using a ZAP stimulus with the PD neuron in the intact network could explain how the phase onset and termination of bursts in the follower neurons changes with cycle frequency. This would provide better insight about the mechanisms used in the intact network to maintain phase constancy.

We have shown a correlation between the burst onset properties and only a single ionic current (I_h). Data on the effects of I_A on the burst onset and burst end were collected but not included in this thesis. Part of my future direction is to understand the role of I_A on burst onset and burst termination, as well as to understand if there is a frequency dependence to this current. As discussed previously, I_h and I_A are coregulated. Therefore, it would be important to understand how these currents operate in synchrony, which would further advance the study of how frequency dependence of ionic currents can drive changes in burst onset during different network demands.

One method to determine the effects of these currents on the phase constancy of the LP neuron is to repeat the experiments (Chapter 4) in the presence of CsCl. By blocking I_h, the belief that the synaptic currents act to activate the intrinsic properties of the neurons can be examined in a frequency dependent manner. We should expect that using the same periodic synaptic input, the presence of I_h should cause a delay in the activity phase of the LP neuron as a function of frequency. Clearly these interaction are not one

directional, but require a bidirectional relationship to promote phase maintenance and stability in an oscillatory network.

7.6 Conclusion

The primary goal of this thesis is to elucidate at what level stability (phase constancy) arises in an oscillatory network. My findings suggest that in order to maintain phase, interactions must occur between the intrinsic properties of a neuron and the properties of its synaptic inputs.

If the synaptically isolated follower neuron was able to maintain phase, then the phase of its burst onset would remain consistent as a function of the input frequency (Figure 7A; Grey line). We have shown, however, that as frequency increased so did the burst onset phase (Chapter 3; Figure 7A; red line -- Schematic diagram based on the Results of Chapter 3). We proposed two mechanisms for this to occur. The first is through a differential influence of I_h relative to I_A at lower and higher frequencies. At lower frequencies, the quantity of I_h is larger than at higher frequencies; at higher frequencies the current does not have enough time to fully activate. I_A, however, is larger at higher frequencies than at lower frequencies. Therefore, at lower frequencies I_h should have a greater influence than I_A, while at higher frequencies the opposite is likely true, which is one candidate explanation for the phase of burst onset increasing with higher frequencies. The second candidate mechanism is through the slope of the input. We proposed that the firing threshold of the neuron changes with the slope of the input. At lower frequencies, because the

time to the peak of the sinusoidal input is longer, the neuron reaches threshold at an earlier phase in the input. At higher frequencies, however, because the time is much shorter, the slope is much steeper and threshold occurs at a later phase of the input, however, only if the threshold V_m remains constant across input frequencies.

Comparably, if the synapse did not need to change TP or G_{max}, then phase would remain constant regardless of which synaptic input was used. However, in order for the pyloric network to maintain phase across different frequencies, the synapse will adjust depending on the frequency (Figure 7B). At lower frequencies, synaptic strength must increase or the TP would delay in order to promote phase maintenance (Chapter 5; Figure 7B1). Conversely, at higher frequencies, a decrease in G_{max} or an advancing of TP would promote phase maintenance (Figure 7B2). These findings are consistent with frequency-dependent short-term synaptic depression. At lower frequencies, the synapse strengthens because longer periods of inactivity in the presynaptic neuron allows for a recovery of the depressing synapse. At higher frequencies, the interval of the synapse is much shorter now allowing for a period of recover of the synapse. In this case, the synapse may not contribute to phase but this may be mainly regulated by the intrinsic properties of the individual neuron.

The networks of the central nervous system are capable of producing a variety of oscillatory behaviors, such as olfaction, locomotion and respiration. In order to understand how these networks produce coherent outputs requires a detailed characterization of both the intrinsic and synaptic properties of the

network. In this thesis, we addressed how stability is produced, by examining the intrinsic and synaptic properties of an oscillatory network and to the extent to which these generate and shape rhythmic network output. Although, a relatively small model system was used, the principles gained in this thesis can be applied to the general understanding of how oscillations are generated, the maintenance of phase relationships and the roles of both the synapses and individual neurons.   This can further our knowledge required to understanding how the cortex can produce stable oscillations.
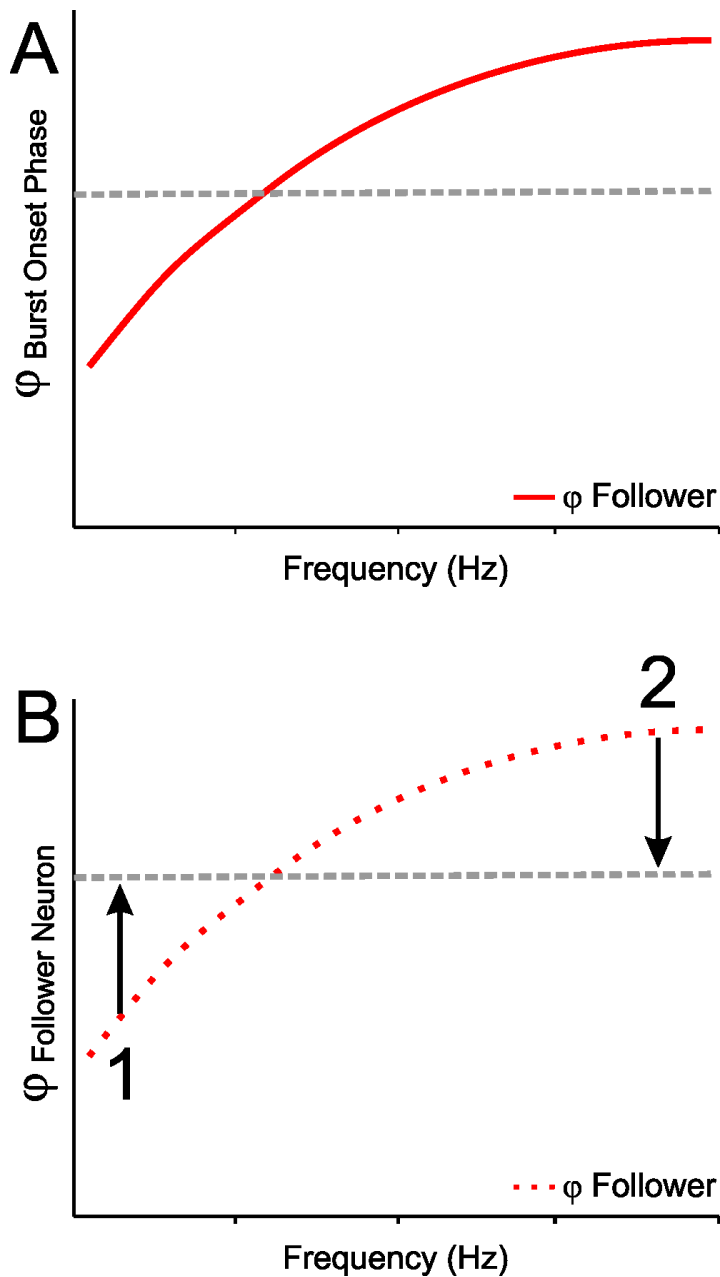
Figure 7.1 Phase constancy can be achieved through short-term synaptic depression. **A.** Schematic diagram of the phase of the burst onset in a synaptically isolated neuron increases with increasing input frequency (red line; based on the Results of Chapter 3). Gray dashed line shows the case of constant phase across input frequencies. **B**. An increase in the synaptic strength (G_{max}) or peak phase (TP) of the inhibitory synaptic input would act to delay the burst onset phase at low input frequencies (1). Similarly a decrease in G_{max} or TP at high input frequencies (2) would advance the burst onset phase.

APPENDIX A

THE CONTRIBUTION OF DIFFERENT PACEMAKER GROUP NEURONS TO SYNAPTIC TRANSMISSION IN THE CRAB *Cancer borealis*

A.1 Introduction

All chemical synapses among pyloric network neurons are inhibitory, however, not all synapses are mediated via the same neurotransmitter. In the lobster *Panulirus interruptus*, the pacemaker neurons AB and PD have distinct synaptic outputs to all follower pyloric neurons (except for VD which only gets an AB synapse) (Eisen and Marder, 1982). The AB and PD neurons are considered the pacemaker ensemble within this network, setting the frequency for the pyloric network. The dilator motor neurons PD and VD in the lobster *P. interruptus* use Acetylcholine (ACh) as their neurotransmitter whereas all the constrictor pyloric neurons and the AB interneuron use glutamate from neurons in the pyloric network occurs as a graded function of membrane potential (Graubard et al., 1980). The threshold for transmitter release is close to the membrane resting potential, with transmitter release increasing as the membrane potential depolarizes. The slow membrane potential oscillations seen during bursting are responsible for most of the transmitter release within the pyloric network (Graubard, 1978, Graubard et al., 1980). Graded synaptic release is found in the retina as well as cells in the olfactory bulb (Morgans, 2000). This type of synaptic release is especially useful for precise control of the postsynaptic membrane potential.

We focused this study on the pacemaker neurons because in the lobster *P. interruptus,* the effects of the two different neurotransmitters (ACh and glutamate) can be easily distinguished through the use of pharmacology. In this study, we are interested in determining whether the two pacemaker neuron types in the crab *Cancer borealis* both contribute to the synaptic inhibition of the follower neurons.

The pacemaker ensemble of the pyloric circuit consists of the AB and two-electrically coupled PD neurons that drive pyloric rhythmic activity (Figure A1). Both neurons oscillate synchronously, due to their strong electrical coupling, to inhibit the follower neurons including LP and PY (Figure A.1A). Each cycle of the triphasic pyloric rhythm is generated through the actions of the AB and PD pacemaker ensemble. During the normal ongoing rhythm the AB and PD neurons, produce a compound IPSP onto the follower neurons, followed by action potentials from the single LP neuron and then by a burst in the PY neurons. Similar to the lobster *P. interruptus* pyloric network, the pyloric pacemaker neurons in the crab *C. borealis* inhibit all pyloric follower neurons, but whether PD uses Ach and forms a synapse onto the followers is not known.

Our hypothesis is that in the crab *C. borealis*, the PD neuron does not make a functional synapse to the follower neurons under control conditions (Figure A1B). We predict that blocking the AB synapse using the known lobster glutamatergic blocker picrotoxin will block all synaptic output from the

pacemaker ensemble to the LP and PY neurons. We also predict that some modulators may rescue the PD synaptic output in the presence of picrotoxin.

We examine the hypothesis by measuring the synaptic output in the LP and PY neuron in response to the activity of the neurons that comprise pacemaker ensemble. The analysis was done in three parts: (1) we aim to examine the dynamics of the synapses from the pacemakers to the LP and PY neurons and examine the short-term depression of these two synapses in the intact network, (2) we block the glutamatergic synapses with picrotoxin and measure the synaptic output from the pacemaker neurons to the LP and PY neurons and (3) we examine whether neuromodulators can rescue the synapses in the presence of picrotoxin.

A.2 Methods

A.2.1 Comparison of Synapses

The synapses between pyloric neurons have two components: spike mediated and graded (Graubard, 1978, Graubard et al., 1980). In this study we focused on the graded component which is believed to be the dominant mode of transmission in pyloric network synapses (Graubard, 1978, Graubard et al., 1980).

After identification of the neurons, we applied 10^{-7} M tetrodotoxin (TTX; Biotium) for 30 minutes to block action potentials and also blocked
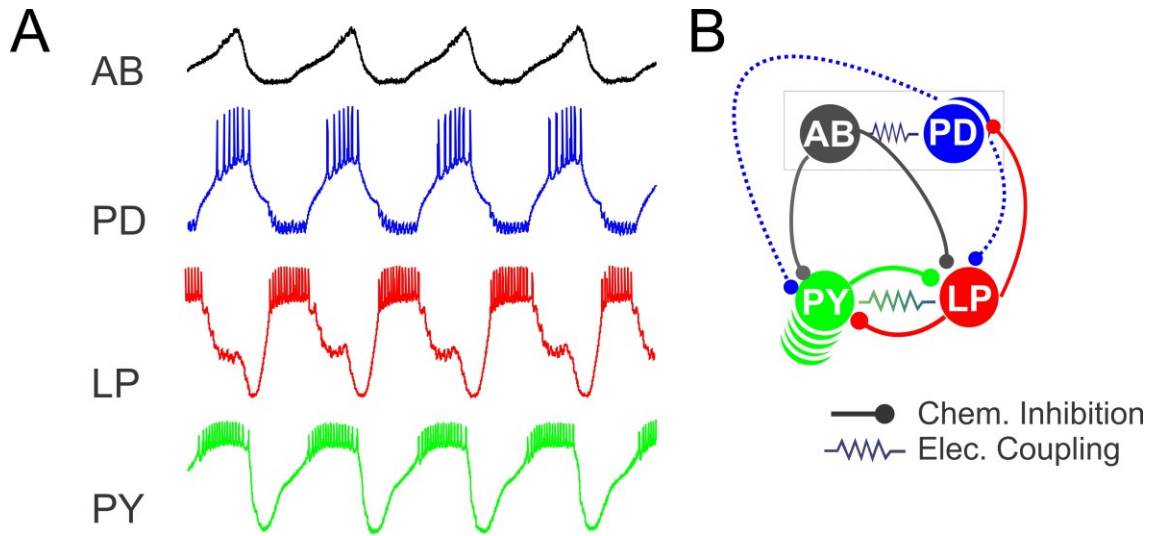
Figure A1 The Pyloric network produces a triphasic rhythm through the synchronous bursting of a pacemaker ensemble comprised of the AB interneuron and the two electrically coupled PD neurons, and the asynchronous bursting of the follower neurons (LP and PY). **A.** Intracellular recordings of the AB, PD, LP and PY neurons. The endogenous oscillator AB interneuron produces a burst which depolarizes the PD neurons, causing them to burst synchronously. Upon termination of this phase, the LP neuron depolarize on rebound with a short delay from the from the pacemaker inhibition. Lastly, PY neurons fire with a burst of action potentials. **B.** Schematic diagram of the pyloric subnetwork consisting of the AB and PD neurons (pacemaker ensemble), the follower LP neuron and the follower PY neuron. In this diagram, the PD neuron (blue-dotted lines) makes functional synapses onto both the PY and LP neuron. The pyloric network contains both electrical and chemical synapses.

endogenously released neuromodulators from projection neurons. We used two electrode voltage clamp (TEVC) and clamped the PD neuron at -60 mV.

The voltage-clamped PD was then depolarized with a train of five pulses (duration: 500 ms; inter-pulse interval: 500 ms) from 15 to 45 mV, in 5 mV intervals. The postsynaptic neurons (PY and LP) were each held at -50 mV, away from the synaptic reversal potential of $\sim$-80mV, in order to record the synaptic current, using a single-electrode in voltage clamp (SEVC). Following measurement of the synapses in control saline (TTX 10^{-7} M) we superfused 10^{-7} M TTX and 10^{-5} M pictrotoxin (PTX) for 30 minutes. Picrotoxin blocks glutamatergic synapses in *Cancer borealis* and has been found to remove synaptic inhibition from the AB neuron in different species of crustaceans (Rabbah and Nadim, 2007). After measurements in PTX, the preparations were then superfused (washed) with control saline for 45 minutes, and the measurements were repeated for wash conditions.

A.2.2 Measuring Synaptic Dynamics

To characterize the synaptic dynamics of the AB and PD neurons, we stimulated the PD neuron in the presence of 10^{-7} M TTX and 10^{-5} M PTX. We measured the extent of the response in both the LP neuron and PY neuron to a train of five square pulses of constant duration (500 ms) and with a constant interpulse interval of 500 ms (Figure A.4A). The extent of synaptic depression in both the LP and PY neuron was quantified as a ratio of the response of the
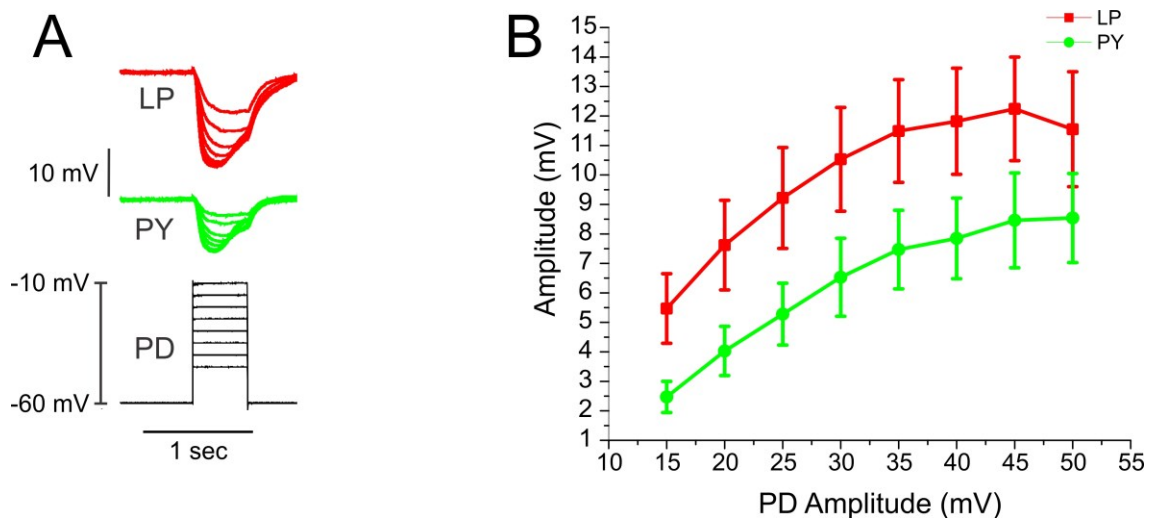
Figure A.2 The amplitude of the PD-evoked IPSP on the follower neurons is voltage dependent as seen in graded synapses. **A.** Voltage trace of the PD depolarization, and the recorded IPSP in both the LP and PY neurons. The PD neuron was depolarized with 15 to 50 mV pulses (delta 5mV) of 500 ms with an interpulse of 500 ms, and recorded the change in voltage in both the LP and PY neurons. **B.** With increased PD depolarization, both the LP and PY IPSP increased in amplitude as expected in a graded synapse. The PY IPSP amplitude is smaller than that of the LP IPSP amplitude across all levels of depolarization (Two-way ANOVA p < 0.001; N=12).

fifth pulse to the first pulse and plotted versus the PD amplitude depolarization Figure A.2B).

A.2.3 Neuromodulator Rescue of Pyloric Synapses

To determine if neuromodulators can rescue the synapse from the pacemaker to follower neuron, we examined the effects of Octopamine in the presence of 10^{-7} M TTX and 10^{-5} M PTX. Octopamine was dissolved in DI water before each experiment and prepared in *Cancer* saline to a final concentration of 10^{-5}M (Johnson and Harris-Warrick, 1990, Kvarta et al., 2012).

We used the same stimulus protocol and bath applied either Octopamine (Oct 10^{-4}M) for thirty minutes in the presence of both 10^{-7} M TTX and 10^{-5} M PTX. The neuromodulator was then washed with TTX and PTX for 45 minutes and the stimulus protocol was repeated.

A.2.4 Recording, Analysis and Statistics

Data were acquired using pClamp 10.1 (Molecular Devices), sampled at 5 kHz on a PC using a Digidata 1332A (Molecular Devices). Statistical and graphical analyses were done using Sigmaplot 11.0 and Origin 8.0. For statistical analysis, mean, standard error and p-value are reported.

A.3 Results

During the ongoing pyloric rhythm, the PD neurons and AB interneuron fire simultaneously to inhibit the different follower neurons. We are interested in determining if these two neuron types use different neurotransmitters, specifically to examine if the PD makes a functional synapse onto the follower neurons. We characterize the amplitude and dynamics of the graded PD to LP and PD to PY synapse at different depolarization steps of PD.

A.3.1. Examining the PD-evoked LP, and PY neuron IPSP amplitudes

To measure synaptic strength, we first examined the differences in amplitude of the pacemaker-evoked IPSPs in the LP and PY neurons in response to the PD neuron depolarization. We activated the synapses using 500 ms steps when the PD neuron was depolarized from -60 to -10mV. The IPSPs elicited in both the LP neuron and PY neuron increased with increased PD depolarization as expected from a graded synapse. At the different membrane voltages of the PD neuron, we see that the PY neuron IPSP was significantly smaller than that of the LP neuron. However, with increasing PD depolarization both the LP and PY neuron IPSP each showed significantly different IPSP amplitudes (Two-way ANOVA $p < 0.001$; N=12; Figure A.2B).

A.3.2 Does the PD neuron make a functional synapse onto the LP and PY neurons?

The AB and PD neurons make a compound inhibitory synapse onto both the LP neuron and the PY neuron in *P. interruptus* (Rabbah and Nadim, 2007). However, each neuron of the pacemaker ensemble contributes to this compound synapse. We were interested in understanding if the PD neuron makes a functional synapse onto both the LP and PD neuron in crab as well.

We used picrotoxin (PTX 10^{-5} M) to block the glutamatergic synapses from the AB neuron. We then repeated our pulse protocol as shown previously (Figure A.3A). In the LP neuron, when we remove the AB synapse with picrotoxin, we see a drastic decrease in the amplitude of the IPSP both for the 20mV and 40mV step when compared to control (20mV-- 7.62 ± 1.52 CTL, 1.17 ± 0.23 PTX; 40mV 11.82 ± 1.80 CTL, 1.34 ± 0.25 PTX) (One-way ANOVA; $p<0.05$; N=12; Figure A.3B). Similarly, in the PY neuron, we see a drastic decrease in both the 20mV and 40mV amplitude when compared to control (20mV -- 4.03 ± 0.83 CTL, 0.71 ± 0.18 PTX; 40mV − 7.87 ± 1.36, 1.34 ± 0.25 PTX). When picrotoxin was washed, the LP and PY IPSP amplitude recovered but not to the same level as seen in control.

A 3.3 Characterization of Synaptic Dynamics

Thus far we have characterized the IPSP amplitudes in the PY and LP neurons. We were also interested in examining the short-term dynamics (depression and
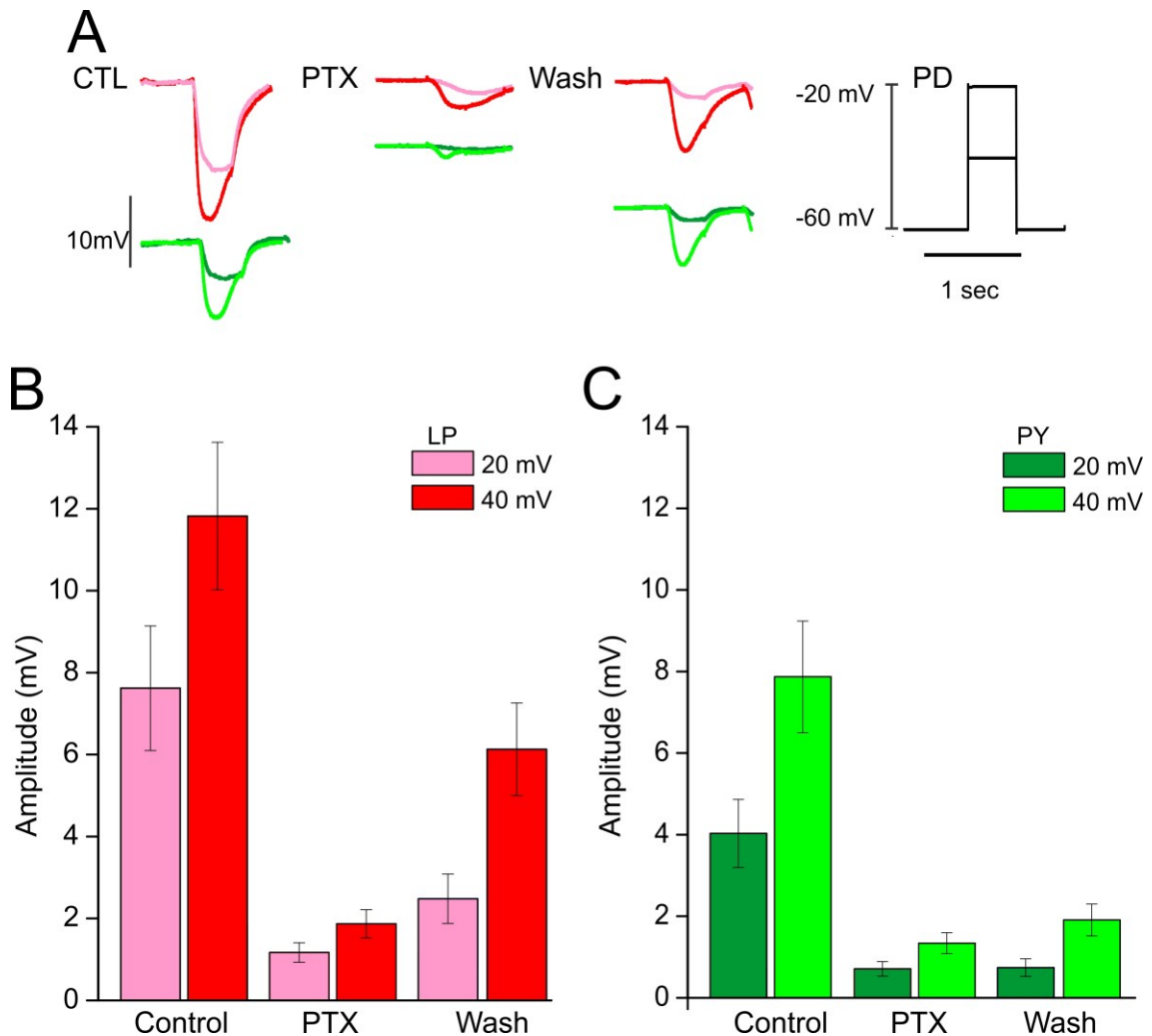
Figure A.3 Picrotoxin blocks the majority of the synapse from the pacemaker ensemble onto the follower neurons. **A.** PD depolarization of 20 mV and 40 mV is shown for both the PY neuron (dark green, light green) and LP neuron (pink, red). **B.** The LP response is shown both the 20 mV (pink) and 40 mV (red). In control the LP response is larger than that in the presence of the glutamatergic blocker picrotoxin. Wash of picrotoxin restored the response of the LP neuron but not to control levels. (20mV-- 7.62 ± 1.52 CTL, 1.17 ± 0.23 PTX, 2.48 ± 0.60 Wash; 40mV 11.82 ± 1.80 CTL, 1.34 ± 0.25 PTX, 6.13 ± 1.13) (One-way ANOVA; $p < 0.05$; N=12) **C.** The PY neuron response to both the 20 mV and 40 mV PD depolarization. Picrotoxin eliminated a majority of the PY neuron response to the PD depolarization, similar to the LP response. Wash of picrotoxin restore the response of the PY neuron to the PD depolarization, similarly to the LP neuron (20mV -- 4.03 ± 0.83 CTL, 0.71 ± 0.18 PTX, 0.74 ± 0.21 Wash; 40mV – 7.87 ± 1.36, 1.34 ± 0.25 PTX, 1.91 ± 0.39 Wash).

time of recovery) of the pacemaker to follower neurons. We depolarized the PD neuron with square pulses of different amplitudes and recorded the changes in membrane voltage in the LP and PY neuron.

The extent of synaptic depression was quantified as a ratio of the fifth IPSP to the first (Mamiya et al., 2003). We see that the IPSP amplitudes decreased between the first and fifth pulse across all levels of PD depolarization (A.4A). As PD depolarization increased so did the level of depression for each neuron (Two-way ANOVA; $p < 0.001$; N=12; Figure A.4B). The extent of depression was greater in the PY neuron than in the LP neuron.

We measured the level of depression in the LP and PY neurons as described previously, in both control and in the presence of picrotoxin when we depolarized the PD neuron by 40 mV (Figure A.5A). In the LP neuron, there is an increase in depression at 40mV in picrotoxin, this effect is reversed when picrotoxin is washed (Two-way ANOVA; $p<0.001$; N=12; Figure A.5B). However, in the PY neuron, the level of depression does not differ between control and picrotoxin.

A 3.4 Neuromodulators and Synapses

Thus far, we have shown the voltage dependence of the graded synapse of the LP and PY neurons. Additionally, we have shown that picrotoxin eliminates a majority of the synapse from the pacemaker ensemble. We were next
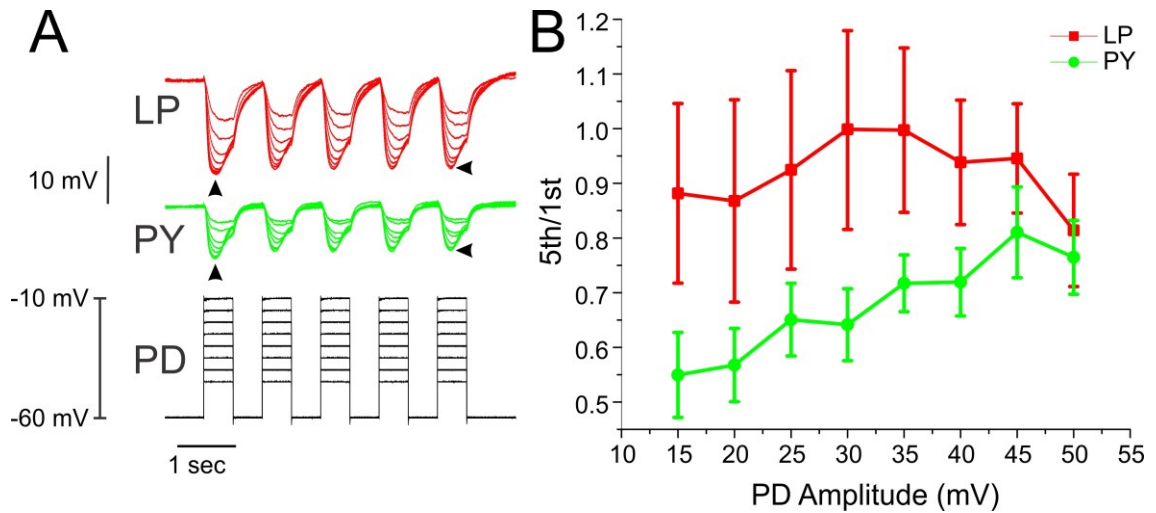
Figure A.4 Synaptic dynamics of the PD-evoked depolarization in the LP and PY neuron. **A.** The PD neuron was stimulated with a series of five pulses of a range of amplitudes from -60 mV 500ms each with an interpulse interval of 500ms while the response in both the PY neuron (green trace) and LP neuron (red trace) was recorded. The vertical arrow denotes the 1st pulse and the vertical arrow denotes the 5th pulse. **B.** Ratio between 5th/1st peak in response to the different amplitude of the PD depolarization of the LP neuron and PY neuron. Synaptic depression was calculated as a ratio between the 5th and 1st pulse. The LP neuron exhibits a smaller level of depression when compared to the PY neuron at different PD depolarization (Two-way ANOVA; p<0.00; N=12).

interested in determining if the synapse from PD to LP and PY cab be upregulated in the presence of different neuromodulators.

Octopamine has been found to enhance the graded synapse between the PD neuron and the PY neuron as well as the PD neuron to the LP neuron in *P. interruptus* (Johnson and Harris-Warrick, 1990). Octopamine (N=3) (and PTX to remove the synapse from AB) did not upregulate the PD onto the LP or PY neurons.

A.4 Discussion

To produce meaningful behavior, neural networks ensure coordination of the motor neurons involved in such a behavior. Specifically, the member neurons of the network should make effective synapses in order to produce rhythmic output in the network, which can translate into a specific behavior. In order to fully understand, a network, the connections, such as those from pacemakers to follower neurons must be characterized and understood. Using the pyloric network of the crab *Cancer borealis,* we were interested in determining if a pacemaker neuron (PD) makes a functional synapse onto the follower neurons as it does in *P. interruptus*. we find that the PD neuron does not make a functional synapse onto the follower neurons, and the AB interneuron is the sole contributor to inhibiting the LP and PY neurons.
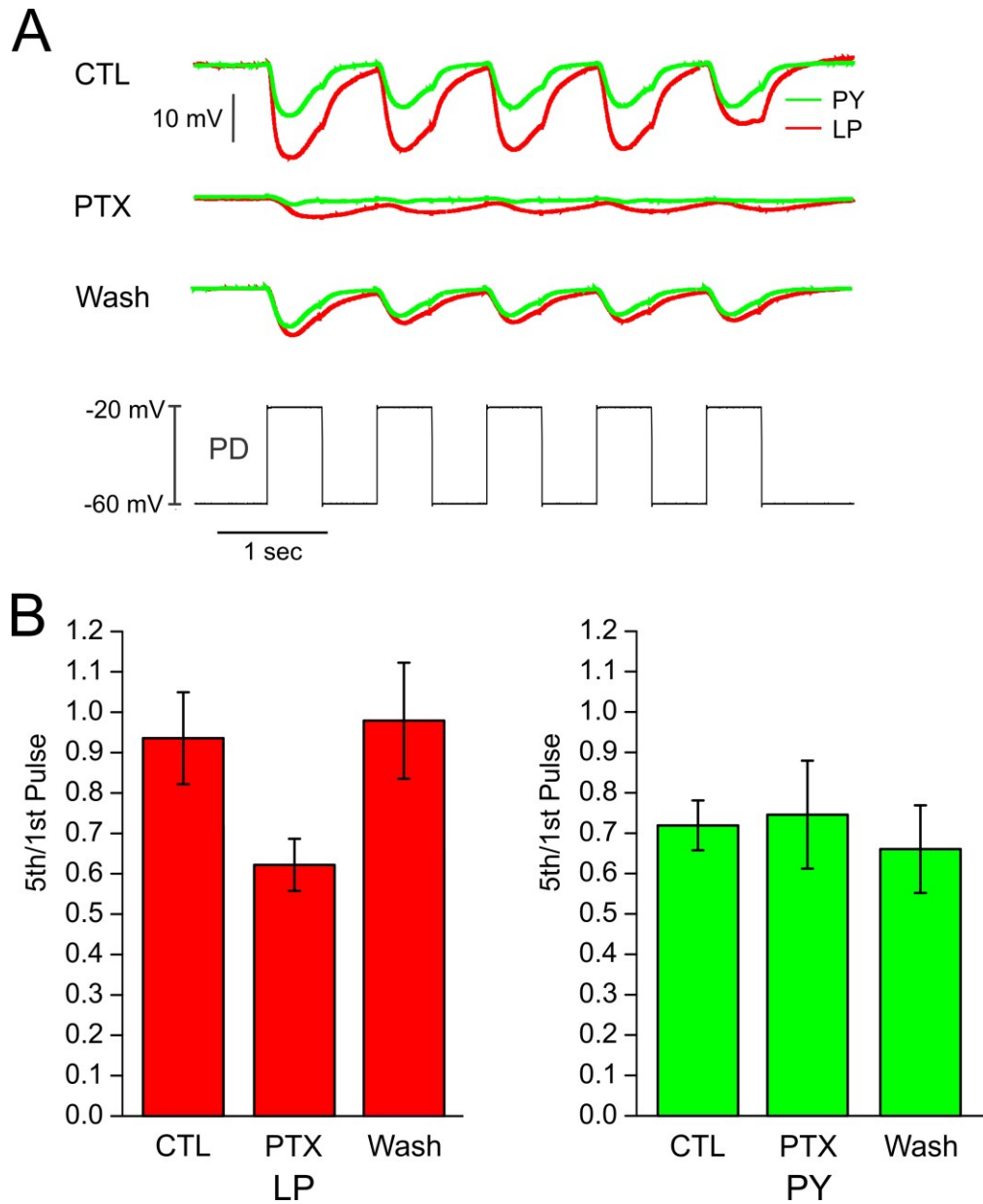
Figure A.5 Synaptic dynamics of the PD-evoked depolarization in the LP and PY neuron in the presence of PTX. **A.** The PD neuron was voltage clamped at -60mV and stimulated with five 40mV pulses. The PY neuron (green trace) and the LP neuron (red trace) exhibits depression when comparing the 5th and 1st pulse. **B.** The level of depression differs between the LP neuron and PY neuron with the 40mV PD depolarization. In control conditions, the PY neuron exhibits a greater level of depression (5th/1st ratio) than the LP neuron. However, during PTX treatment the LP neuron exhibits a greater level of depression in comparison to the PY neuron. (LP – 0.93 ± 0.11, 0.62 ± 0.06 PTX, 0.97 ± 0.14 Wash Two-way ANOVA; $p < 0.001$; N=12; PY -- 0.71 ± 0.06, 0.74 ± 0.13 PTX, 0.66 ± 0.10 Wash; N=12).

While picrotoxin significantly decreased the amplitude of the synapse from the pacemaker ensemble on to the LP and PY neurons, it did not abolish it. This shows us that AB neuron does not solely contribute to the synapse onto the follower neurons but the PD neuron also contributes to inhibiting the follower neurons as well or PTX is not 100% effective. In order to conclusively demonstrate the nature of the PD synapse onto the followers, a cholinergic blocker such as atropine should be used to block the PD synapse onto the follower neurons (Marder and Eisen, 1984b).

The difference between the contributions of the AB neuron and PD neuron in both *P. interruptus and C.borealis,* may also account for differences in the response elicited via neuromodulators. In our study, octopamine did not increase the amplitude of the pacemaker to LP neuron synapse. This may be due to the higher contribution of the PD neuron in *P. interruptus* than in *C. borealis.* This may be the reason for the differential response in this synapse in the presence of neuromodulators.

CHAPTER B

THE EFFECTS OF NEUROMODULATORY PROJECTION NEURONS ON NEURONAL ACTIVITY AND SYNAPTIC STRENGTH

B.1 Introduction

Neuromodulators reach the STG in a variety of ways: released neurally from the terminals of projection neurons as well as from sensory neurons, or hormonally via the bloodstream (Nusbaum and Beenhakker, 2002, Dickinson, 2006). Extensive studies into the connectivity of modulatory projection neurons and their effects on the STG circuits, in particular the pyloric network, have shown how neuromodulators can alter network activity. Neuromodulator released from projection neurons such as MCN1 and MCN5 can increase pyloric frequency, alter synapses and alter intrinsic properties of the pyloric neurons (Swensen and Marder, 2001, Zhao et al., 2011). In total, they release a multitude of peptides, amines and classical neurotransmitters.

Often a single projection neuron releases multiple neuromodulators that can affect a neural circuit (Blitz et al., 1999). For example, modulatory commissural neuron (MCN1) projects from the CoG onto the STG and releases three identified neurotransmitters: *Cancer borealis* tachykinin-related peptide 1a (CabTRP Ia), GABA and the peptide proctolin (Coleman et al., 1995, Blitz et al., 1999, Swensen et al., 2000). MCN1 uses CabTRP Ia and GABA to influence the gastric mill network (Wood et al., 2000). In contrast, proctolin and CabTRP Ia target neurons within the pyloric network (Swensen and Marder, 2001).

Synapses in the pyloric network show short-term synaptic depression in control conditions (Manor et al., 1997).The LP neuron provides the sole chemical synaptic feedback to the pacemaker group (Manor et al., 1997). This synapse is important in the maintenance of the frequency of the triphasic pyloric rhythm (Nadim et al., 2011) and is known to be modulated by both proctolin (Zhao et al., 2011) and CabTRP Ia (Shebanie and Nadim, 2009). The LP to PD synapse, normally depressing, becomes a facilitating synapse in the presence of proctolin with low-amplitude presynaptic input (Zhao et al., 2011).

Projection neurons including MCN1 have a strong effect on the pyloric and gastric mill networks (Coleman and Nusbaum, 1994, Norris et al., 1996, Bartos and Nusbaum, 1997). MCN1 is presynaptically inhibited by the lateral gastric (LG) neuron, one of the rhythm-generating neurons in the gastric mill network, which results in the inhibition of synaptic release from MCN1 onto the neurons of the STG (Nusbaum et al., 1992, Coleman and Nusbaum, 1994). We are interested in determining how the set of co-transmitters released from MCN1 exerts its influence on the pyloric network through modifying network properties. MCN1 can influence the pyloric network in two ways. MCN1 can directly modulate the pacemaker neurons and thereby change pyloric activity (Bartos and Nusbaum, 1997). MCN1 can also have direct effects on the pyloric synapses, as seen through the effects of proctolin on the LP to PD synapse (Zhao et al., 2011). As we propose in this chapter, MCN1 can act directly on the pyloric synapses and thereby influence pyloric activity. These two ways in which MCN1 may exert its influence the pyloric network are not exclusive, and

may induce changes directly on the synapse through both. To determine the effects MCN1 has on the synapses, we characterize the effect of MCN1 on the pyloric neurons and on the synapses. We then examined whether removing the LP to PD synapse influences the rhythm when MCN1 is active.

B 2.2 Materials and Methods

B.2.1 Stimulation of Projection Neurons

The bilateral MCN1 neurons project from the CoGs, through the inferior esophageal nerves (*ions*) and down the stomatogastric nerve (*stn*) synapsing onto neurons of the STG (Figure B.1)(Coleman and Nusbaum, 1994). In order to selectively stimulate MCN1, we transected the *ions* isolated the bilateral *ions* by building a Vaseline well around each, and used an extracellular pulse stimulator to stimulate each *ion* (A-M Systems Isolated Pulse Stimulator, Model 2100)*.* We only transected the left *son* so that the pyloric network remained rhythmic. Previous work had confirmed that intrasomatic stimulation of MCN1 produced the same results as *ion* stimulation (Bartos and Nusbaum, 1997). Because MCN5, another projection neuron, also sends projections through the *ion (Norris et al., 1996)* it is necessary to determine that the stimulation of the *ion* only activated MCN1. Because MCN5 possesses a smaller diameter axon, it requires stronger stimulation to activate (Coleman and Nusbaum, 1994, Norris et al., 1996, Bartos and Nusbaum, 1997). The stimulation threshold was adjusted to a level to activate MCN1 but not MCN5, whose distinct actions on the pyloric network are easily monitored on the *lvn*, as MCN5 activation inhibits

all non-pacemaker neurons such as LP and PY (Norris et al., 1996). The stimulation pattern was tonic with a constant frequency (10, 15, 20, 25, 30, 35 Hz).

MCN1 is presynaptically inhibited in the STG by the lateral gastric (LG) neuron (Coleman et al., 1995). Each action potential in MCN1 elicits an electrical excitatory postsynaptic potential in the LG neuron. Therefore, to ensure that each *ion* stimulus elicited an MCN1 action potential, we impaled the LG neuron and monitored the electrical EPSPs. We hyperpolarized LG sufficiently to prevent it from firing spikes during MCN1 stimulation, and in turn interfering with the MCN1 excitation of the pyloric network. The protocol was sufficient that one single spike stimulus of MCN1 elicited one electrical EPSP in the LG neuron (Coleman et al., 1995) (1:1 ratio of stimulus to one LG EPSP).

B.2.2 Effects of projection neuron stimulation on the ongoing rhythm

Once we verified that one single spike stimulus of MCN1 elicited a 1:1 action potential in the LG neuron, we impaled the PD and LP neuron while recording the LG neuron, and we hyperpolarized the LG neuron to remove its effect on MCN1. We recorded the rhythm for 30 seconds, and then stimulated for 25 seconds and then recorded for another 60 seconds post-stimulation. After recording PD activity, we two-electrode voltage clamped (TEVC) the PD neuron and held it at

-50mV, away from the synaptic reversal potential of -80mV, in order to also measure the LP to PD synaptic current during the ongoing rhythm.

We measured the following parameters of PD to LP activity before and during MCN1 stimulation: amplitude, burst duration, pyloric period, spike number and duty cycle (Figure B.2). Amplitude was calculated as the average of five cycles (after the waveform is low-pass filtered using a Butterworth filter with a cut-off of 10 Hz) by calculating the change in membrane voltage. Spike number was determined by taking the average of spikes in each cycle for five cycles. The duty cycle was calculated by taking the burst duration/cycle period.

B.2.3 Effect of projection neuron stimulation on pyloric synapses

In order to understand if the LP to PD synapse has an effect on the pyloric network during MCN1 stimulation, we measured the pyloric network frequency in control and after removing the LP to PD synapse. We voltage clamped the presynaptic neuron (pacemaker to LP, or LP to PD) at -60mV and the postsynaptic neuron was held with TEVC at -50mV.

B.2.4 Generation of the representative PD and LP neuron waveform

In order to determine the effects of altering the presynaptic waveform on the synapse, we developed representative realistic waveforms of both the LP and PD neurons from intracellular recordings using the Readscope software (version 8.0) as described below. This representative realistic waveform was generated by averaging 5 cycles of consecutive activity of either the LP or PD
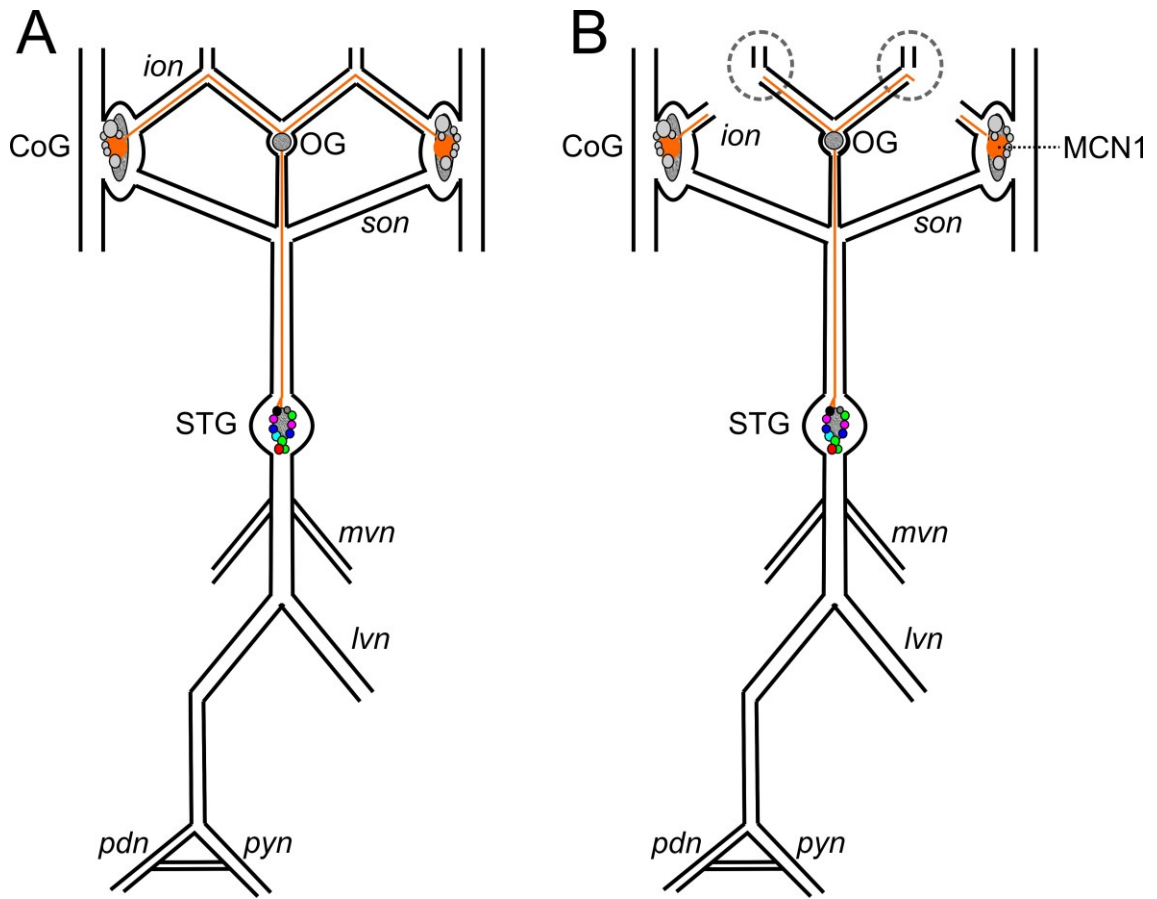
Figure B.1 MCN1 can be stimulated through its axon. **A.** In the intact STNS, the MCN1 axon exits the commissural ganglion (CoG), traverses the inferior oesophageal nerve (*ion*), travels through the stomatogastric nerve (*stn*) and synapses onto cells of the stomatogastric ganglion (STG). **B.** The *ions* were cut in order to stimulate the MCN1 axon. The MCN1 axon was stimulated, by placing a Vaseline well (dotted circle) around the each bilateral *ion* and placing a stimulating wire electrode into each well.
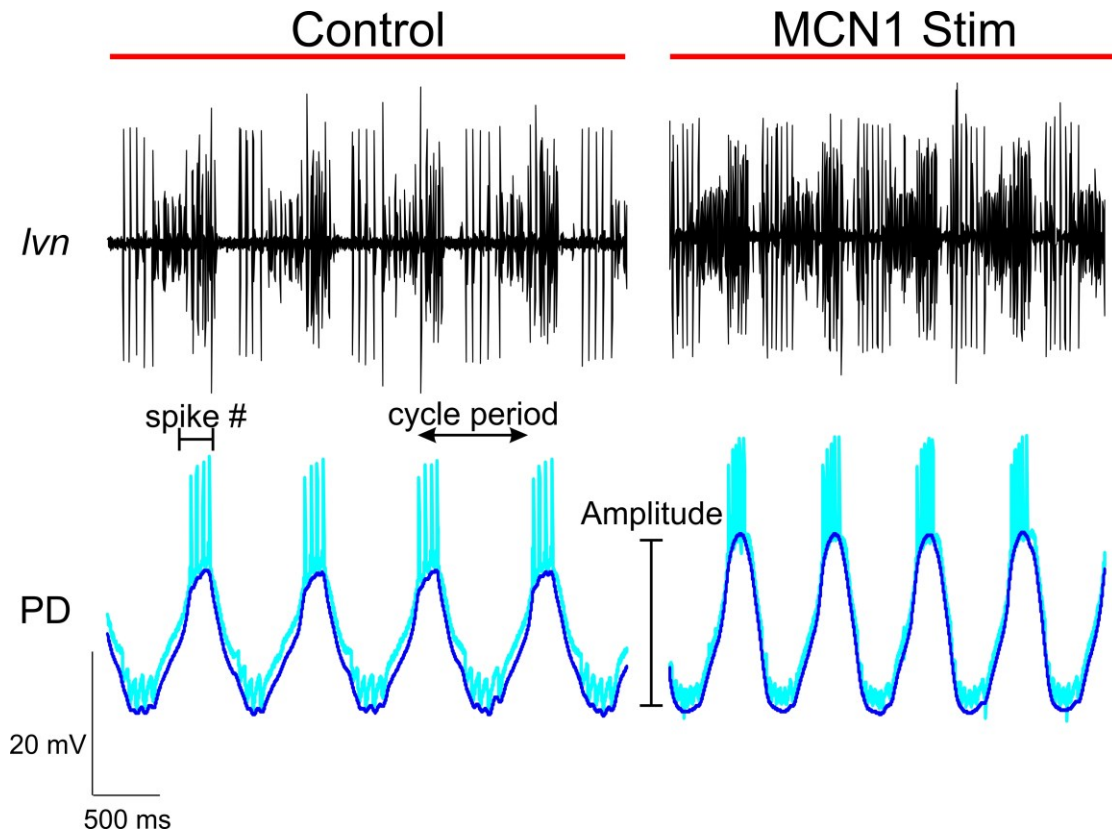
Figure B.2 The effects of MCN1 stimulation is measured by quantifying changes in the pyloric network. A recording of the *mvn* and *lvn,* and an intracellular recording of the PD neuron (light blue trace) in CTL and with MCN1 stimulation (20Hz). In order to determine the effects of MCN1 stimulation, we measured different parameters including: amplitude, spike number (per cycle) and cycle period. In order to determine the amplitude, the intracellular recording was low pass filtered at 10 Hz to remove spikes. Amplitude is measured from the baseline of the recording to the peak in the filtered oscillation (dark blue line). Cycle period was measured from the onset of the PD burst to the onset to the next PD burst.

neuron during the ongoing rhythm. The average membrane potential in the five selected cycles was used as the voltage threshold to align and average these cycles to generate a single averaged waveform. The generated waveform was sampled at 1000 points and rescaled between 0 and 1 to produce a unitary realistic waveform. The realistic waveform was then applied repetitively to the voltage clamped presynaptic neuron at different amplitudes and cycle periods to control the membrane potential of the presynaptic neuron. The same waveform was used across all experiments.

We drove the presynaptic neuron with the realistic waveform at different periods for 20 cycles. We used cycle periods of 500, 750, 1000, 1250, 1500, 2000, 2500 ms, and compared the effects of the waveforms on the postsynaptic current in control and in MCN1 stimulation. During MCN1 stimulation, we recorded 10 seconds before driving the presynaptic neuron with the waveform in order to establish a baseline. We then recorded during the 20 seconds and 10 seconds after the presynaptic neuron was driven by the waveform.

B.2.5 Software

Data were acquired using both pClamp 9.0+ (Axon Instruments) as well as Scope 7.4 to record and stimulate each neuron. The software Readscope and Scope were developed and maintained by the Nadim lab and can be downloaded at http://stg.rutgers.edu/Resources.html. All data were sampled at 5 kHz and saved on a PC using a Digidata 1332A (Molecular Devices) and a PCI-6070-E data acquisition board (National Instruments).

B.2.6 Statistical Analysis

Statistical analysis was performed using Sigmaplot 12.0 (Systat). Significance was evaluated at an α value of 0.05, error bars shown and error values reported denote standard error unless noted.

B.3 Results

B.3.1 Which neuron properties are altered during MCN1 stimulation?

As originally shown by Bartos and Nusbaum (1997), we found that pyloric frequency significantly increased with increasing MCN1 stimulation across all experiments when compared to control (Two way repeated measures ANOVA; N=8; p=0.006; Figure B.3A). We also measured the changes in the individual neurons in control and in MCN1 stimulation (Figure B.3, 2.4). The change in the number of spikes in the PD neuron increased significantly with MCN1 stimulation across frequencies (Two way repeated measures ANOVA; N=6; p=0.039; Figure B.4). However, the LP neuron's spike number was not different across MCN1 stimulation frequencies when compared to control (N=6; p=0.068; Figure B.3B). Both the PD and LP duty cycles remained unchanged with MCN1 stimulation at different frequencies ((PD: Figure B.4C (Two way repeated measures ANOVA; N=6; p=0.306, LP: Figure B.4D (Two way repeated measures ANOVA; N=6; p=0.109)). The PD neuron's slow membrane potential waveform amplitude increased significantly when compared to control across all MCN1 stimulation frequencies (Two-Way Repeated Measures ANOVA with

Holm-Sidak Method; N=7; p=< 0.001 Figure B.3). The LP neuron membrane

potential waveform amplitude, however, remained unaffected by MCN1

stimulation.

Table B.1 Pyloric frequency, PD burst duration and LP burst duration in control
and with MCN1 stimulation

MCN1 Freq (Hz)	Pyloric Freq (Hz)		PD Amplitude (mV)		LP Amplitude (mV)	
	CTL	+MCN1	CTL	+MCN1	CTL	+MCN1
15	0.805 ± 0.06	0.844 ± 0.05	24.64 ± 2.32	28.13 ± 2.85	26.30 ± 1.99	29.19 ± 2.97
20	0.756 ± 0.08	0.818 ± 0.04	24.91 ± 2.30	29.39 ± 2.42	27.04 ± 2.10	30.26 ± 2.83
25	0.731 ± 0.08	0.797 ± 0.08	25.87 ± 2.21	29.87 ± 2.43	26.67 ± 2.67	29.61 ± 2.80
30	0.709 ± 0.07	0.785 ± 0.08	26.30 ± 2.24	31.38 ± 2.29	27.07 ± 2.67	29.44 ± 2.15
35	0.708 ± 0.08	0.768 ± 0.08	26.64 ± 2.43	31.95 ± 2.15	26.99 ± 3.12	29.17 ± 2.86

Pyloric frequency, PD amplitude and LP amplitude are shown in control
conditions and during different MCN1 stimulation frequencies. Values shown
are mean and standard error. Pyloric frequency and PD amplitude were
statistically different between control and MCN1 stimulation. LP amplitude was
not statistically different.
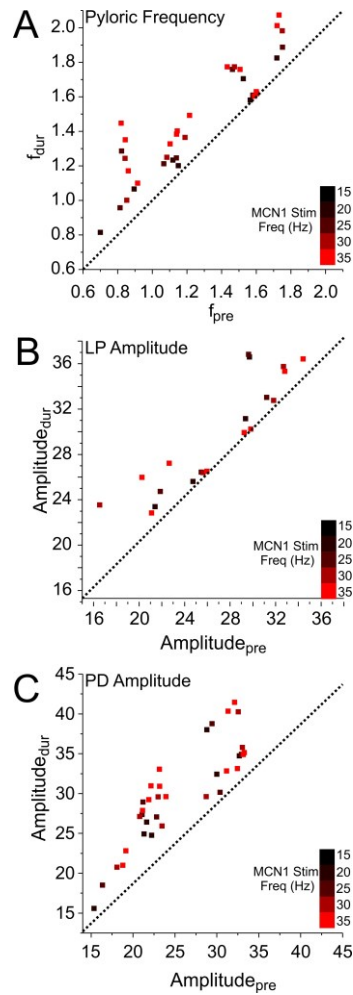
Figure B.3 Pyloric frequency, LP amplitude and PD amplitude were increased at all MCN1 stimulation frequencies. In each panel, the x-axis represents the control condition and the y-axis represents MCN1 stimulation. The dotted line is the reflection line (x=y). Each color from black to red represents increasing MCN1 stimulation frequency. Data from all experiments can be found in Table 2.1 **A**. Pyloric frequency was determined at each of the different MCN1 stimulation frequencies. We compared pyloric frequency during MCN1 stimulation and in control conditions. We compared the control frequency and frequency during MCN1 stimulation. As the MCN1 stimulation increased so did the pyloric frequency which was highest at MCN1 stimulation frequency of 35 Hz. **B.** LP amplitude increased with MCN1 stimulation but did not change as a function of MCN1 stimulation frequency. **C.** PD amplitude increased as a function of MCN1 stimulation and was highest at MCN1 stimulation frequency of 35Hz.
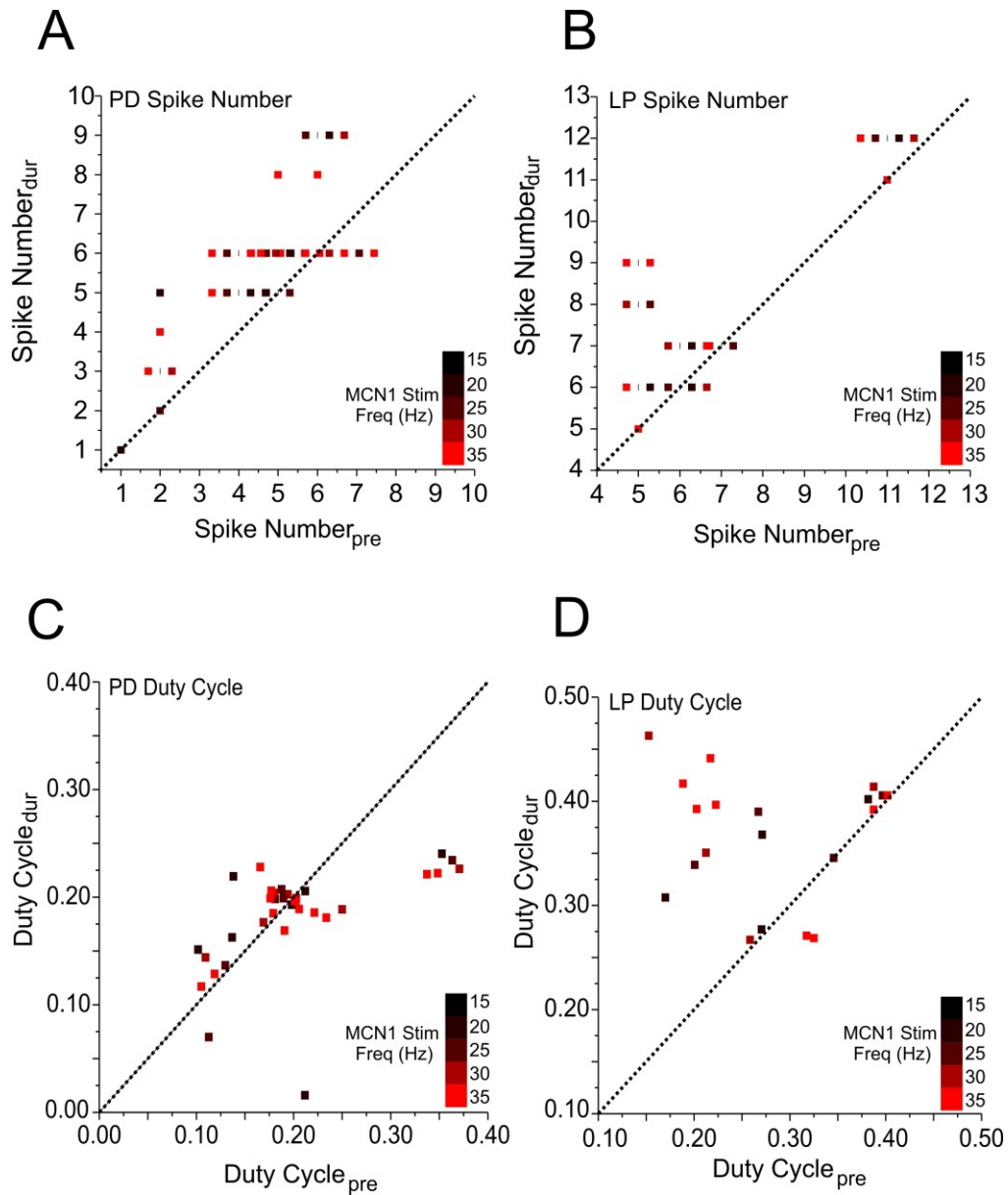
Figure B.4 PD spike number, LP spike number but not PD or LP duty cycle are different in control and MCN1 stimulation. In each panel, the x-axis represents the control condition and the y-axis MCN1 stimulation. The dotted line is the reflection line (x=y). Each color from black to red represents increasing MCN1 stimulation frequency. Data from all experiments can be found in Table 2.2. **A.** PD spike number was compared in control and at the different MCN1 stimulation frequencies. PD spike number increased with increasing MCN1 frequency stimulation (N=8). **B.** LP spike number did not increase significantly from control. **C.** Duty cycle was calculated as the burst duration/period for both control and MCN1 stimulation. Neither the PD neuron (D) nor the LP neuron (C) duty cycle was significantly changed with MCN1 stimulation.

Table B.2 PD amplitude, LP amplitude, PD and LP spike number in control and during MCN1 stimulation

MCN1 Freq	PD Duty Cycle		LP Duty Cycle		PD SN		LP SN	
	CTL	+MCN1	CTL	+MCN1	CTL	+MCN1	CTL	+MCN1
15	0.193 ± 0.03	0.170 ± 0.02	0.273 ± 0.04	0.339 ± 0.02	4.14 ± 0.73	5.29 ± 0.89	7.00 ± 1.35	7.75 ± 1.43
20	0.193 ± 0.03	0.178 ± 0.02	0.302 ± 0.04	0.370 ± 0.01	4.57 ± 0.52	5.57 ± 0.78	7.25 ± 1.31	8.25 ± 1.31
25	0.211 ± 0.03	0.192 ± 0.009	0.253 ± 0.04	0.374 ± 0.04	4.71 ± 0.56	5.85 ± 0.67	7.00 ± 1.35	8.25 ± 1.31
30	0.201 ± 0.02	0.190 ± 0.01	0.281 ± 0.04	0.374 ± 0.03	4.57 ± 0.53	5.85 ± 0.45	7.00 ± 1.41	8.00 ± 1.29
35	0.208 ± 0.02	0.185 ± 0.01	0.284 ± 0.04	0.372 ± 0.03	4.71 ± 0.57	5.85 ± 0.55	6.75 ± 1.43	8.50 ± 1.32

PD duty cycle, LP duty cycle, PD spike number, and LP spike number are shown in control conditions and during different MCN1 stimulation frequencies. Values shown are mean and standard error. PD spike number is statistically different in control and MCN1 stimulation, however LP duty cycle, PD duty cycle and LP spike number are not.

B.3.2 Does removing the LP to PD Synapse affect network properties in the presence of MCN stimulation?

In order to understand the contribution of the LP to PD synapse to the pyloric frequency, we examined two different conditions: removing the LP to PD synapse by hyperpolarizing the LP neuron (CTL) and by removing the LP to PD synapse in the presence of MCN1 stimulation. Hyperpolarizing the LP neuron alone did not have a significant change in frequency than when LP was not hyperpolarized (Two way RM ANOVA with *post hoc* Holm Sidak test p = 0.410).

When LP was hyperpolarized to remove the synapse to the pacemakers, the pyloric network frequency did not increase in the presence of MCN1 stimulation at 15, 20 and 25 Hz (Two way RM ANOVA with *post hoc* Holm Sidak test 15 Hz p= 0.876; 20 Hz p=0.279; 25 Hz p=0.089; Figure B.5A). However, with LP hyperpolarized with MCN1 stimulation of 30 and 35 Hz, there was a significant increase in the pyloric frequency (Two way RM ANOVA with

post hoc Holm Sidak test 30 Hz p=0.018; 35 Hz p=0.048; Figure B.5A). Differences in frequency were not seen when LP was hyperpolarized alone (Two way RM ANOVA with *post hoc* Holm Sidak test p = 0.101; Figure B.5A). PD burst duration (Two way RM ANOVA; N=4, p=0.389), PD amplitude (Two way RM ANOVA; N=4, p=0.147) and PD duty cycle (Two way RM ANOVA; N=4, p=0.675) were not statistically different between LP hyperpolarized alone and in the presence of MCN1 stimulation.

Table B.3 Effect of LP to PD Synapse on Pyloric Network Properties

MCN1 Freq	PD Amp. (mV)		Pyloric Freq. (Hz)		Spike Number		PD Burst Dur (ms)		PD Duty Cycle	
	LP Hype (CTL)	+MCN1	LP Hype (CTL)	+MCN1	LP Hype (CTL)	+MCN1	LP Hype (CTL)	+MCN1	LP Hype (CTL)	+MCN1
15	24.06 ± 1.37	25.31 ± 0.79	1.41 ± 0.16	1.56 ± 0.11	4.75 ± 0.41	5.25 ± 0.21	0.173 ± 0.03	0.185 ± 0.01	0.213 ± 0.02	0.185 ± 0.01
20	24.15 ± 1.22	26.26 ± 0.75	1.46 ± 0.18	1.69 ± 0.10	4.75 ± 0.41	5.25 ± 0.21	0.177 ± 0.03	0.186 ± 0.02	0.204 ± 0.02	0.186 ± 0.02
25	23.80 ± 1.44	27.01 ± 1.19	1.41 ± 0.16	1.69 ± 0.10	5.0 ± 0.35	5.25 ± 0.21	0.176 ± 0.03	0.179 ± 0.01	0.209 ± 0.01	0.179 ± 0.01
30	23.88 ± 1.42	27.16 ± 0.64	1.44 ± 0.11	1.85 ± 0.11	5.0 ± 0.50	5.75 ± 0.21	0.181 ± 0.04	0.179 ± 0.02	0.206 ± 0.01	0.179 ± 0.02
35	24.12 ± 1.50	28.61 ± 1.66	1.57 ± 0.10	1.91 ± 0.10	4.75 ± 0.41	6.0 ± 0.00	0.176 ± 0.03	0.188 ± 0.03	0.156 ± 0.04	0.188 ± 0.03

The effect on PD amplitude, pyloric frequency, spike number, PD spike burst duration, and PD duty cycle with removal of the LP to PD synapse and in the presence of MCN1 stimulation. The values shown are mean and standard deviation.

B.3.3 How does the Presynaptic Period affect the LP to PD Synapse?

Thus far, we have shown that MCN1 stimulation can alter the properties of the individual neurons. We have also shown that removing the LP to PD synapse influences the cycle period in the presence of MCN1 stimulation. Therefore, we were interested in determining if changing the properties of the LP neuron, such

as the period would cause changes to synaptic properties such as area and amplitude (Figure B.6A; 2.5B). Additionally, how does MCN1 stimulation affect changes in both the synaptic area and synaptic amplitude.

The LP to PD synapse exhibits differences with respect to changes in both synaptic amplitude and synaptic area when changing the presynaptic neuron waveform period in control conditions (Figure B.6; Table 2.2). If we compare the IPSC amplitude and area across all of the different periods, we see that not all responses are statistically different. With a 1250ms period, there is no significant difference in IPSC amplitude between the control and the MCN1 group (Two way RM ANOVA with *post hoc* Holm Sidak test; N=8, p=0.109). However, at all other periods of 500, 750, 1000, 1500, 2000 and 2500 (Figure B.5A), when comparing control and MCN1 stimulation the IPSC amplitude was statistically significant when compared to each other in control and MCN1 stimulation. Synaptic area (Figure B.5B) was significantly different between the control and MCN1 stimulation group (Two-Way Repeated Measures ANOVA; N=8; p <0.001).

Table B.4 Presynaptic Period Effects on Synapse in Control and MCN1 Stimulation

Period	CTL IPSC amplitude	+MCN1 IPSC amplitude	CTL Area (nA*ms)	MCN1 Area (nA*ms)
500	3.66 ± 0.36	5.06 ± 0.35	864.75 ± 206.72	1317.23 ± 137.76
750	3.60 ± 0.38	5.15 ± 0.34	1151.93 ± 180.25	1785.60 ± 160.81
1000	3.78 ± 0.36	5.22 ± 0.45	1521.46 ± 226.00	2055.57 ± 172.81
1250	3.83 ± 0.31	4.79 ± 0.24	1664.21 ± 217.45	2399.30 ± 266.87
1500	3.85 ± 0.29	5.25 ± 0.29	2030.42 ± 266.61	3231.07 ± 347.56
2000	3.77 ± 0.24	5.15 ± 0.36	2415.9 ± 305.76	3618.97 ± 355.44
2500	3.90 ± 0.32	5.19 ± 0.27	3034.00 ± 287.33	4674.23 ± 677.60

The IPSC and area of the LP to PD neuron was compared in control and at different MCN1 stimulation frequencies.
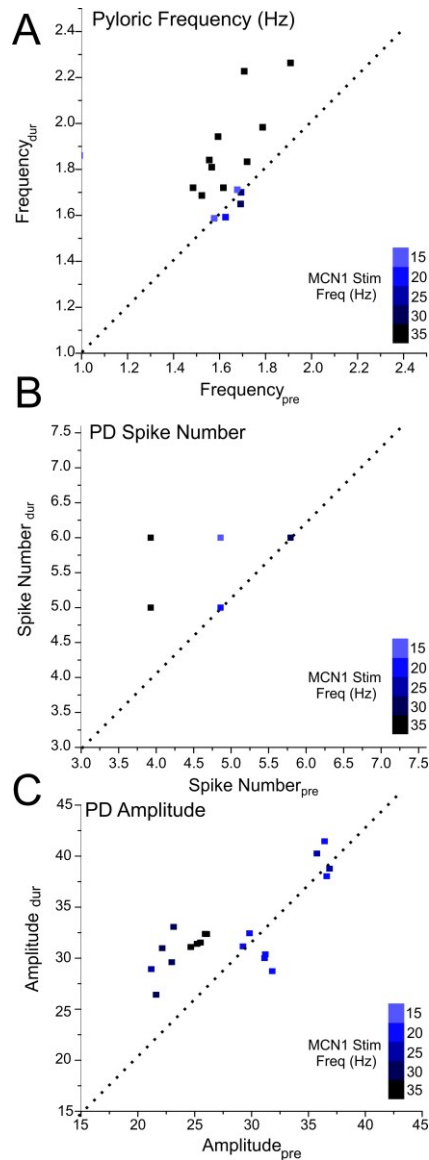
Figure B.5 Pyloric frequency, PD amplitude but not PD spike number are different with the LP neuron hyperpolarized alone and with MCN1 stimulation. In each panel, the x-axis represents the control condition and the y-axis represents MCN1 stimulation. The dotted line is the reflection line (x=y). Each color from light blue to dark blue (to indicate this figure differs from the others as LP is hyperpolarized) represents increasing MCN1 stimulation frequency. Data from all experiments can be found in Table 2.3 **A.** Pyloric frequency did not significantly increase when LP was hyperpolarized alone or with MCN1 stimulation at 15, 20 and 25 Hz. Pyloric frequency was only significantly different at 30 and 35 Hz. **B.** PD spike number was not different between these two groups. **C.** PD amplitude is statistically different between LP hyperpolarized alone and with MCN1 stimulation.
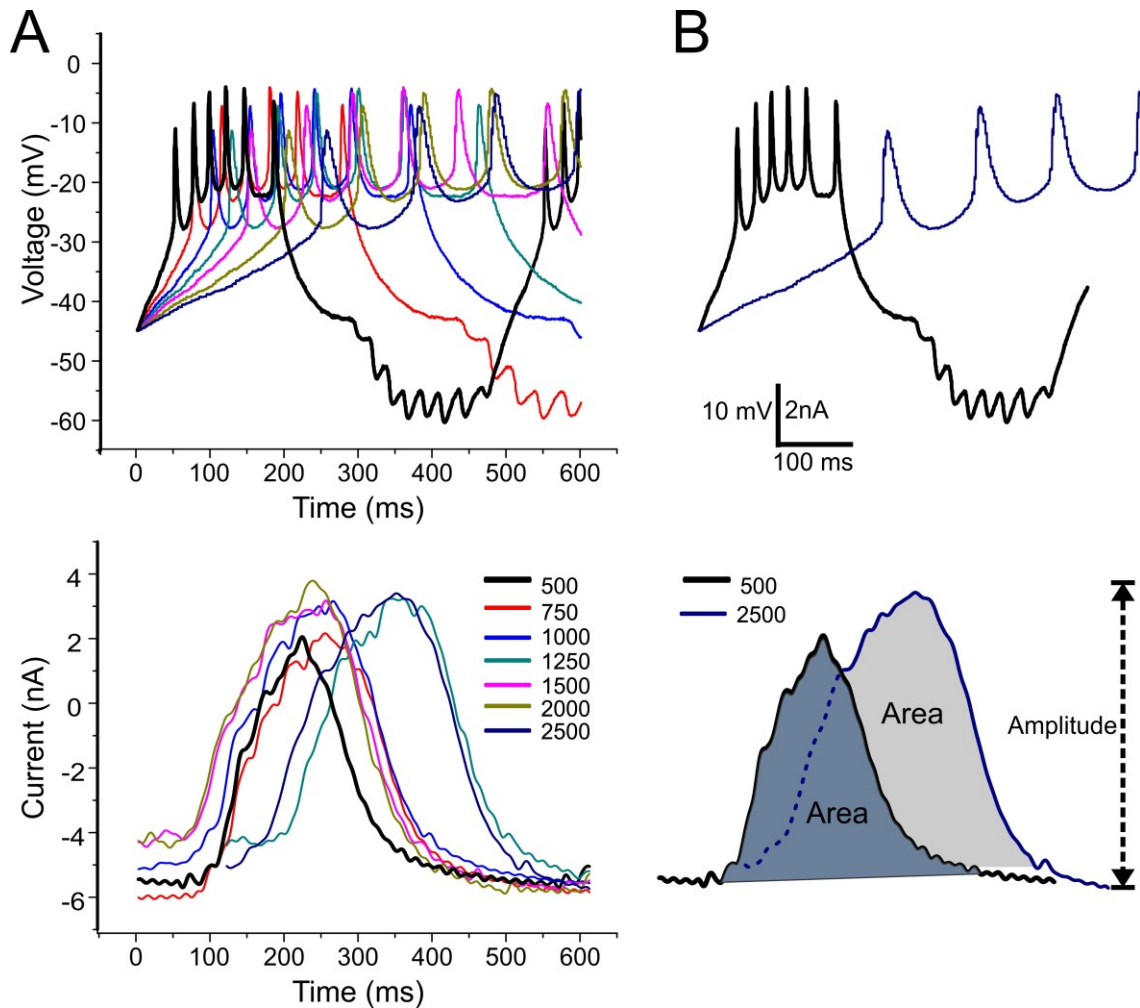
Figure B.6 The presynaptic PD neuron period affects the amplitude of the IPSC and synaptic area. Data from all experiments can be found in Table 2.4. **A.** Top panel: The PD neuron was driven using a unitary waveform of different periods (500, 750, 1000, 1250, 1500, 2000, and 2500). The values were normalized to 500 ms to make it easier to compare. Bottom panel: The synaptic amplitude was measured at each different period waveform and compared before and during MCN1 stimulation. **B.** Top panel, two waveforms of different periods (500 and 2000ms) are compared. The bottom panels, shows the area and amplitude of the synapse at both 500ms and 2000ms. Synaptic area was measured as the integral of the synaptic amplitude change over time (nA*ms). The synaptic area increased with waveform period. Amplitude also increased as a function of the presynaptic neuron period.

B.3.4 Does bath application of neuromodulators occlude the effect of projection neuron release?

Swensen and Marder (2000) showed that saturating concentrations of both proctolin and CabTRP Ia occlude each other's actions. Now that we have shown the effects of MCN1 stimulation on the pyloric neurons and synapses, we were interested in determining if MCN1 stimulation in the presence of proctolin will cause a change in the pyloric frequency and pyloric parameters we have tested. Furthermore, we wanted to determine whether proctolin will occlude the actions of MCN1 stimulation on the pyloric network.

We found that pyloric frequency was statistically different between the bath-applied proctolin and the proctolin/MCN1 stim group (Two-Way ANOVA; $p<0.001$, N=3). However, at a frequency of 15 Hz MCN1 stimulation there was no statistically significant difference. Both the LP amplitude increased and was statistically significant between proctolin and proctolin/MCN1 (LP: Two Way ANOVA; $p = 0.031$, N=3). PD amplitude (Two Way ANOVA; $p = 0.247$ N=3), LP spike number (Two Way ANOVA; $p = 0.356$ N=3), PD spike number (Two Way ANOVA; $p = 0.109$ N=3), PD burst duration (Two Way ANOVA; $p = 0.295$ N=3), and LP burst duration (Two Way ANOVA; $p = 0.344$ N=3), were not significant between the proctolin and proctolin/MCN1 group. These preliminary results indicate that proctolin does not fully occlude the actions of MCN1 stimulation at all parameters tested.

B.4 Discussion

A fundamental characteristic of many oscillatory neural networks is their ability to adapt to changes through neuromodulation. Different behavioral needs of an organism often require for networks to alter their output without changing the constituents (Marder and Thirumalai, 2002). It is important to understand how neuromodulation affects the network, as well as both the individual neurons and the synapses in the network. Modulation of the output of neural networks allows for flexibility in network output. To understand where the flexibility in the network originates we used a known modulatory projection neuron to determine how neuromodulators can modify synaptic properties and promote changes in a neural network. We have found that modulation through a projection neuron can occur both through changes in the individual neurons, as well as the synapses.

We explored the effect of endogenously released neuromodulators on network characteristics, synapses, and individual neurons. We found that endogenously released neuromodulators from MCN1 exerts its action through the LP to PD synapse. Changes in the individual parameters of the neurons may be explains through the modulation of the synapse. This may indicate that differential modulation of neurons and synapse may be necessary for proper network function.

B.4.1 The effect of neuromodulation on individual neurons

Previous work has shown that neuromodulators can affect the properties of individual neurons and that this effect can also be selective (Swensen and Marder, 2001). Here we add to the previous understanding of the effects of MCN1 on the individual neurons, by showing how voltage amplitude of the individual neurons changes as a result of neuromodulation. First, we show that the amplitude of the PD neuron and not of the LP neuron increases in the presence of MCN1 stimulation. This confirms previous work showing that bath-application of proctolin increases the amplitude of both AB and the PD neuron (Nusbaum and Marder, 1989, Swensen and Marder, 2001). Second, we show that changes in LP spike number, LP amplitude, LP duty cycle and PD duty cycle do not change in the presence of MCN1 stimulation. The PD neuron's amplitude, however, did increase with MCN1 stimulation. This finding is consistent with the results of Bartos and Nusbaum (1997) who found that with MCN1 stimulation, the amplitude of the AB neuron, the other member of the pyloric pacemaker group, increased.

Similar to the differential effects of neuromodulators in the pyloric network, cell type-specific neuromodulation also occurs in cortical neurons. The changes in the cortical circuit that occur during the sleep and wake states have been proposed to arise from the cell-type specific actions of adenosine (van Aerde et al., 2015). Adenosine exerts differential effects on both different neuronal types as well as laminar location. For instance, some interneurons in layer 2 were insensitive to adenosine modulation, while pyramidal neurons in

layer 3-6 were hyperpolarized (van Aerde et al., 2015). The differential actions of neuromodulatory release of MCN1 onto the pyloric network neurons, are also selective (Swensen and Marder, 2001). The effects on the different pyloric neurons, are not identical across different neuron types, and the manner in which they effect the cells may provide some answers to explain the methods in which adenosine also effects neurons differentially (Swensen and Marder, 2001).

Neuromodulators can alter ionic channel quantity, spatial distribution of channels, expression levels, and gating properties of channels (Nadim and Bucher, 2014). Therefore, it is not surprising that the same complement of neuromodulators released from MCN1 (GABA, CabTrp1a and proctolin) would affect certain properties of the PD neuron and not those of the LP neuron. Schulz et al (2006) demonstrated that although both the LP neuron and the PD neuron each possess the same types of ion channels, they possess different quantities of each. These difference in ionic channel quantities may be a reason that one neuron will respond differentially to neuromodulators than the other. Another reason that may account for the differences in response to neuromodulators may be the distribution of receptors that these neurons possess. If the PD neuron and the LP neuron possess different types or numbers of receptors, their response endogenously released neuromodulators would be different and may be a way to induce different types of changes in the network. Therefore, the actions of the neuromodulator on the network may not

be present at all times, but depend on the current state of the network and its components.

B.4.2. Does removing the LP to PD Synapse affect the pyloric frequency in the presence of MCN1 stimulation?

The LP to PD synapse is the sole chemical feedback from the pyloric follower neurons to the pacemaker group. We found that when we hyperpolarized LP to remove the synapse to the pacemakers, the pyloric network frequency did not increase significantly in the presence of MCN1 stimulation at frequencies of 15, 20 and 25 Hz. MCN1 stimulation frequencies of 30 and 35 Hz, however, did increase the pyloric network frequency. Additionally, differences in frequency were not seen when LP was hyperpolarized alone without MCN1 stimulation. Therefore, removing the LP to PD synapse does not influence the rhythm when MCN1 is active. This supports the hypothesis that MCN1 can exert its actions on the synapse directly and not on the pacemaker neurons.

The question is therefore, in what manner does MCN1 exert its actions on the synapse directly? Neuromodulators can modify and target synapse through actions on both postsynaptic and presynaptic mechanisms. Presynaptically, neuromodulators can target ion channels, Ca^{+2} influx, and proteins in the active zone (Man-Son-Hing et al., 1989, Dittman and Regehr, 1996, Betz et al., 1998, Oh et al., 2012) and modify synaptic release. Postsynaptic changes include the expression of receptors and changes in membrane properties of the neuron. In this case, we hyperpolarized the LP neuron and removed the presynaptic neuron completely. Therefore, the release

of neuromodulators through MCN1 may work at least to alter the properties of the presynaptic neuron. Quantifying changes in receptor content of the postsynaptic (PD) neuron is beyond the scope of this study. The PD neuron parameters measured (burst duration, amplitude and duty cycle) were found not to be different between the LP hyperpolarized alone and LP hyperpolarized in the presence of MCN1 stimulation. This indicates that MCN1 may exert its actions directly on the synapse rather than through changes in the pacemaker neurons. Even though Bartos and Nusbaum (1997) showed that MCN stimulation increased the slow waveform amplitude of the AB neuron and the pyloric frequency, this study was done without removing the LP to PD synapse. The increase in the AB amplitude may be explained through changes in the LP to PD synapse, which increases the PD slow wave amplitude. Because the PD neuron is electrically coupled to the AB neuron, increases in the PD neuron's slow wave amplitude may therefore influence the increase in the amplitude of the AB neuron.

B.4.3. What affect does the presynaptic waveform period have on the synapse?

Traditionally, short-term plasticity has been measured using a paired pulse protocol, to understand changes in both synaptic dynamics and synaptic strength. However, we were interested in understanding how the presynaptic neuron's dynamics would affect these parameters and in turn the pyloric network. We have shown that individual changes in the pyloric neurons can be cell-specific under the influence of neuromodulation. This led us to examine the

effects of the waveform of the presynaptic neuron, and how that may affect the synapse both in MCN1 stimulation and control.

Altering the period of the presynaptic waveform can alter dynamics of ionic currents. In leech heart interneurons, increasing the period of the presynaptic waveform increased I_h (Olsen and Calabrese, 1996). This suggests that I_h may be a candidate for changing the period of the oscillation but also may provide negative feedback to increase the oscillations (Olsen and Calabrese, 1996). Here we have shown that increasing the presynaptic period increased both synaptic amplitude and synaptic area. Additional analysis of our results is needed to see if changing the amplitude and not only the period of the presynaptic waveform would have similar results. The longer the period, the longer the amount of time provided for I_h to fully activate.

Altering the period of the presynaptic waveform may allow for changes in ionic channel currents and other possible mechanisms that may influence release of neuromodulators. One possibility is that the longer the period, the more calcium enters the presynaptic neuron allowing for longer release of neurotransmitter, affecting both synaptic current and synaptic area. Similar studies have shown the effect of increasing spike width of the granule cell. Increasing the spike width of the presynaptic waveform, led to a 25% increase in the influx of calcium to the presynaptic neuron, which in turn doubled synaptic strength to the Purkinje cell (Sabatini and Regehr, 1997). Studies in *Xenopus laevis*, examined the effect of calcium release at the NMJ using R-roscovotine (a kinase inhibitor)(Cho and Meriney, 2006). They found that increasing calcium

entry into the presynaptic neuron also increased transmitter release at the adult frog NMJ. This finding on the increase in calcium entry, supports the belief that that the longer the period of the presynaptic neuron, the greater the increase in calcium entry (Cho and Meriney, 2006).

We were able to manipulate the period of the presynaptic waveform using a prerecorded waveform. We found that as the period of the presynaptic waveform increased, so did the IPSC amplitude and synaptic area. This can be a way in which increased calcium entry into the presynaptic neuron can then increase the amount of neurotransmitter increasing both IPSC amplitude and synaptic area. The amount which these two properties are increased is enhanced in the presence of neuromodulators from MCN1, as seen through my results. Multiple modulators can act on the same synapse in order to modify it to alter circuit dynamics, however, this is only assuming that there is a need for a change in network output (Tseng et al., 2014). Proctolin for instance, only facilitates the LP to PD synapse under certain conditions (Zhao et al., 2011). The increase in the IPSC and synaptic area, seen in the presence of MCN1 stimulation, only occurs at specific periods. Modulation of the synapses can either be through direct modulation of the synapse, or through changes in the properties of the individual neurons, such as the presynaptic LP neuron.

Ayali A, Harris-Warrick RM (1999) Monoamine control of the pacemaker kernel and cycle frequency in the lobster pyloric network. J Neurosci 19:6712-6722.

Bal T, McCormick DA (1997) Synchronized oscillations in the inferior olive are controlled by the hyperpolarization-activated cation current I(h). J Neurophysiol 77:3145-3156.

Bal T, Nagy F, Moulins M (1988) The pyloric central pattern generator in Crustacea: a set of conditional neuronal oscillators. Journal of Comparative Physiology A 163:715-727.

Barnes NM, Sharp T (1999) A review of central 5-HT receptors and their function. Neuropharmacology 38:1083-1152.

Bartos M, Nusbaum MP (1997) Intercircuit control of motor pattern modulation by presynaptic inhibition. J Neurosci 17:2247-2256.

Beaumont V, Zucker RS (2000) Enhancement of synaptic transmission by cyclic AMP modulation of presynaptic Ih channels. Nat Neurosci 3:133-141.

Berger T, Senn W, Luscher HR (2003) Hyperpolarization-activated current Ih disconnects somatic and dendritic spike initiation zones in layer V pyramidal neurons. J Neurophysiol 90:2428-2437.

Betz A, Ashery U, Rickmann M, Augustin I, Neher E, Sudhof TC, Rettig J, Brose N (1998) Munc13-1 is a presynaptic phorbol ester receptor that enhances neurotransmitter release. Neuron 21:123-136.

Billimoria CP, Li L, Marder E (2005) Profiling of neuropeptides released at the stomatogastric ganglion of the crab, Cancer borealis with mass spectrometry. J Neurochem 95:191-199.

Blitz DM, Christie AE, Coleman MJ, Norris BJ, Marder E, Nusbaum MP (1999) Different proctolin neurons elicit distinct motor patterns from a multifunctional neuronal network. J Neurosci 19:5449-5463.

Blitz DM, Nusbaum MP (1997) Motor pattern selection via inhibition of parallel pathways. J Neurosci 17:4965-4975.

Boschert U, Amara DA, Segu L, Hen R (1994) The mouse 5-hydroxytryptamine1B receptor is localized predominantly on axon terminals. Neuroscience 58:167-182.

Bose A, Manor Y, Nadim F (2004) The activity phase of postsynaptic neurons in a simplified rhythmic network. J Comput Neurosci 17:245-261.

Brochini L, Carelli PV, Pinto RD (2011) Single synapse information coding in intraburst spike patterns of central pattern generator motor neurons. J Neurosci 31:12297-12306.

Bucher D, Prinz AA, Marder E (2005) Animal-to-animal variability in motor pattern production in adults and during growth. J Neurosci 25:1611-1619.

Burger RM, Cramer KS, Pfeiffer JD, Rubel EW (2005) Avian superior olivary nucleus provides divergent inhibitory input to parallel auditory pathways. J Comp Neurol 481:6-18.

Burger RM, Fukui I, Ohmori H, Rubel EW (2011) Inhibition in the balance: binaurally coupled inhibitory feedback in sound localization circuitry. J Neurophysiol 106:4-14.

Butt SJ, Harris-Warrick RM, Kiehn O (2002) Firing properties of identified interneuron populations in the mammalian hindlimb central pattern generator. J Neurosci 22:9961-9971.

Calabrese RL (1995) Oscillation in motor pattern-generating networks. Curr Opin Neurobiol 5:816-823.

Cardin JA, Carlen M, Meletis K, Knoblich U, Zhang F, Deisseroth K, Tsai LH, Moore CI (2009) Driving fast-spiking cells induces gamma rhythm and controls sensory responses. Nature 459:663-667.

Cho S, Meriney SD (2006) The effects of presynaptic calcium channel modulation by roscovitine on transmitter release at the adult frog neuromuscular junction. Eur J Neurosci 23:3200-3208.

Christie AE, Lundquist CT, Nassel DR, Nusbaum MP (1997) Two novel tachykinin-related peptides from the nervous system of the crab Cancer borealis. J Exp Biol 200:2279-2294.

Coleman MJ, Meyrand P, Nusbaum MP (1995) A switch between two modes of synaptic transmission mediated by presynaptic inhibition. Nature 378:502-505.

Coleman MJ, Nusbaum MP (1994) Functional consequences of compartmentalization of synaptic input. J Neurosci 14:6544-6552.

Cuttle MF, Rusznak Z, Wong AY, Owens S, Forsythe ID (2001) Modulation of a presynaptic hyperpolarization-activated cationic current (I(h)) at an excitatory synaptic terminal in the rat auditory brainstem. J Physiol 534:733-744.

D'Angelo E, Nieus T, Maffei A, Armano S, Rossi P, Taglietti V, Fontana A, Naldi G (2001) Theta-frequency bursting and resonance in cerebellar granule cells: experimental evidence and modeling of a slow k+-dependent mechanism. J Neurosci 21:759-770.

Dickinson PS (2006) Neuromodulation of central pattern generators in invertebrates and vertebrates. Curr Opin Neurobiol 16:604-614.

Dittman JS, Regehr WG (1996) Contributions of calcium-dependent and calcium-independent mechanisms to presynaptic inhibition at a cerebellar synapse. J Neurosci 16:1623-1633.

Doi A, Ramirez JM (2008) Neuromodulation and the orchestration of the respiratory rhythm. Respir Physiol Neurobiol 164:96-104.

Eckhorn R, Bauer R, Jordan W, Brosch M, Kruse W, Munk M, Reitboeck HJ (1988) Coherent oscillations: a mechanism of feature linking in the visual cortex? Multiple electrode and correlation analyses in the cat. Biol Cybern 60:121-130.

Eisen JS, Marder E (1982) Mechanisms underlying pattern generation in lobster stomatogastric ganglion as determined by selective inactivation of identified neurons. III. Synaptic connections of electrically coupled pyloric neurons. J Neurophysiol 48:1392-1415.

Eisen JS, Marder E (1984) A mechanism for production of phase shifts in a pattern generator. J Neurophysiol 51:1375-1393.

Elliott CJ, Vehovszky A (2000) Polycyclic neuromodulation of the feeding rhythm of the pond snail Lymnaea stagnalis by the intrinsic octopaminergic interneuron, OC. Brain Res 887:63-69.

Engel TA, Schimansky-Geier L, Herz AV, Schreiber S, Erchova I (2008) Subthreshold membrane-potential resonances shape spike-train patterns in the entorhinal cortex. J Neurophysiol 100:1576-1589.

Fan Y, Fricker D, Brager DH, Chen X, Lu HC, Chitwood RA, Johnston D (2005) Activity-dependent decrease of excitability in rat hippocampal neurons through increases in I(h). Nat Neurosci 8:1542-1551.

Feldman JL, Del Negro CA (2006) Looking for inspiration: new perspectives on respiratory rhythm. Nat Rev Neurosci 7:232-242.

Fell J, Axmacher N (2011) The role of phase synchronization in memory processes. Nat Rev Neurosci 12:105-118.

Fink KB, Gothert M (2007) 5-HT receptor regulation of neurotransmitter release. Pharmacol Rev 59:360-417.

Flamm RE, Harris-Warrick RM (1986) Aminergic modulation in lobster stomatogastric ganglion. II. Target neurons of dopamine, octopamine, and serotonin within the pyloric circuit. J Neurophysiol 55:866-881.

Fries P (2005) A mechanism for cognitive dynamics: neuronal communication through neuronal coherence. Trends Cogn Sci 9:474-480.

Fukuda T, Kosaka T (2000) Gap junctions linking the dendritic network of GABAergic interneurons in the hippocampus. J Neurosci 20:1519-1528.

Getting PA (1983) Neural control of swimming in Tritonia. Symp Soc Exp Biol 37:89-128.

Getting PA (1989) Emerging principles governing the operation of neural networks. Annu Rev Neurosci 12:185-204.

Goaillard JM, Taylor AL, Schulz DJ, Marder E (2009) Functional consequences of animal-to-animal variation in circuit parameters. Nat Neurosci 12:1424-1430.

Goeritz ML, Ouyang Q, Harris-Warrick RM (2011) Localization and function of Ih channels in a small neural network. J Neurophysiol 106:44-58.

Golowasch J, Abbott LF, Marder E (1999) Activity-dependent regulation of potassium currents in an identified neuron of the stomatogastric ganglion of the crab Cancer borealis. J Neurosci 19:RC33.

Golowasch J, Buchholtz F, Epstein IR, Marder E (1992) Contribution of individual ionic currents to activity of a model stomatogastric ganglion neuron. J Neurophysiol 67:341-349.

Golowasch J, Marder E (1992a) Ionic currents of the lateral pyloric neuron of the stomatogastric ganglion of the crab. J Neurophysiol 67:318-331.

Golowasch J, Marder E (1992b) Proctolin activates an inward current whose voltage dependence is modified by extracellular Ca2+. J Neurosci 12:810-817.

Graubard K (1978) Synaptic transmission without action potentials: input-output properties of a nonspiking presynaptic neuron. J Neurophysiol 41:1014-1025.

Graubard K, Raper JA, Hartline DK (1980) Graded synaptic transmission between spiking neurons. Proc Natl Acad Sci U S A 77:3733-3735.

Graubard K, Raper JA, Hartline DK (1983) Graded synaptic transmission between identified spiking neurons. J Neurophysiol 50:508-521.

Grillner S (1974) On the generation of locomotion in the spinal dogfish. Exp Brain Res 20:459-470.

Hahn G, Bujan AF, Fregnac Y, Aertsen A, Kumar A (2014) Communication through resonance in spiking neuronal networks. PLoS Comput Biol 10:e1003811.

Harris-Warrick RM (1992) Dynamic biological networks: the stomatogastric nervous system: MIT Press.

Harris-Warrick RM, Coniglio LM, Barazangi N, Guckenheimer J, Gueron S (1995a) Dopamine modulation of transient potassium current evokes phase shifts in a central pattern generator network. J Neurosci 15:342-358.

Harris-Warrick RM, Coniglio LM, Levini RM, Gueron S, Guckenheimer J (1995b) Dopamine modulation of two subthreshold currents produces phase shifts in activity of an identified motoneuron. J Neurophysiol 74:1404-1420.

Harris-Warrick RM, Johnson BR (2010) Checks and balances in neuromodulation. Front Behav Neurosci 4.

Harris-Warrick RM, Johnson BR, Peck JH, Kloppenburg P, Ayali A, Skarbinski J (1998) Distributed Effects of Dopamine Modulation in the Crustacean Pyloric Networka. Ann N Y Acad Sci 860:155-167.

Heidelberger R (2007) Mechanisms of tonic, graded release: lessons from the vertebrate photoreceptor. J Physiol 585:663-667.

Hill AA, Masino MA, Calabrese RL (2002) Model of intersegmental coordination in the leech heartbeat neuronal network. J Neurophysiol 87:1586-1602.

Hill AA, Masino MA, Calabrese RL (2003) Intersegmental coordination of rhythmic motor patterns. J Neurophysiol 90:531-538.

Hooper SL, Buchman E, Weaver AL, Thuma JB, Hobbs KH (2009) Slow conductances could underlie intrinsic phase-maintaining properties of isolated lobster (Panulirus interruptus) pyloric neurons. J Neurosci 29:1834-1845.

Hooper SL, Hobbs KH, Thuma JB (2008) Invertebrate muscles: thin and thick filament structure; molecular basis of contraction and its regulation, catch and asynchronous muscle. Prog Neurobiol 86:72-127.

Hooper SL, Marder E (1987) Modulation of the lobster pyloric rhythm by the peptide proctolin. J Neurosci 7:2097-2112.

Hooper SL, Moulins M (1990) Cellular and synaptic mechanisms responsible for a long-lasting restructuring of the lobster pyloric network. J Neurophysiol 64:1574-1589.

Hooper SL, O'Neil MB, Wagner R, Ewer J, Golowasch J, Marder E (1986) The innervation of the pyloric region of the crab, Cancer borealis: homologous muscles in decapod species are differently innervated. J Comp Physiol A 159:227-240.

Hormuzdi SG, Filippov MA, Mitropoulou G, Monyer H, Bruzzone R (2004) Electrical synapses: a dynamic signaling system that shapes the activity of neuronal networks. Biochim Biophys Acta 1662:113-137.

Hutcheon B, Yarom Y (2000) Resonance, oscillation and the intrinsic frequency preferences of neurons. Trends Neurosci 23:216-222.

Johnson BR, Harris-Warrick RM (1990) Aminergic modulation of graded synaptic transmission in the lobster stomatogastric ganglion. J Neurosci 10:2066-2076.

Khorkova O, Golowasch J (2007) Neuromodulators, not activity, control coordinated expression of ionic currents. J Neurosci 27:8709-8718.

Kilman VL, Marder E (1996) Ultrastructure of the stomatogastric ganglion neuropil of the crab, Cancer borealis. J Comp Neurol 374:362-375.

Kloppenburg P, Levini RM, Harris-Warrick RM (1999) Dopamine modulates two potassium currents and inhibits the intrinsic firing properties of an identified motor neuron in a central pattern generator network. J Neurophysiol 81:29-38.

Kvarta MD, Harris-Warrick RM, Johnson BR (2012) Neuromodulator-evoked synaptic metaplasticity within a central pattern generator network. J Neurophysiol 108:2846-2856.

Lampl I, Yarom Y (1997) Subthreshold oscillations and resonant behavior: two manifestations of the same mechanism. Neuroscience 78:325-341.

Landisman CE, Long MA, Beierlein M, Deans MR, Paul DL, Connors BW (2002) Electrical synapses in the thalamic reticular nucleus. J Neurosci 22:1002-1009.

Levi R, Akanyeti O, Ballo A, Liao JC (2015) Frequency response properties of primary afferent neurons in the posterior lateral line system of larval zebrafish. J Neurophysiol 113:657-668.

Liu Q, Hollopeter G, Jorgensen EM (2009) Graded synaptic transmission at the Caenorhabditis elegans neuromuscular junction. Proc Natl Acad Sci U S A 106:10823-10828.

Llinas R, Yarom Y (1981) Electrophysiology of mammalian inferior olivary neurones in vitro. Different types of voltage-dependent ionic conductances. J Physiol 315:549-567.

Llinas RR (1988) The intrinsic electrophysiological properties of mammalian neurons: insights into central nervous system function. Science 242:1654-1664.

Luther JA, Robie AA, Yarotsky J, Reina C, Marder E, Golowasch J (2003) Episodic bouts of activity accompany recovery of rhythmic output by a neuromodulator- and activity-deprived adult neural network. J Neurophysiol 90:2720-2730.

MacLean JN, Zhang Y, Johnson BR, Harris-Warrick RM (2003) Activity-independent homeostasis in rhythmically active neurons. Neuron 37:109-120.

Magee JC (1998) Dendritic hyperpolarization-activated currents modify the integrative properties of hippocampal CA1 pyramidal neurons. J Neurosci 18:7613-7624.

Magee JC (1999) Dendritic lh normalizes temporal summation in hippocampal CA1 neurons. Nat Neurosci 2:508-514.

Mamiya A, Manor Y, Nadim F (2003) Short-term dynamics of a mixed chemical and electrical synapse in a rhythmic network. J Neurosci 23:9557-9564.

Mamiya A, Nadim F (2004) Dynamic interaction of oscillatory neurons coupled with reciprocally inhibitory synapses acts to stabilize the rhythm period. J Neurosci 24:5140-5150.

Mamiya A, Nadim F (2005) Target-specific short-term dynamics are important for the function of synapses in an oscillatory neural network. J Neurophysiol 94:2590-2602.

Man-Son-Hing H, Zoran MJ, Lukowiak K, Haydon PG (1989) A neuromodulator of synaptic transmission acts on the secretory apparatus as well as on ion channels. Nature 341:237-239.

Manor Y, Bose A, Booth V, Nadim F (2003) Contribution of synaptic depression to phase maintenance in a model rhythmic network. J Neurophysiol 90:3513-3528.

Manor Y, Nadim F, Abbott LF, Marder E (1997) Temporal dynamics of graded synaptic transmission in the lobster stomatogastric ganglion. J Neurosci 17:5610-5621.

Marder E (1984) Roles for electrical coupling in neural circuits as revealed by selective neuronal deletions. J Exp Biol 112:147-167.

Marder E (2012) Neuromodulation of neuronal circuits: back to the future. Neuron 76:1-11.

Marder E, Bucher D (2007) Understanding circuit dynamics using the stomatogastric nervous system of lobsters and crabs. Annu Rev Physiol 69:291-316.

Marder E, Bucher D, Schulz DJ, Taylor AL (2005) Invertebrate central pattern generation moves along. Curr Biol 15:R685-699.

Marder E, Calabrese RL (1996) Principles of rhythmic motor pattern generation. Physiol Rev 76:687-717.

Marder E, Eisen JS (1984a) Electrically coupled pacemaker neurons respond differently to same physiological inputs and neurotransmitters. J Neurophysiol 51:1362-1374.

Marder E, Eisen JS (1984b) Transmitter identification of pyloric neurons: electrically coupled neurons use different transmitters. J Neurophysiol 51:1345-1361.

Marder E, Goaillard JM (2006) Variability, compensation and homeostasis in neuron and network function. Nat Rev Neurosci 7:563-574.

Marder E, Thirumalai V (2002) Cellular, synaptic and network effects of neuromodulation. Neural Netw 15:479-493.

Matsushima T, Grillner S (1992) Neural mechanisms of intersegmental coordination in lamprey: local excitability changes modify the phase coupling along the spinal cord. J Neurophysiol 67:373-388.

Maynard D, Selverston A (1975) Organization of the stomatogastric ganglion of the spiny lobster. J Comp Physiol 100:161-182.

Migliore M, Ferrante M, Ascoli GA (2005) Signal propagation in oblique dendrites of CA1 pyramidal cells. J Neurophysiol 94:4145-4155.

Migliore M, Messineo L, Ferrante M (2004) Dendritic Ih selectively blocks temporal summation of unsynchronized distal inputs in CA1 pyramidal neurons. J Comput Neurosci 16:5-13.

Miles GB, Sillar KT (2011) Neuromodulation of vertebrate locomotor control networks. Physiology (Bethesda) 26:393-411.

Miller JP, Selverston AI (1982a) Mechanisms underlying pattern generation in lobster stomatogastric ganglion as determined by selective inactivation of identified neurons. II. Oscillatory properties of pyloric neurons. J Neurophysiol 48:1378-1391.

Miller JP, Selverston AI (1982b) Mechanisms underlying pattern generation in lobster stomatogastric ganglion as determined by selective inactivation of identified neurons. IV. Network properties of pyloric system. J Neurophysiol 48:1416-1432.

Monsivais P, Yang L, Rubel EW (2000) GABAergic inhibition in nucleus magnocellularis: implications for phase locking in the avian auditory brainstem. J Neurosci 20:2954-2963.

Morgans CW (2000) Neurotransmitter release at ribbon synapses in the retina. Immunol Cell Biol 78:442-446.

Morris LG, Hooper SL (1997) Muscle response to changing neuronal input in the lobster (Panulirus interruptus) stomatogastric system: spike number- versus spike frequency-dependent domains. J Neurosci 17:5956-5971.

Mouser C, Nadim F, Bose A (2008) Maintaining phase of the crustacean tri-phasic pyloric rhythm. J Math Biol 57:161-181.

Mullins OJ, Hackett JT, Buchanan JT, Friesen WO (2011) Neuronal control of swimming behavior: comparison of vertebrate and invertebrate model systems. Prog Neurobiol 93:244-269.

Mulloney B, Smarandache-Wellmann C (2012) Neurobiology of the crustacean swimmeret system. Prog Neurobiol 96:242-267.

Nadim F, Bucher D (2014) Neuromodulation of neurons and synapses. Curr Opin Neurobiol 29C:48-56.

Nadim F, Manor Y, Nusbaum MP, Marder E (1998) Frequency regulation of a slow rhythm by a fast periodic input. J Neurosci 18:5053-5067.

Nadim F, Zhao S, Bose A (2012) A PRC Description of How Inhibitory Feedback Promotes Oscillation Stability. In: Phase Response Curves in Neuroscience, vol. 6 (Schultheiss, N. W. et al., eds), pp 399-417: Springer New York.

Nadim F, Zhao S, Zhou L, Bose A (2011) Inhibitory feedback promotes stability in an oscillatory network. J Neural Eng 8:065001.

Nokia MS, Wikgren J (2010) Hippocampal theta activity is selectively associated with contingency detection but not discrimination in rabbit discrimination-reversal eyeblink conditioning. Hippocampus 20:457-460.

Nolan MF, Malleret G, Dudman JT, Buhl DL, Santoro B, Gibbs E, Vronskaya S, Buzsaki G, Siegelbaum SA, Kandel ER, Morozov A (2004) A behavioral role for dendritic integration: HCN1 channels constrain spatial memory and plasticity at inputs to distal dendrites of CA1 pyramidal neurons. Cell 119:719-732.

Norris BJ, Coleman MJ, Nusbaum MP (1994) Recruitment of a projection neuron determines gastric mill motor pattern selection in the stomatogastric nervous system of the crab, Cancer borealis. J Neurophysiol 72:1451-1463.

Norris BJ, Coleman MJ, Nusbaum MP (1996) Pyloric motor pattern modification by a newly identified projection neuron in the crab stomatogastric nervous system. J Neurophysiol 75:97-108.

Norris BJ, Weaver AL, Wenning A, Garcia PS, Calabrese RL (2007a) A central pattern generator producing alternative outputs: pattern, strength, and dynamics of premotor synaptic input to leech heart motor neurons. J Neurophysiol 98:2992-3005.

Norris BJ, Weaver AL, Wenning A, Garcia PS, Calabrese RL (2007b) A central pattern generator producing alternative outputs: phase relations of leech heart motor neurons with respect to premotor synaptic input. J Neurophysiol 98:2983-2991.

Nusbaum MP, Beenhakker MP (2002) A small-systems approach to motor pattern generation. Nature 417:343-350.

Nusbaum MP, Blitz DM, Swensen AM, Wood D, Marder E (2001) The roles of co-transmission in neural network modulation. Trends Neurosci 24:146-154.

Nusbaum MP, Marder E (1989) A modulatory proctolin-containing neuron (MPN). II. State-dependent modulation of rhythmic motor activity. J Neurosci 9:1600-1607.

Nusbaum MP, Weimann JM, Golowasch J, Marder E (1992) Presynaptic control of modulatory fibers by their neural network targets. J Neurosci 12:2706-2714.

Oh M, Zhao S, Matveev V, Nadim F (2012) Neuromodulatory changes in short-term synaptic dynamics may be mediated by two distinct mechanisms of presynaptic calcium entry. J Comput Neurosci 33:573-585.

Olsen OH, Calabrese RL (1996) Activation of intrinsic and synaptic currents in leech heart interneurons by realistic waveforms. J Neurosci 16:4958-4970.

Pape HC (1996) Queer current and pacemaker: the hyperpolarization-activated cation current in neurons. Annu Rev Physiol 58:299-327.

Peck JH, Gaier E, Stevens E, Repicky S, Harris-Warrick RM (2006) Amine modulation of Ih in a small neural network. J Neurophysiol 96:2931-2940.

Peck JH, Nakanishi ST, Yaple R, Harris-Warrick RM (2001) Amine modulation of the transient potassium current in identified cells of the lobster stomatogastric ganglion. J Neurophysiol 86:2957-2965.

Pena F, Parkis MA, Tryba AK, Ramirez JM (2004) Differential contribution of pacemaker properties to the generation of respiratory rhythms during normoxia and hypoxia. Neuron 43:105-117.

Pereda AE (2014) Electrical synapses and their functional interactions with chemical synapses. Nat Rev Neurosci 15:250-263.

Pouille F, Scanziani M (2004) Routing of spike series by dynamic circuits in the hippocampus. Nature 429:717-723.

Prinz AA, Thirumalai V, Marder E (2003) The functional consequences of changes in the strength and duration of synaptic inputs to oscillatory neurons. J Neurosci 23:943-954.

Rabbah P, Nadim F (2007) Distinct synaptic dynamics of heterogeneous pacemaker neurons in an oscillatory network. J Neurophysiol 97:2239-2253.

Ramirez JM, Koch H, Garcia AJ, 3rd, Doi A, Zanella S (2011) The role of spiking and bursting pacemakers in the neuronal control of breathing. J Biol Phys 37:241-261.

Ramirez JM, Tryba AK, Pena F (2004) Pacemaker neurons and neuronal networks: an integrative view. Curr Opin Neurobiol 14:665-674.

Robinson RB, Siegelbaum SA (2003) Hyperpolarization-activated cation currents: from molecules to physiological function. Annu Rev Physiol 65:453-480.

Sabatini BL, Regehr WG (1997) Control of neurotransmitter release by presynaptic waveform at the granule cell to Purkinje cell synapse. J Neurosci 17:3425-3435.

Sari Y (2004) Serotonin1B receptors: from protein to physiological function and behavior. Neurosci Biobehav Rev 28:565-582.

Schulz DJ, Goaillard JM, Marder E (2006) Variable channel expression in identified single and electrically coupled neurons in different animals. Nat Neurosci 9:356-362.

Selverston A, Elson R, Rabinovich M, Huerta R, Abarbanel H (1998) Basic Principles for Generating Motor Output in the Stomatogastric Ganglion. Ann N Y Acad Sci 860:35-50.

Selverston AI, Miller JP (1980) Mechanisms underlying pattern generation in lobster stomatogastric ganglion as determined by selective inactivation of identified neurons. I. Pyloric system. J Neurophysiol 44:1102-1121.

Selverston AI, Russell DF, Miller JP (1976) The stomatogastric nervous system: structure and function of a small neural network. Prog Neurobiol 7:215-290.

Shebanie A, Nadim F (2009) Co-modulation of synaptic strengths by distinct co-released neurotransmitters. Soc Neurosci Abstract 35: 270.276.

Sillar KT (1996) The development of central pattern generators for vertebrate locomotion. In: Advances in Psychology, vol. Volume 115 (María, A. P. and Julio, A., eds), pp 205-221: North-Holland.

Sirota A, Buzsaki G (2005) Interaction between neocortical and hippocampal networks via slow oscillations. Thalamus Relat Syst 3:245-259.

Smarandache C, Hall WM, Mulloney B (2009) Coordination of rhythmic motor activity by gradients of synaptic strength in a neural circuit that couples modular neural oscillators. J Neurosci 29:9351-9360.

Smith M, Pereda AE (2003) Chemical synaptic activity modulates nearby electrical synapses. Proc Natl Acad Sci U S A 100:4849-4854.

Soofi W, Archila S, Prinz AA (2012) Co-variation of ionic conductances supports phase maintenance in stomatogastric neurons. J Comput Neurosci 33:77-95.

Southan AP, Morris NP, Stephens GJ, Robertson B (2000) Hyperpolarization-activated currents in presynaptic terminals of mouse cerebellar basket cells. J Physiol 526 Pt 1:91-97.

Stein W (2009) Modulation of stomatogastric rhythms. J Comp Physiol A Neuroethol Sens Neural Behav Physiol 195:989-1009.

Suzuki N, Bekkers JM (2012) Microcircuits mediating feedforward and feedback synaptic inhibition in the piriform cortex. J Neurosci 32:919-931.

Swensen AM, Golowasch J, Christie AE, Coleman MJ, Nusbaum MP, Marder E (2000) GABA and responses to GABA in the stomatogastric ganglion of the crab Cancer borealis. J Exp Biol 203:2075-2092.

Swensen AM, Marder E (2000) Multiple peptides converge to activate the same voltage-dependent current in a central pattern-generating circuit. J Neurosci 20:6752-6759.

Swensen AM, Marder E (2001) Modulators with convergent cellular actions elicit distinct circuit outputs. J Neurosci 21:4050-4058.

Szucs A, Pinto RD, Rabinovich MI, Abarbanel HD, Selverston AI (2003) Synaptic modulation of the interspike interval signatures of bursting pyloric neurons. J Neurophysiol 89:1363-1377.

Tang LS, Goeritz ML, Caplan JS, Taylor AL, Fisek M, Marder E (2010) Precise temperature compensation of phase in a rhythmic motor pattern. PLoS Biol 8.

Tchumatchenko T, Clopath C (2014) Oscillations emerging from noise-driven steady state in networks with electrical synapses and subthreshold resonance. Nat Commun 5:5512.

Tepper JM, Koos T, Wilson CJ (2004) GABAergic microcircuits in the neostriatum. Trends Neurosci 27:662-669.

Thirumalai V, Prinz AA, Johnson CD, Marder E (2006) Red pigment concentrating hormone strongly enhances the strength of the feedback to the pyloric rhythm oscillator but has little effect on pyloric rhythm period. J Neurophysiol 95:1762-1770.

Tierney AJ, Harris-Warrick RM (1992) Physiological role of the transient potassium current in the pyloric circuit of the lobster stomatogastric ganglion. J Neurophysiol 67:599-609.

Tohidi V, Nadim F (2009) Membrane resonance in bursting pacemaker neurons of an oscillatory network is correlated with network frequency. J Neurosci 29:6427-6435.

Tseng HA, Martinez D, Nadim F (2014) The frequency preference of neurons and synapses in a recurrent oscillatory network. J Neurosci 34:12933-12945.

Tseng HA, Nadim F (2010) The membrane potential waveform of bursting pacemaker neurons is a predictor of their preferred frequency and the network cycle frequency. J Neurosci 30:10809-10819.

van Aerde KI, Qi G, Feldmeyer D (2015) Cell type-specific effects of adenosine on cortical neurons. Cereb Cortex 25:772-787.

Weimann JM, Marder E (1994) Switching neurons are integral members of multiple oscillatory networks. Curr Biol 4:896-902.

Weimann JM, Meyrand P, Marder E (1991) Neurons that form multiple pattern generators: identification and multiple activity patterns of gastric/pyloric neurons in the crab stomatogastric system. J Neurophysiol 65:111-122.

Winterer J, Stempel AV, Dugladze T, Foldy C, Maziashvili N, Zivkovic AR, Priller J, Soltesz I, Gloveli T, Schmitz D (2011) Cell-type-specific modulation of feedback inhibition by serotonin in the hippocampus. J Neurosci 31:8464-8475.

Wood DE, Manor Y, Nadim F, Nusbaum MP (2004) Intercircuit control via rhythmic regulation of projection neuron activity. J Neurosci 24:7455-7463.

Wood DE, Nusbaum MP (2002) Extracellular peptidase activity tunes motor pattern modulation. J Neurosci 22:4185-4195.

Wood DE, Stein W, Nusbaum MP (2000) Projection neurons with shared cotransmitters elicit different motor patterns from the same neural circuit. J Neurosci 20:8943-8953.

Wright TM, Jr., Calabrese RL (2011) Patterns of presynaptic activity and synaptic strength interact to produce motor output. J Neurosci 31:17555-17571.

Yang L, Monsivais P, Rubel EW (1999) The superior olivary nucleus and its influence on nucleus laminaris: a source of inhibitory feedback for coincidence detection in the avian auditory brainstem. J Neurosci 19:2313-2325.

Zhang H, Rodgers EW, Krenz WD, Clark MC, Baro DJ (2010) Cell specific dopamine modulation of the transient potassium current in the pyloric network by the canonical D1 receptor signal transduction cascade. J Neurophysiol 104:873-884.

Zhao S, Golowasch J (2012) Ionic current correlations underlie the global tuning of large numbers of neuronal activity attributes. J Neurosci 32:13380-13388.

Zhao S, Sheibanie AF, Oh M, Rabbah P, Nadim F (2011) Peptide
neuromodulation of synaptic dynamics in an oscillatory network. J
Neurosci 31:13991-14004.